THE JOURNAL
OF
CHEMICAL PHYSICS

VOLUME 4 OCTOBER, 1936 NUMBER 10

The Infrared Absorption Spectra of H_2S, HDS and D_2S

C. R. BAILEY, J. W. THOMPSON AND J. B. HALE, *Department of Chemistry, University College, London, England*

(Received May 15, 1936)

The infrared spectra of H_2S, HDS and D_2S have been examined up to 15 μ with a monochromating prism spectrometer, and the results compared with the Raman spectra. The fundamental frequencies have been assigned with reasonable certainty, and a calculation has been made of the frequencies corresponding to infinitesimal amplitude. The cruder methods of the vibrational-rotational spectrum suggest a vertical angle of 110°, as compared with 92° obtained previously from a rotational analysis.

THERE have been many investigations of the infrared absorption spectrum of hydrogen sulphide.[1–7] The possible presence of impurities has led to the postulation of bands which do not exist,[1, 2, 4] and to the denial of others which are really there.[3, 5] We have re-examined the spectra of this compound and its deuterium isotopes between 1 and 15 μ with a monochromating prism spectrometer.

The weakness of absorption throughout the spectrum has increased the difficulties of observation and interpretation; and although finality is not claimed, we think we have presented at least a concordant account of the three isotopic molecules, while we have stressed in what follows the uncertainties which would justify further investigation.

EXPERIMENTAL

1. Apparatus

The general arrangement has been fully described,[8] the only important modifications being the replacement of the Downing galvanometer by a photo-relay using a Zernicke and a Moll galvanometer, and the fitting of the absorption cells and thermopile with potassium bromide endplates. We would emphasize the need for great care in the calibration of a prism spectrometer, particularly in the use of the unresolved maxima of atmospheric CO_2 bands, since the position of these changes considerably with the percentage of carbon dioxide present. In our experience the use of two absorption cells, one evacuated and the other containing the gas under examination, seems to be essential. The omission of this precaution inevitably leads to the inclusion of false absorption regions, and to a good deal of imaginary resolution.

A preliminary run was made with the rocksalt prism, and the located regions of absorption were then more closely examined with the appropriate

[1] W. W. Coblentz, Pub. Carnegie Inst., No. 35, pp. 52 and 178 (1902).
[2] A. H. Rollefson, Phys. Rev. **34**, 604 (1929).
[3] H. H. Nielsen and E. F. Barker, Phys. Rev. **37**, 727 (1931).
[4] W. Mischke, Zeits. f. Physik **67**, 106 (1931).
[5] H. H. Nielsen and A. D. Sprague, Phys. Rev. **37**, 1183 (1931).
[6] A. D. Sprague and H. H. Nielsen, Phys. Rev. **43**, 375 (1933).
[7] P. C. Cross, Phys. Rev. **47**, 7 (1935).
[8] A. B. D. Cassie and C. R. Bailey, Proc. Roy. Soc. **A132**, 252 (1931).

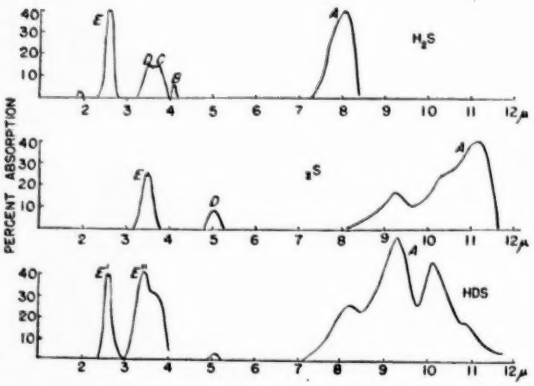

FIG. 1. The infrared spectra of H_2S, D_2S and HDS.

prism of quartz, fluorite, or rocksalt. Readings were taken at intervals of approximately 0.02 μ in order to have full advantage of the available resolution. The slit widths used and the spectral interval included are as already given.[9] Corrections were made for the temperature of setting and of observing, and for the error in setting at minimum deviation. The absorption cell length was 45 cm.

2. Preparation of the gases

H_2S was prepared by three different methods: (i) by warming calcium sulphide with a saturated solution of magnesium chloride; the gas was then bubbled through water and baryta solution and over P_2O_5: it was then liquefied by solid CO_2 and fractionated; (ii) by passing H_2S into a suspension of magnesium oxide in water, and gently warming the resulting $Mg(HS)_2$: the gas so obtained was washed and dried as before; (iii) as a check, a sample was prepared from aluminum sulphide: an apparatus was devised which could be swept out with dry, CO_2-free air and evacuated: water was dropped onto Al_2S_3 from within the apparatus and the resulting H_2S passed over baked calcium chloride and P_2O_5, and collected in a trap from which it could be fractionated; the sample so prepared was found to be free from CO_2. It was found that neither KHS nor baryta saturated with H_2S removed CO_2 completely.

D_2S was first obtained by method (iii) above, with 99.2 percent D_2O. Additional Al_2S_3 was introduced as a drying agent. Curve (a) (Fig. 2) shows that the sample contained HDS, probably derived from the calcium chloride and Al_2S_3. The former was therefore discarded, and the latter baked in vacuum before use, when curve (b) (Fig. 2) was obtained: it will be seen that although the amount of HDS was considerably reduced, complete elimination was not effected.

HDS was obtained by mixing equal volumes of H_2S and D_2S, and allowing the mixture to come to equilibrium.

[9] C. R. Bailey, A. B. D. Cassie and W. R. Angus, Proc. Roy. Soc. **A130**, 134 (1930).

EXPERIMENTAL RESULTS

A general comparison of the three spectra is given in Fig. 1, from which a rough measure of the relative intensities can be made. The adjusted percentage absorptions of Figs. 2–4 should not be used for that purpose.

H_2S

Band A: 8.089 μ; 1236 cm^{-1} (rocksalt); Fig. 2. There has been much discussion as to the existence of this band, but we have found it in all samples of H_2S, and all doubt is removed by the appearance of the corresponding isotopic bands. Although a good deal of the rotational structure is revealed, there is no evidence of separation into *P* and *R* branches, and the band is altogether different in appearance from the corresponding

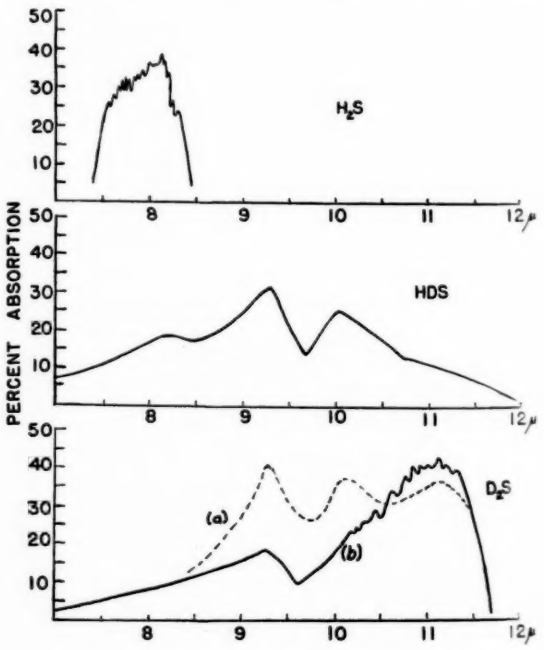

FIG. 2. ω_2 or band *A*.

fundamentals of D_2O and H_2O. It is just possible that the band may be overlaid by a difference tone. A number of the most prominent lines show a separation of the order of 7 cm^{-1}.

Band B: 4.127 μ; 2423 cm^{-1} (fluorite). This band of low intensity is probably real and different from that located at 4.25 μ by Coblentz,[1] Rollefson,[2] and Mischke,[4] which is most likely due to CO_2.

Bands C and D: 3.8 μ; (fluorite) Fig. 3. In this region there are peaks at 3.91 μ (2558 cm^{-1}), 3.70 μ (2703 cm^{-1}), and 3.435 μ (2911 cm^{-1}). The separation between 3.70 and 3.43 μ is 208 cm^{-1}, and is much too large to enable these peaks to be considered as a doublet: we therefore conclude that 3.70 μ consists of the unresolved Q and R branches of a band, C, whose P branch is at 3.91 μ. The line (−7) of Nielsen and Barker's Curve C[3] may perhaps be the weak Q branch.

Band E: 2.636 μ; 3794 cm^{-1} (quartz); Fig. 4. The contour shows the presence of P, Q, and R branches in agreement with the complete resolution obtained by Nielsen and Barker.[3]

Band F: 1.94 μ; 5155 cm^{-1} (quartz). The band was not resolved, but has been shown to be a doublet by Sprague and Nielsen,[6] whose value for the center is 5130 cm^{-1}.

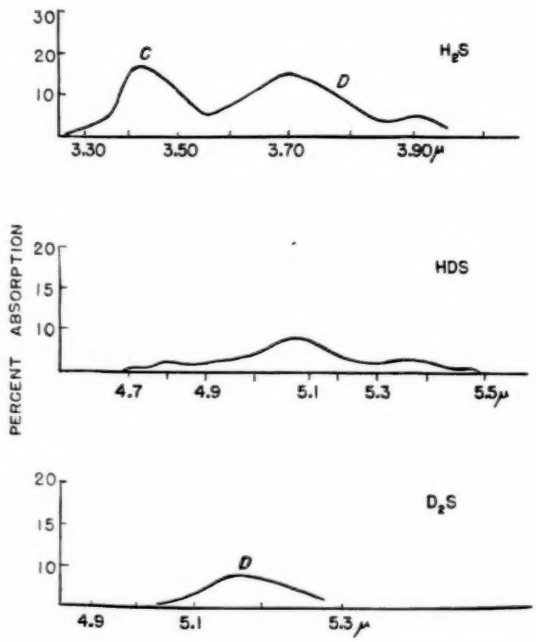

FIG. 3. Bands C and D.

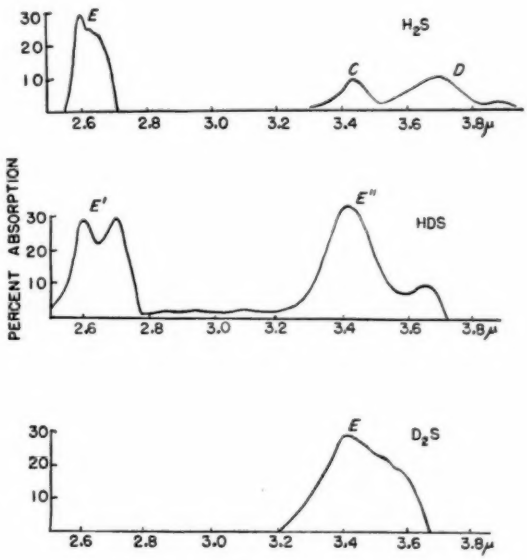

FIG. 4. Band E.

D_2S

Band A: 11.14 μ; 898 cm^{-1} (rocksalt); Fig. 2 (b). The band is similar in structure to Band A of H_2S; there is some faint evidence of rotational structure, but a spacing of 3.5 cm^{-1} corresponding to the 7 cm^{-1} is hardly within the limits of resolution of our spectrometer.

Band C: 5.155 μ; 1940 cm^{-1} (fluorite); Fig. 3. The band was extremely weak, but has the one-sided appearance often associated with the presence of a Q branch.

Band E: 3.57 μ; 2798 cm^{-1} (quartz); Fig. 4. The band resembles that of H_2S, but again no resolution was obtained.

HDS

Band A: 9.28 μ; 1078 cm^{-1} (rocksalt); Fig. 2. The shape of the band serves to emphasize the difficulties in the interpretation of the spectra. Two peaks are observed at 1078 and 988 cm^{-1}. The separation between them is some 90 cm^{-1}, a not unlikely value for a P–R spacing in HDS; but the total frequency range included in the band is some 340 cm^{-1} against 180 for H_2S and 135 for D_2S. We are faced with the absence or extreme weakness of a P branch in the latter substances, or alternatively the appearance of a new band in HDS. The determination below of the force constant k_3 makes it certain that the three peaks 1236, 898, and 1078 cm^{-1} correspond in the three

substances. Since HDS is asymmetric, ω_2 for this molecule should possess a small component of change of electric moment along the least axis of inertia, and the band should therefore show a weak Q branch, and it is tempting to find in the sharper character of the peak at 1078 cm^{-1} some faint evidence for its existence.

Band C at 5 μ: (fluorite); Fig. 3. There is a much extended region of weak absorption from 4.5 to 6.0 μ, with peaks in the neighborhood of 4.7 and 5.1 μ.

Band E′: 3.5 μ; (quartz); Fig. 4. The peak at 2721 cm^{-1} is probably due to H_2S, and that at 2938 cm^{-1} to D_2S and HDS (see assignments).

Band E″: 2.7 μ; (quartz); Fig. 4. The peaks at 3724 and 3849 cm^{-1} are probably both due to HDS and to H_2S.

Theoretical

A very striking and complete analysis of the band at 9911 cm^{-1} has been carried out by Cross[7] from measurements in the photographic infrared. The bond angle in the normal state was found to be 92° 20′, while for water vapor the corresponding value is 105° 6′.[10] It is difficult to predict qualitatively the effect upon the vertical angle of the exchange of sulphur for oxygen: the distance of the hydrogen atom from the central atom increases from 0.97 to 1.34A so that lessened interaction between the extreme hydrogen atoms would favor closer approach to the theoretical valence angle for p-s binding of 90°; on the other hand the electronic structure of the sulphur atom tends to make the angular rigidity less.

An investigation of a purely vibrational spectrum will not yield results of the same high order as those obtained by Cross, but for the purpose of comparison with heavier molecules whose rotational structure cannot as yet be unravelled, it is interesting to enquire what accuracy may be expected when the number of approximations is reduced as far as possible. We therefore propose to apply the potential energy expression used by Van Vleck and Cross in their consideration of the water vapor molecule.[11] For this purpose we require an estimate of the mechanical frequencies ν_i associated with infinitesimal amplitudes; and we now proceed to an attempted assignment of frequencies.

Assignments

We will adopt the conventional numbering of Dennison, in which ν_3 is the asymmetrical frequency, ν_1 the short wave and ν_2 the long wave symmetrical frequencies. The limiting angle above which the axis of least inertia is perpendicular to the symmetry axis is 88° 16′ for H_2S, and for D_2S is 86° 38′: hence we may expect ν_3 to have a more or less well developed Q branch. A, the smallest moment of inertia, is about $0.9B$, whereas for water, $A=0.5B$; and from Dennison's curves[12] we see that this Q branch will be much weaker in H_2S than in H_2O. This may account for our inability to resolve the band. For H_2S we therefore take 2632 cm^{-1} as ω_3. The peak at 2911 cm^{-1} gives a force constant of some 4.9×10^5 dynes per cm which seems to be too high to allow this band to count as an H_2S fundamental, although the possibility should not be overlooked. We have to confess that we can offer no reasonable assignment for it, and since it appears in all samples of the gas we do not think it can be ascribed to an impurity. ω_1 is found in the Raman spectrum of the gas at 2615 cm^{-1}.[13] ω_2 we must place at 8 μ, although the peculiar structure of the band again makes it difficult to determine the center exactly: a comparison of our own and Rollefson's curve[2] suggests 1236 cm^{-1} as the most reasonable value, and the data for the isotopic molecules are in agreement. 2432 cm^{-1} is then $2\omega_2$, and since 3794 cm^{-1} has a Q branch it must be $\omega_3+\omega_2$. As far as one can say from our own work and that of Sprague and Nielsen[6] the band at 1.9 μ has no Q branch and may be $2\omega_1$, rather than $\omega_1+\omega_3$. Weizel[14] has shown for H_2O that even overtones of ω_3 are not to be expected, and we may probably transfer his reasoning to this case. 9911 cm^{-1} $(\omega_3+3\omega_1)$ and 10,100 cm^{-1} $(3\omega_3+\omega_1)$ have already been assigned by Cross.[7]

D_2S. We assign 898 cm^{-1} to ω_2, 1940 cm^{-1}, to ω_3, and 2793 cm^{-1} to $\omega_3+\omega_2$. The only reference we have been able to find to the Raman spectrum occurs in an authors' abstract of a paper presented last year to the Vienna Academy;[15] as far

[10] R. Mecke, Zeits. f. Physik **81**, 313 (1933).
[11] J. H. Van Vleck and P. Cross, J. Chem. Phys. **1**, 357 (1933).
[12] D. M. Dennison, Rev. Mod. Phys. **3**, 280 (1931).
[13] S. Bhagavantam, Nature **126**, 502 (1930).
[14] W. Weizel, Zeits. f. Physik **88**, 214 (1934).
[15] A. Dadieu and H. Kopper, Nature **136**, 235 (1935).

TABLE I. *Proposed assignment of Raman and infrared bands of H_2S, HDS, and D_2S.*

	H_2S (cm^{-1})	HDS (cm^{-1})	D_2S (cm^{-1})
ω_2	1236	1078	898
ω_1	2615	(1910) calc.	1906
ω_3	2632	(2619) calc.	1940
$2\omega_2$	2423	2110	—
$\omega_3+\omega_2$	3794	3724	2798
$\omega_1+\omega_2$	—	2938	—
$2\omega_1$	5155	3849	—
$3\omega_1+\omega_3$	9911	—	—
$3\omega_3+\omega_1$	10100	—	—
?	2911	—	—
	—	988	—

as we can say, the paper has not yet been published. The mixture of H_2S and D_2S gives lines at 1880 and 2585 cm^{-1}. These are certainly the values for the liquid state, and we find for D_2O and H_2O that the percentage change in frequency in passing from the liquid to the gaseous state is the same for both molecules. Hence we may assume that the change in D_2S is of the same order as in H_2S, and take the calculated gaseous frequency 1906 cm^{-1} as ω_1.

HDS. The peculiar double nature of ω_2 has already been described, and the additional possibilities discussed should be borne in mind. For the purposes of approximate calculation of ω_3 and ω_1, we may use the valence force expression derived by Lechner[16] for the asymmetrical triatomic molecule. The somewhat complicated expression is a cubic for the frequencies, and on inserting the values $K_{H_2S}=3.92$, $K_{D_2S}=4.09$, and $d(=2k_3$ as determined below$)=0.47\times10^5$ dynes/cm, together with the observed frequency $\omega_2=1078$ cm^{-1}, we find $\omega_3\doteq2619$ and $\omega_1=1910$ cm^{-1} in agreement with the values calculated for the gas from Dadieu and Kopper's results. We may thus assume that the weak, extended region of absorption at 5 μ contains ω_1 of HDS together with ω_3 of D_2S. 3.5 μ (band D') contains ω_3 of H_2S, ω_3 of HDS, and $\omega_1+\omega_2$ of HDS at 2938 cm^{-1}. Band D'' at 2.64 μ contains $2\omega_1$ and $\omega_3+\omega_2$ of HDS, with $\omega_3+\omega_2$ of H_2S. There are indications of $2\omega_2$ for HDS at 4.8 μ.

The above conclusions are summarized in Table I.

[16] F. Lechner, Wien. Ber. **141**, 291 (1932).

DETERMINATION OF THE FORCE CONSTANTS

The significance of the force constants will be seen from the potential energy expression used by Van Vleck and Cross:[11]

$$V=\tfrac{1}{2}[k_1(\Delta r_1)^2+k_2(\Delta r_2)^2+2k_3r_1^{0^2}(\Delta\gamma)^2]+k_{12}\Delta r_1\Delta r_2+2^{\frac{1}{2}}k_{13}r_1^0(\Delta r_1\Delta\gamma+\Delta r_2\Delta\gamma). \quad (1)$$

On the assumption $r_1^0=r_2^0$, and $k_1=k_2$, the solution of the secular equation yields

$$\begin{aligned}&(a_{11}-a_{12})\lambda_3{}^2-k_1+k_{12}=0,\\ &[(a_{11}+a_{12})\lambda_{1,\,2}{}^2-k_1-k_{12}][a_{33}\lambda_{1,\,2}{}^2-k_3]\\ &\qquad-2[a_{13}\lambda^2-k_{13}]^2=0.\end{aligned} \quad (2)$$

The coefficients a_{ij} are not given explicitly in the original. They have therefore been deduced and recorded for various values of the vertical angle, γ (Table II). If m and M are the relative atomic masses of H and S, respectively,

$$\mu=m(m+M)/(2m+M), \quad \mu_3=m^2/(2m+M).$$

Since the coefficients are all of dimensions $[M]^1$, we may write $\lambda^2=4\pi^2c^2\nu^2=5.863\times10^{-2}\nu^2$, and thus obtain the k's in dynes per cm.

The frequency equations apply to the corrected frequencies, ν_i, and not to the observed frequencies, ω_i. We have therefore adopted an expression of the type

$$\begin{aligned}E_{000}=&X_1V_1+X_2V_2+X_3V_3\\ &+X_{11}V_1{}^2+X_{22}V_2{}^2+X_{33}V_3{}^2\\ &+X_{12}V_1V_2+X_{23}V_2V_3+X_{31}V_3V_1,\end{aligned} \quad (3)$$

where $V_i=(n_i+\frac{1}{2})$, and have attempted a solution from the observed data. We have, for example, $\omega_{100}=E_{100}-E_{000}$ when E is expressed in cm^{-1}, and the values of X_i give the required frequencies ν_i: unfortunately only eight bands can be located and assigned with reasonable certainty for H_2S, and it has been necessary to calculate X_{12} from the D_2S spectrum on the assumption that the anharmonic constants in the

TABLE II.

a_{ij}	H_2S			D_2S		
	92°20′	105°	110°	92°20′	105°	110°
$a_{11}=a_{22}=\mu-\mu_3^2\sin^2\gamma/2(\mu-\mu_3\cos\gamma)$	0.971	0.971	0.971	1.886	1.886	1.884
$a_{12}\quad=-\mu_3\cos\gamma$						
$\quad+(\mu_3^2\sin^2\gamma)/2(\mu-\mu_3\cos\gamma)$	.001	.008	.010	0.008	0.032	0.043
$a_{13}=a_{23}=(1/2\sqrt{2})\mu_2\sin\gamma$	.010	.010	.010	.039	.038	.037
$a_{33}\quad=\frac{1}{2}(\mu+\mu_3\cos\gamma)$	.242	.240	.240	.473	.465	.462

two molecules show the same ratio (determinable from the reduced masses) as is found for the fundamentals,[17] e.g., $(\omega_2/\omega_2^*)^2=1.87$. The results for H_2S are $X_1=2719$, $X_2=1294$, $X_3=2749$, $X_{11}=-37$, $X_{22}=-24$, $X_{33}=-11$, $X_{12}=+57$, $X_{23}=-74$, $X_{31}=-114$, and for D_2S, $X_1=1961$, $X_2=929$, $X_3=2003$, $X_{11}=-20$, $X_{22}=-13$, $X_{33}=-6$, $X_{12}=30$, $X_{23}=-40$, $X_{31}=-62$, all in cm^{-1}. The high positive value for X_{12} is in accordance with the other observed data: furthermore we can now apply Teller's relationship[17] between the symmetrical frequency ν_1 for the two molecules H_2S and D_2S and thus make an estimate of the vertical angle, γ. We have $(\nu_1/\nu_1^*)^2=D(S+2H\sin^2\gamma/2)/H(S+2D\sin^2\gamma/2)$ where H, D, and S are the atomic masses of the respective atoms, and hence from $(2719/1969)^2$ we have $\gamma=110°$. This value is considerably greater than that of 92° 20′ deduced by Cross[7] from the rotational structure of the band at 9911 cm^{-1}, but as will be seen below, it furnishes better agreement among the force constants in the vibrational spectrum, and on the whole one would expect the vertical angle for H_2S to be certainly not less than that of the water molecule, which is 105°.

That the mechanical frequencies so deduced cannot be far from true may be seen by solving a simplified valence force system for the two molecules.[18] Without a knowledge of the force constants we can construct a cubic in the frequencies for the vertical angle:

$$\frac{p_1^2p_2^2}{p_3^2}\cdot\frac{x^3}{1+(2m/M)}-(p_1^2+p_2^2+p_3^2)x+2p_3^2\left(1+\frac{m}{M}\right)=0; \quad (4)$$

where $x=1+(2m/M)\sin^2\alpha$, α being the semi-vertical angle, and $p_i=2\pi\nu_i c$. On insertion of the frequencies deduced for infinitesimal amplitude, we find for H_2S that 2α is 111° 26′, and for D_2S that 2α is 111° 30′. The uncorrected frequencies give no such measure of agreement, the value for H_2S being 102° and for D_2S, 119°.

We may note in passing that the expression deduced by Rosenthal[19] for the vibrational effect in ω_3, the asymmetric vibration, is incorrect. As given it is

$$\omega_3^*/\omega_3=[1-2k\mu(\sin^2\alpha+\mu\cos^2\alpha)^{-1}], \quad (5)$$

where $k=\frac{1}{2}\Delta m(m+\Delta m)^{-1}$; $\mu=M/(2m+M)$; and 2α is the vertical angle. If the term on the left is squared, one obtains results of the right order. Miss Rosenthal's formula for the ratio of the two symmetric frequencies is useful: we have

$$(\omega_1^*/\omega_1)(\omega_2^*/\omega_2)=(1-2k\mu)^{\frac{1}{2}}(1-2k)^{\frac{1}{2}}. \quad (6)$$

Inserting $\nu_1=2719$, $\nu_2=1294$, and $\nu_1^*=1961$, we have $\nu_2^*=925$ compared with $\nu_2^*=929$ cm^{-1} observed, and so obtain a good check on our assignments and observations.

TABLE III. *The force constants for H_2S and D_2S (in dynes/cm$\times 10^{-5}$).*

		k_1-k_{12}	k_1+k_{12}	k_3	k_{13}
92° 20′	H_2S	4.29	4.21	0.238	0.04
	D_2S	4.40	4.27	0.239	0.04
110°	H_2S	4.26	4.25	0.236	0.04
	D_2S	4.33	4.34	0.234	0.04

THE FORCE CONSTANTS

We have solved the frequency Eq. (2) using the calculated values of γ for H_2S and D_2S. On comparison with H_2O it now seems fairly certain that the potential energy curves of a polyatomic molecule do not correspond sufficiently closely with those of the isotopic molecule to enable them to be used to give highly accurate values of the vertical angle, and in fact no reasonable solution for this angle can be obtained on the assumption that the force constants are the same for the two molecules. We have therefore examined the Van Vleck and Cross relationship for certain values of the angle, and summarize those for 92° 20′ and 110° in Table III.

Although the absolute value for k_1 must not be taken too literally, nevertheless it is significant that the larger value for γ tends to remove the discrepancies between H_2S and D_2S, and between k_1-k_{12} and k_1+k_{12}. For HDS, with $a_{33}=0.632$ for 110°, the uncorrected frequency 1078 cm^{-1} gives k_3 as approximately 0.216×10^5 dynes per per cm as compared with 0.219 for H_2S and 0.218 for D_2S. It is interesting to record approximate

[17] E. Teller, Det kgl. Danske Videnskaternes Selskab (1934).
[18] C. R. Bailey and A. B. D. Cassie, Proc. Roy. Soc. **A137**, 622 (1932).
[19] J. E. Rosenthal, Phys. Rev. **45**, 426 (1934).

values for k_1 in the series H_2O, H_2S, and H_2Se: with uncorrected data these are 7.8, 4.0, and 3.2×10^5 dynes/cm.

For the sake of completeness we will remark that Végard[20] from an x-ray analysis gave a rectilinear structure for H_2S, at least in the solid. It is noteworthy that the observed frequencies give reasonable force constants if introduced into equations for a rectilinear model: the peculiar shape of the long wave fundamental would then have to be explained by invoking the presence of an unresolved Q branch; while all observed bands other than ω_2 and ω_3 must be interpreted as combination tones involving an inactive frequency. The only band in H_2S which cannot be so assigned is $2\omega_2$ at 2423 cm^{-1}, but the last point, together with the irregular nature of the rotational lines in the band at 2.6 μ resolved by Nielsen and Barker,[3] is sufficient to exclude the rectilinear structure.

While this paper was in preparation, Nielsen and Nielsen[21] published a brief note as a preliminary account of similar work. They confirm the existence of the long wave band at 8.0 μ for H_2S, and the corresponding bands for D_2S and HDS. They do not appear to have located the fundamental ω_2 for D_2S; in its place they give a band at 4.55 μ and relate it to ω_3 of H_2S. This wave-length corresponds to a force constant of some 5.2×10^5 dynes/cm, and hence the frequency is much too high. The strong peak in HDS at 988 cm^{-1} also seems to have escaped observation. The following comparative table is given by Nielsen and Nielsen:

H_2S	HDS	D_2S
1.9 μ	2.1 μ	—
2.65	3.15	3.65μ
3.70	4.1	4.55
7.9	9.0	10.8

We wish to express our acknowledgments to Professor F. G. Donnan, F.R.S., for his continued interest in our work.

[20] L. Végard, Nature **126**, 916 (1930).

[21] A. H. Nielsen and H. H. Nielsen, J. Chem. Phys. **4**, 229 (1936).

OCTOBER, 1936 JOURNAL OF CHEMICAL PHYSICS VOLUME 4

The Rate of Thermal Decomposition of Deuterium Iodide

JOHN C. L. BLAGG AND G. M. MURPHY,* *Chemical Laboratory of Columbia University*

(Received August 7, 1936)

The partition functions for deuterium iodide have been calculated at temperatures from 300 to 1500°K. Constants were calculated for an equation to give the value of the free energy function at any temperature within this range. A similar calculation was made for D_2 using the data of Johnston and Long. Combining these with the data for the other molecules involved, the equilibrium constant for the decomposition of deuterium iodide and for the exchange reaction was calculated. These results can be differentiated and integrated to give values for ΔH^0, ΔC_p and ΔS^0. The equilibrium constant for the reaction $H_2+2DI\rightleftarrows D_2+2HI$ has been plotted against the temperature from 300 to 1500°K. The equilibrium constant for the reaction $DI\rightleftarrows\frac{1}{2}D_2+\frac{1}{2}I_2$ has been calculated. The rate of thermal decomposition of deuterium iodide was measured between 660 and 719°K. The experimental ratio of the rate constants for the reactions $HI\rightarrow\frac{1}{2}H_2+\frac{1}{2}I_2$ and $DI\rightarrow\frac{1}{2}D_2+\frac{1}{2}I_2$ has been compared with the theoretical value of Wheeler, Topley and Eyring. Contrary to their expectations, it was found to be lower than the theoretical value.

THE effect on the rate of several chemical reactions produced by substituting deuterium for hydrogen has been studied by various investigators.[1] Because of the simple homogeneous and bimolecular character of the thermal decomposition of hydrogen iodide, the corresponding reaction with deuterium appears to be one of the most important reactions to study at the present time, since theoretical calculations can be made for this case with some certainty. We have therefore studied the rate of thermal decomposition of deuterium iodide between 660 and 719°K.

Since the reverse reaction also occurs, the rate of decomposition of hydrogen iodide depends

* Present address, Sterling Chemistry Laboratory, Yale University, New Haven, Conn.

[1] For a review of the subject, see Urey and Teal, Rev. Mod. Phys. **7**, 34 (1935).

TABLE I.

	DI
B_e	3.301
α	6.180×10^{-2}
D_e	-5.347×10^{-5}
ω_e	1640.307
$x_e\omega_e$	20.043

TABLE II.

T	Q	$-(F^0-E_0^0)/T$
300	64.550	43.828
500	108.585	47.399
800	182.750	50.768
1000	240.238	52.420
1500	404.875	55.471

upon the equilibrium constant. The latter has been determined experimentally by Bodenstein[2] who has also made an extensive study of the rates of formation and decomposition. Additional experiments have been made by Kistiakowsky[3] and others and a critical review of both the experimental and theoretical aspects of the reaction has been given by Kassel.[4] The equilibrium constant for deuterium iodide has not yet been measured but Rittenberg and Urey[5] have investigated the reaction

$$H_2+2DI\rightarrow D_2+2HI \qquad (1)$$

and have shown that the experimentally determined equilibrium constants are in agreement with those calculated from spectroscopic data. Since the energy levels and their statistical weights are well known for hydrogen, iodine and hydrogen iodide and since the corresponding data for the isotopic deuterium compound are readily obtainable,[6] we may proceed with confidence and use the equilibrium constant for deuterium iodide as calculated from the statistical theory. This calculation has been made recently for hydrogen iodide by Murphy[7] who has shown that the experimental results are in reasonable agreement with the theory. It appears, however, that the temperatures at which Bodenstein has worked may be in error and an attempt has been made to correct them. The other difficulty lies in the uncertainty in the heat of dissociation of hydrogen iodide which cannot be determined from spectroscopic data. We have therefore used Bodenstein's data to determine this quantity.[8] The calculated values of log K are plotted against the reciprocal of the absolute temperature in Fig. 1 together with the experimental points of Bodenstein and of Rittenberg and Urey. A more certain value of the heat of dissociation of hydrogen iodide would only result in a parallel shift of the whole curve in either direction, but it seems impossible to adjust the statistical theory in any way so as to obtain agreement with experiment at the highest and lowest temperatures studied by Bodenstein.

The method of calculating the equilibrium constants for deuterium iodide is similar to that for hydrogen iodide, the partition functions,

$$Q=\sum_{v,\ J} p_J \exp\left[-E(v,\ J)/kT\right], \qquad (2)$$

being summed by the method of Kassel.[9] The summation is taken over vibrational and rotational quantum numbers, v and J, $p_J=(2J+1)$ is the quantum weight of the Jth rotational level and E is the vibrational and rotational energy of the molecule as given by analysis of the molecular spectra. The molecular constants were obtained from those of hydrogen iodide and are given in Table I. Following Giauque and his co-workers, the natural constants found in the International Critical Tables[10] were used. The summation was made at 300, 500, 800, 1000 and 1500°K and the values for the partition function, Q, are given in Table II. The free energy may then be obtained by the relation

$$-(F^0-E_0^0)/T=(3/2)R\ln M+(5/2)R\ln T+R\ln Q-7.267 \qquad (3)$$

[2] Bodenstein, Zeits. f. physik. Chemie **13**, 56 (1894); **22**, 1 (1897); **29**, 295 (1899).

[3] Kistiakowsky, J. Am. Chem. Soc. **50**, 2315 (1928).

[4] Kassel, *Kinetics of Homogeneous Gas Reactions* (The Chemical Catalog Co., New York, 1932), p. 148.

[5] Rittenberg and Urey, J. Am. Chem. Soc. **56**, 1885 (1934).

[6] Jevons, *Report on Band-Spectra of Diatomic Molecules* (The University Press, Cambridge, 1932).

[7] Murphy, J. Chem. Phys. **4**, 344 (1936).

[8] Bodenstein has also neglected to correct for the decomposition of iodine molecules into atoms. This has been done in the points as plotted in Fig. 1, although it is nearly negligible at his temperatures. The decomposition of H_2 and D_2 into atoms is also negligible at these temperatures. We have therefore neglected these slight corrections in our rate constant.

[9] Kassel, J. Chem. Phys. **1**, 576 (1933); Phys. Rev. **43**, 364 (1933).

[10] Int. Crit. Tab., Vol. I, p. 16. The numerical constant of the free energy equation was taken as 7.267; $R=1.9869$; $hc/k=1.4324$.

where M is the molecular weight, E_0^0 is the energy at the absolute zero and the other quantities have their usual thermodynamic meaning. Since the normal state of deuterium iodide is $^1\Sigma$ the electronic statistical weight is unity. There are no other electronic states to be considered. The nuclear spin contributions have been omitted which is valid for temperatures above 25°C as shown by Gibson and Heitler.[11] With the use of Eq. (3) and the values of the Q's as shown in Table II, we have obtained values for the free energy function as given in the same table. The atomic weights for deuterium and iodine were taken as 2.01363[1] and 126.932,[12] respectively. For convenience in interpolation, the values obtained from Eq. (3) have been fitted to a formula of the type

$$-(F^0-E_0^0)/T=a/T+b\log T+cT+dT^2+i. \quad (4)$$

The coefficients in this equation for deuterium iodide together with those obtained for D_2 from the calculations of Johnston and Long[13] are shown in Table III. An equation of the form of (4) will reproduce the value of the free energy function to within at least 0.001 cal./mole between the temperatures of 298.1 and 1500°K as shown by comparison with the results obtained by summation at other temperatures within this range. It should probably not be extrapolated beyond these limits. The coefficients in Eq. (4) may now be combined with the corresponding constants for I_2 as calculated by Murphy,[7] to give

$$-R\ln K=\Delta F^0/T=\Delta H_0/T-\Delta\Gamma_0\ln T-\tfrac{1}{2}\Delta\Gamma_1 T-\tfrac{1}{6}\Delta\Gamma_2 T^2+I, \quad (5)$$

providing the value for ΔE_0^0 is known. This may be obtained from the value 971.83 14 cal./mole

TABLE III.

	DI	D_2
a	−365.512	−6.92285
b	11.1051	15.7301
c	3.642×10^{-3}	2.85×10^{-5}
d	-6.78×10^{-7}	1.09×10^{-7}
i	16.5063	−11.1506

[11] Gibson and Heitler, Zeits. f. Physik **49**, 465 (1928).
[12] Int. Crit. Tab., Vol. I, p. 44.
[13] Johnston and Long, J. Chem. Phys. **2**, 389 (1934).

TABLE IV.

	$DI\rightarrow\frac{1}{2}D_2+\frac{1}{2}I_2$
ΔH_0	562.08
$\Delta\Gamma_0$	2.8930
$\Delta\Gamma_1$	-6.8113×10^{-3}
$\Delta\Gamma_2$	4.1889×10^{-6}
I	19.8513

for the hydrogen iodide reaction and the zero-point energies of the various molecules involved, by using the equation

$$^2\Delta E_0^0={}^1\Delta E_0^0+(\tfrac{1}{2}E_{0D_2}{}^0-E_{0DI}{}^0-\tfrac{1}{2}E_{0H_2}{}^0+E_{0HI}{}^0), \quad (6)$$

where the superscripts one and two refer to reactions (7) and (8) respectively.

$$HI\rightarrow\tfrac{1}{2}H_2+\tfrac{1}{2}I_2, \quad (7)$$

$$DI\tfrac{1}{2}\rightarrow D_2+\tfrac{1}{2}I_2 \quad (8)$$

and $$E_0^0=(\tfrac{1}{2}\omega_e-\tfrac{1}{4}x_e\omega_e)\cdot hcN. \quad (9)$$

We have used constants as given by Urey and Teal[1] from the spectroscopic data of Jeppeson[14] for H_2 and D_2, obtaining for the zero-point energies of H_2, D_2, hydrogen iodide and deuterium iodide the values 2175.02 1545.62, 1144.84 and 815.142 cm^{-1}, respectively.[15] The value of $^2\Delta E_0^0$ obtained from Eq. (6) is 1014.52 cal./mole. The principal uncertainty in this quantity is that due to $^1\Delta E_0^0$ and therefore $^2\Delta E_0^0$ is probably good to about 14 calories. The constants for Eq. (5) are given in Table IV.

The equilibrium constant for reaction (8) is now obtained from Eq. (5), the constants of

[14] Jeppeson, Phys. Rev. **44**, 165 (1933).
[15] The vibrational constants used by Giauque (J. Am. Chem. Soc. **52**, 4816 (1930)) and by Johnston and Long, reference 13, which we have used in calculating the partition functions for H_2 and D_2 give somewhat different zero-point energies for these two molecules than the ones we give above. The use of their zero-point energies changes $^2\Delta E_0^0$ by about 50 cal. but this affects the final constants by a negligible amount as we have discovered by calculation. It seems better to use the more recent vibrational constant for H_2 and D_2 as determined by Jeppeson. A similar conclusion was reached by Davis and Johnston (J. Am. Chem. Soc. **56**, 1045 (1934)) who report that the use of Jeppeson's data in place of that used by Giauque changes the entropy by only 0.001 cal./mole/degree. Teal and MacWood (J. Chem. Phys. **3**, 760 (1935)) have given vibrational constants for H_2 and D_2, obtained from Raman Spectra, which differ slightly from those of Jeppeson and which are probably better due to the method in which they were obtained. However, the use of these constants instead of those of Jeppeson would change ΔE_0^0 for reaction (8) by only 0.98 cal./mole which is much less than the other uncertainties involved. We have taken 1 $cm^{-1}=2.8461$ cal./mole.

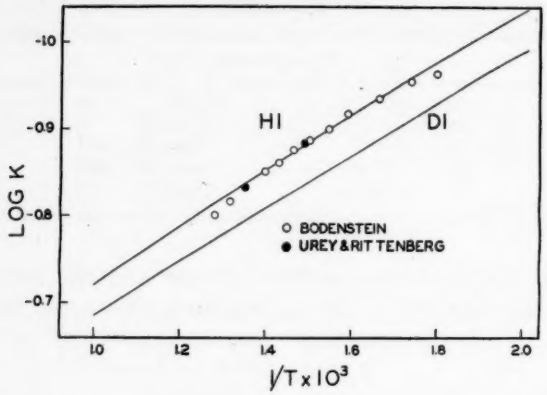

FIG. 1.

Table IV and this value of $^2\Delta E_0^0$, and the results are shown in Fig. 1. Since the principal uncertainty in the whole procedure is that in $^1\Delta E_0^0$, a better value of this would only shift both curves parallel to themselves in either direction by an equal amount. There are at present no experimental data to check the deuterium iodide curve.

The well-known methods of thermodynamics[16] may also be used to give reliable values of ΔS^0, ΔC_p, and ΔH^0 from Eq. (4). Although the results obtained are not as exact as those for the free energy, the precision is sufficient for most applications and the tedious task of summing the partition functions a second time is unnecessary. We obtain in this way, from the constants of Table IV

$$\Delta H^0_{298.1} = 1159 \pm 15 \text{ cal./mole}$$

and

$$\Delta S^0_{298.1} = -1.303 \text{ cal./mole.}$$

Using the value $S_{298.1}(I_2) = 62.29$ as calculated by Giauque[17] and $S_{298.1}(D_2) = 34.36$ as given by Johnston and Long,[13] we find $S_{298.1}(DI) = 49.62$ cal./mole. The values of ΔH^0 and ΔS^0 at this temperature are higher than the corresponding quantities for hydrogen iodide by 46 and 0.1 cal./mole, respectively.

TABLE IVa.

$H_2+2DI \rightarrow D_2+2HI$	
ΔH_0	−306.80
$\Delta\Gamma_0$	2.6378
$\Delta\Gamma_1$	-1.03694×10^{-2}
$\Delta\Gamma_2$	7.7832×10^{-6}
I	14.3158

[16] Lewis and Randall, Thermodynamics (McGraw-Hill Book Co., New York, 1923), Chapter XV, p. 173.
[17] Giauque, J. Am. Chem. Soc. **53**, 507 (1931).

The equilibrium constant for reaction (1) may also be calculated from the constants of Table IV and smilar constants for reaction (7) as obtained by Murphy.[7] The resulting coefficients in Eq. (5) are found in Table IVa and a plot of K against temperature is shown in Fig. 2. The partition functions of the four molecules involved vary in a very complicated way with the temperature and so it is difficult to make any exact statements as to the way in which the various factors involved contribute to the free energy change of the reaction. There is no reason, however, to doubt the statistical calculations and, if the equilibrium should be measured for this exchange reaction over a wide temperature range, this curious variation with temperature will probably be found.

RATE OF DECOMPOSITION OF DEUTERIUM IODIDE

The rate constant for the decomposition of deuterium iodide is given by the expression

$$k_2 = (K_2/(0.4343 \cdot a \cdot t)) \log ((\alpha+z)/(\alpha-z)), \quad (10)$$

where K_2 is the equilibrium constant for reaction (8), a is the initial concentration of deuterium iodide in moles per cc, t is the time expressed in seconds, $\alpha = 2K_2(1-z)$ and z is the fraction of deuterium iodide decomposed at time t. This is essentially the equation used by Bodenstein, although expressed in different units and rearranged to facilitate computation. As may be seen from Eq. (10) and as pointed out by Kistiakowsky,[3] the errors involved in determining k_2 are smallest when the time of heating is so

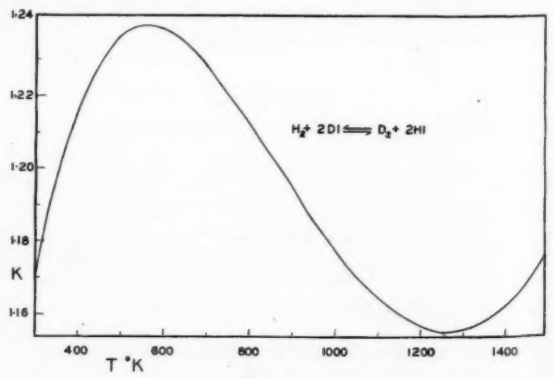

FIG. 2.

chosen that a small but uniform decomposition occurs as far as possible from the equilibrium concentration. Our experiments have been carried out, for the most part, at the same time for each temperature. This is valid for the deuterium iodide decomposition since the reaction is known to be homogeneous and bimolecular from Bodenstein's work on hydrogen iodide.

Experimental Materials

Deuterium was prepared by decomposing 99.9 percent deuterium oxide in an electrolytic cell so designed as to separate the oxygen and deuterium as they were generated. The iodine was resublimed before using. Deuterium iodide was prepared by passing a mixture of deuterium and iodine gases over two platinum spirals, burning at red heat, in the manner described by Cook and Bates.[18] An excess of iodine was used to insure almost complete combination of the deuterium. The deuterium iodide was purified by distillation from a trap surrounded by a dry ice-alcohol mixture to a trap immersed in liquid air. Three or four distillations were made to insure the purity of the deuterium iodide as shown by the colorless product which was obtained. The deuterium iodide was kept frozen by liquid air until the cells were ready to be filled. Hydrogen iodide was prepared in a similar manner using tank hydrogen, which had been passed over a roll of red hot copper screen, and was used to check our experimental procedure as described below. All chemicals used in the analysis were of high grade analytical purity.

Furnace and Reaction Vessels

The furnace was a sulfur boiler in which the temperature was controlled by keeping the pressure over the sulfur constant. The device for controlling the pressure was developed in this laboratory and is described by Rittenberg and Urey[5] and independently by C. C. Coffin.[19]

The temperature was measured with a thermocouple made from No. 28 Chromel-*P* and No. 28 Alumel wire and the voltage read with a Leeds and Northrup type K potentiometer. The standard cell used with the potentiometer was a new Eppley cell which had a negligible temperature coefficient. The thermocouple was calibrated against the ice point and boiling point of water, the boiling point of naphthalene and the boiling point of sulfur. These are all approved standards of pyrometry.[20] The boiling points were corrected to atmospheric pressure by the equations given in the *International Critical Tables*.[20] A least square equation was calculated for the temperature. The temperature remained constant to better than $\frac{1}{2}°$ since it was impossible to notice fluctuations with the potentiometer.

Quartz reaction cells were used. They were approximately six inches long with an outside diameter of about one inch. The volumes were between 50 and 60 cc. The volume of each cell was determined by one of two methods. One, by weighing empty and then filled with water, and two, by filling with water from a burette. The two methods checked to within 0.05 cc. The volume was needed in order to determine a.

Table V.

Run	Temp. (°K)	Time (sec.)	Mol./cc $\times 10^5$	z (%)	k_2 $\times 10$	k_2 ave. $\times 10$	K $\times 10$
25	660	18,003	1.963	3.90	1.16		
26		15,421	1.970	3.68	1.26		
27		18,063	1.963	3.92	1.16	1.19	1.430
22	671	14,457	1.949	5.29	2.01		
23		12,354	1.967	4.73	2.06		
24		14,344	1.935	4.93	1.88	1.98	1.455
11	686	10,805	1.933	7.19	3.80		
12		10,857	1.664	6.66	4.03		
13		10,800	1.678	6.57	3.96		
14		10,810	1.683	6.50	3.89	3.92	1.487
15	708	3,599	1.948	7.30	11.49		
16		3,600	1.959	6.92	10.75		
17		18,003	1.963	20.83	11.12	11.12	1.537
18	719	3,623	1.924	11.03	18.82		
19		3,602	1.925	10.54	17.88		
20		3,734	1.693	10.02	18.43		
21		3,603	1.709	9.74	18.23	18.34	1.560
1*	681	3,630	2.144	3.94	5.31		
2		3,599	2.159	3.86	5.21		
3		7,219	1.819	5.92	4.88		
4		7,207	1.832	6.23	5.10		
5		7,203	2.064	5.70	4.14		
6		7,196	2.057	6.36	4.69		
7		7,204	2.011	5.80	4.33		
8		7,208	2.024	6.68	5.03	4.84	1.332

* Runs 1 to 8 inclusive were made with hydrogen iodide. All other runs were made with deuterium iodide.

[18] Cook and Bates, J. Am. Chem. Soc. **57**, 1775 (1935).
[19] C. C. Coffin, J. Am. Chem. Soc. **55**, 3636 (1933).
[20] Int. Crit. Tab., Vol. I, p. 53.

Experimental Procedure

The cells were pumped for from twelve to twenty-four hours and heated to a dull red heat four or five times during the pumping. When the cells were ready to be filled, the liquid air was removed from the storage trap containing the deuterium iodide and a bath of alcohol dry ice was substituted. The amount of dry ice used was such that the temperature of the bath was between -50 and -45°C as measured by a pentane thermometer. This gave a pressure of deuterium iodide desirable for our experiments and was reproducible as can be seen from column four in Table V. The pressure of deuterium iodide was allowed to build up for about ten minutes and then a stopcock between the storage trap and the cells was opened. The gas flowed into the cells through capillary stopcocks which were closed after about fifteen minutes from the time the liquid air was removed from the storage trap. The gas in the cells was then frozen with liquid air and the cells sealed off from the vacuum system. Contact with the stopcock grease caused a slight amount of decomposition, but since the cells were filled through capillary tubes the diffusion of the decomposition products was slow and no color was shown by the deuterium iodide in the cells. Bates and Lavin[21] have shown that stopcocks lubricated with vaseline may be used with hydrogen iodide. In these experiments Lubriseal was used throughout. The cells for runs with hydrogen iodide were filled in a similar manner and, since a good check with Bodenstein's results was obtained, any error introduced by the use of greased stopcocks is negligible. Before each set of runs the deuterium iodide was redistilled.

After a measured length of time in which the cells were kept in the constant temperature furnace, the reaction was stopped by placing the cells in a blast of cold air and then freezing the deuterium iodide and iodine with liquid air. The total time elapsed between removal from the furnace and complete freezing never exceeded two minutes. Any error thus introduced was balanced out by the time necessary to bring the cell up to temperature when placed in the furnace. The reaction was timed by an electric clock and was measured to the nearest second from the time the cell was placed in the furnace until it was removed and placed in the blast of air. The cells were then opened, sealed to the vacuum system and the gases collected in a trap filled with a four percent solution of potassium iodide which was free from dissolved carbon dioxide and which had been tested for neutrality and for the presence of iodate.[22]

Method of Analysis

The trap containing the iodine and deuterium iodide dissolved in potassium iodide was emptied into a flask and thoroughly washed. A standard solution of sodium thiosulfate, free from dissolved carbon dioxide, was used to titrate the iodine. The thiosulfate solution was standardized each day by means of a standard ceric sulfate solution.[23] This latter solution had been standardized against Bureau of Standards sodium oxalate, using orthophenanthroline ferrous complex, as the indicator since a back titration with ferrous sulfate was necessary. For iodine-thiosulfate titrations a one percent freshly prepared potato starch solution was used. Weight burettes were used for all titrations and all titrations were made in a reproducible light.

The iodate method for acid determination was used in analyzing for deuterium iodide.[24] After analysis for iodine had been made, two grams of potassium iodate were added and the solution allowed to stand for twenty minutes and then titrated with thiosulfate. The titration was completed within twenty-five minutes after the addition of the iodate. A blank was run over the same period of time by adding the same amount of iodate to twenty-five cc of the same potassium iodide solution in which the deuterium iodide and iodine were dissolved. Since the volume of each cell was known, the number of moles of deuterium iodide at the start could be calculated. The fraction decomposed was determined by dividing the number of grams of thiosulfate solution used to titrate the iodine by the total number of grams used in both titrations.

The validity of our experimental method was tested by means of eight experiments on the rate

[21] Bates and Lavin, J. Am. Chem. Soc. **55**, 81 (1933).

[22] Fales, *Inorganic Quantitative Analysis* (The Century Co., New York, 1925), p. 353.

[23] Suggested by Dr. G. W. Walden of this laboratory.

[24] Kolthoff and Furman, *Volumetric Analysis*, Vol. II, p. 389.

of decomposition of hydrogen iodide and the results obtained were in good agreement with those of Bodenstein. The data obtained for both hydrogen iodide and deuterium iodide will be found in Table V. The equilibrium constant, K, was calculated for deuterium iodide from Eq. (5) and for hydrogen iodide from a similar equation given by Murphy.[7] The values obtained are given in the last column of Table V. Our constants refer to reactions (7) and (8) and the subscripts one and two refer to the hydrogen iodide and deuterium iodide reactions, respectively. All of our experimental rate constants will be found plotted in Fig. 3, together with those of Bodenstein and Kistiakowsky on hydrogen iodide.

We have considered all the factors involved in calculating our rate constants and each constant is good to the average deviation from the mean which ranges from two to four percent. This precision is as good as that obtained by Bodenstein and Kistiakowsky on the hydrogen iodide reaction. Any error due to K is due to the uncertainty in the zero-point energy and is well within the precision which we have claimed.

Discussion of Results

It is now well known that the simple Arrhenius equation is not valid for reaction rate constants over a very wide temperature range. Moreover, there are objections to the simple collisional formulas as used in the past. We have, however, used the latter theory to derive an equation for our results of the form

$$\log k_2 = -9333/T + 0.5 \log T + 11.799 \quad (11)$$

which may be compared with the similar equation given by Kassel[4] for hydrogen iodide

$$\log k_1 = -9555/T + 0.5 \log T + 12.311. \quad (12)$$

Eq. (11) will reproduce $\log k_2$ to ± 0.01 and should be regarded merely as an interpolation formula, rather than ascribing any reality to the heat of activation, number of collisions, temperature dependence or cross-sectional molecular areas. On the basis of this theory, if we assume that the collision cross sections of HI and DI are equal and that there is no zero-point energy in the activated complex, the ratio of the rate constants for the two reactions is given by

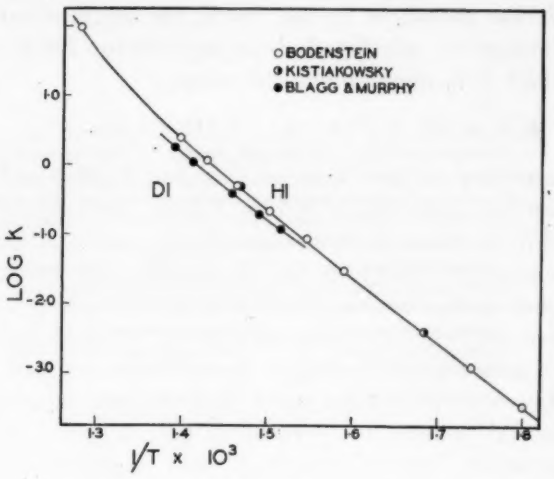

FIG. 3.

$$k_1/k_2 = (M_2/M_1)^{\frac{1}{2}} e^{\Delta E_0^0/RT}, \quad (13)$$

where M_1 and M_2 are the molecular weights of HI and DI and ΔE_0^0 is the difference in their zero-point energies and equals 938.4 cal./mole. Evaluation of Eq. (13) at 700°K gives 1.97 as the ratio of the rate constants. Using Eq. (11) based upon our experimental results and the corresponding constant for HI as determined by Bodenstein, we find the experimentally observed ratio at 700°K of

$$k_1/k_2 = 1.156/0.757 = 1.528.$$

The definitely slower rate for DI seems to indicate that some zero-point in energy is required in the activated state.

Eyring[25] and his collaborators have calculated the absolute rate of reactions in terms of potential surfaces, which in general are those obtained from the Morse formula. Statistical considerations enable the probability of the activated state to be calculated and symmetry considerations furnish considerable information about its potential and vibrational properties. Later developments of this theory by Wheeler, Topley and Eyring[26] have resulted in numerical results for the reaction rates between the halogens and hydrogen and deuterium. They have predicted for the rate of formation of hydrogen and deuterium iodides, the values $k_1'/k_2' = 2.6$, 2.34 and 2.26 at 575, 700 and 781°K where the primes on the rate constants refer to the reverse reaction

[25] Eyring, J. Chem. Phys. **3**, 107 (1935).
[26] Wheeler, Topley and Eyring, J. Chem. Phys. **4**, 178 (1936).

of that measured by us. Using the equilibrium constant as calculated above we find for 700°K, which is in our temperature range,

$$k_1/k_2=(K_1/K_2)^2\cdot k_1'/k_2'=0.818\times 2.34=1.92$$

according to the theory of Wheeler, Topley and Eyring. This result is based upon 14 percent additive binding in the potential surfaces, the zero-point energy of the activated state being ignored. Approximately 20 percent is required to give the experimental result for the HI reaction, if activated zero-point energy is included. However, they have used Bodenstein's experimental results to determine the proper frequencies, activation energy and moments of inertia and since the DI reaction uses the same potential surface, their result should give the correct constant for the DI reaction. Because of the difficulties involved in the theoretical calculations, however, we feel the agreement with our experimental ratio of 1.528 is highly satisfactory. Unfortunately, Wheeler, Topley and Eyring expected the observed ratios to be somewhat larger than the value cited above, since they believe their calculated frequencies for the activated complex to be too stiff. Since the experimental ratio for this reaction has been highly desirable as a check of the theory, it will no doubt suggest to the theoretical chemists the proper way to adjust the potential surfaces in order to obtain closer agreement.

Recently, Geib and Lendle[27] have presented some results on the rate of formation of DI. Their ratio at 700°K is 2.45 and converting to the decomposition reaction as before by means of the equilibrium constant, we find $k_1/k_2=2.00$. This is considerably higher than our result and also somewhat higher than the theoretical one of Wheeler, Topley and Eyring. They followed the course of the reaction by measuring the extinction coefficient of iodine by a photometric method. Since they did not use monochromatic light, rather large corrections were necessary for the effect of H_2 and HI on the calibration curves of the iodine absorption. Their precision is therefore rather low and since their agreement with Bodenstein's results for HI is not very satisfactory, the individual rate constants, as well as their ratio, may be in error.

ACKNOWLEDGMENT

The author wishes to acknowledge his indebtedness to Dr. G. M. Murphy for his helpful advice, criticism and encouragement during this investigation.

He also wishes to thank Professor H. C. Urey for the donation of the deuterium oxide which was used.

[27] Geib and Lendle, Zeits. f. physik. Chemie **B32**, 463–70 (1936).

OCTOBER, 1936 JOURNAL OF CHEMICAL PHYSICS VOLUME 4

The Far Ultraviolet Absorption Spectrum of N_2O

A. B. F. DUNCAN, *Department of Chemistry, Brown University, Providence, R. I.*

(Received July 6, 1936)

The absorption spectrum of nitrous oxide below 2200A has been reinvestigated. Much new material has been found, particularly below 1550A, including some discrete systems of bands, and some continuous regions of absorption. No bands are found below 997A, but only continous absorption down to about 850A, the limit of observation. A Rydberg series was found, converging to an ionization potential of 12.66 volts. Evidence was found for a total of ten electronic states including the members of the Rydberg series. The vibration frequency in the electronic transition around 1500A is 621 cm^{-1}.

THE near ultraviolet absorption spectrum of N_2O has been studied by many investigators.[1–3] The absorption above 2000A appears to be continuous, and very weak. Below 2000A Leifson[4] found two broad bands, one whose center was apparently about 1850A and the other extending from about 1550A to the limit of his observation. These regions have also been studied

[1] A. K. Dutta, Proc. Roy. Soc. **A138**, 84 (1932).
[2] O. R. Wulf and E. H. Melvin, Phys. Rev. **39**, 180 (1932).
[3] L. Henry, Nature **134**, 498 (1934).
[4] S. Leifson, Astrophys. J. **63**, 73 (1926).

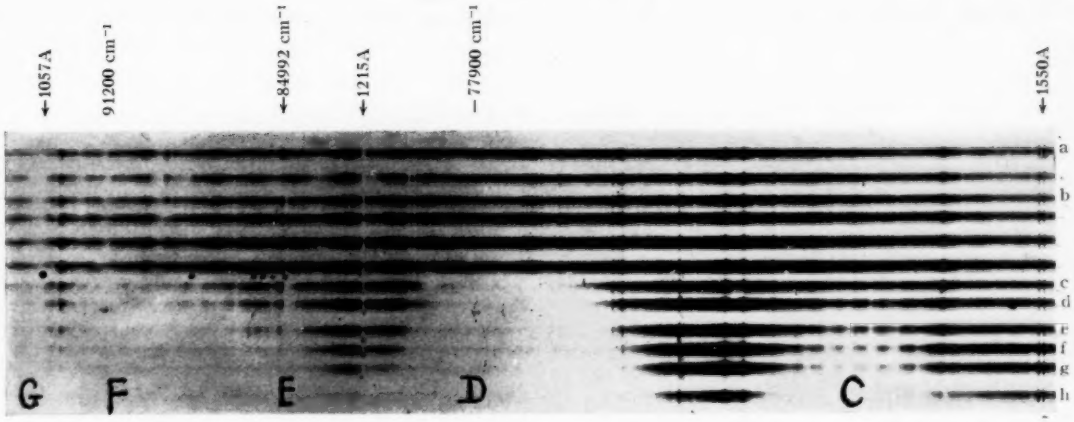

FIG. 1. (a) source, (b) $N_2O-0.001$ mm, (c) $-N_2O-0.01$ mm, (d) $-N_2O-0.02$ mm, (e) $N_2O-0.04$ mm, (f) $N_2O-0.075$, (g) $N_2O-0.09$ mm, (h) $N_2O-0.19$ mm.

by Sen-Gupta[5] who has discussed the relation of this absorption to the decomposition of N_2O into NO and N. The present writer has investigated the absorption of this molecule from 2200A down to about 850A and found several new regions of absorption, some of them showing vibrational structure.

EXPERIMENTAL

The N_2O (a tank product prepared for anesthetic work) was purified by bubbling slowly through a tower filled with strong KOH solution, then dried by passing through P_2O_5. It was collected by liquid air in a large bulb which was attached to the spectrograph. It was then further purified by distillation with liquid air.

The spectra were photographed with a 120,000-line, 1-meter focus, glass grating used at normal incidence. The dispersion was about 8.5A/mm in the first order. The light source was the Lyman continuum with H_2 used as the conducting gas in most cases. Helium, purified with charcoal and liquid air, was used in a few exposures in order to try to improve the Lyman continuum in the region 1150 to 900A where many emission and absorption lines occur in the source. The use of helium leads to no improvement, which might have been anticipated, since most of the lines come from the glass vaporized in the discharge. In spite of this the strong bands below 1100 could be located without difficulty, but weak bands in this region may have been missed.

[5] P. K. Sen-Gupta, Nature **136**, 513 (1935).

The pressure of N_2O was varied from 0.001 to 0.53 mm in this work. The spectrograph served as the absorbing column, giving a two-meter path. At these pressures no absorption whatever appeared at wave-lengths longer than 1530A. In one exposure the spectrograph was filled to a pressure of 7.3 mm by separating the spectrograph from the discharge with a fluorite window.[6] The region found by Leifson and Sen-Gupta about 1850 appeared at this pressure, extending from 1768 to 2068A. This region was not investigated further.

RESULTS

The general appearance of the spectrum between 1550 and 1050A is shown in Fig. 1 which is an enlargement (about four diameters) of a representative plate.

The first electronic transition (called *C*) below 1550A consists of narrow bands shaded to the red, which widen rapidly with increase in pressure. They first appear at about 0.01 mm. Above 0.1 mm the bands merge in a continuum whose limits appear to increase slowly with increasing pressure. At 0.53 absorption extends up to 1528A. At 7.3 mm strong absorption extends to 1700A, and the region between 1700 and 1768 is partly absorbed. Thus the "long wave limit" of this region given by Sen-Gupta[5] (1580A) is far from constant.[7] The apparent

[6] A pressure greater than about 1 mm cannot be used in this spectrograph, because of diffusion through the slit into the discharge.

[7] The absorption limits in this paper are given solely for the practical use of photochemists who may wish to study the decomposition or other reactions of N_2O by light in

TABLE I. *Bands of electronic transition C.*

Calc.	Obs.	Calc.−obs.
65939	65912	+27
66548	66569	−21
67135	67166	−31
67699	67697	+ 2
68239	68224	+15
68756	68740	+16
69251	69232	+19
69722	69745	−23
70170	70148	+22

centers of nine bands observed fit a formula

$$\nu = 65{,}939 + 621.2n - 11.54n^2 \quad (n = 0,1,2\cdots).$$

The frequencies of these bands and the agreement with values calculated from the above equation may be seen in Table I. The bands do not appear to be very sharp but this does not imply predissociation here, since the rotational structure could not be resolved in any case with our instrument. The maximum of intensity occurs at the band 68,224 cm^{-1}.

Since no discrete absorption in the ultraviolet had been reported for N_2O, we investigated the possibility that these bands might be due to N_2 or to NO. We had some plates of pure N_2 at pressures about 100 times that necessary to develop these N_2O bands clearly. N_2 showed no absorption whatever in this region. NO present in the original gas would have been removed, but some may have been formed during exposures.[2-3] We then tried irradiating N_2O in the spectrograph for 30 minutes (longer than the longest exposure) with the Lyman continuum. The absorption spectrum was then taken and showed no additional bands, while the original bands were unchanged in appearance. The frequency separation is also too low for any of the known bands of NO in the Schumann region. We must conclude, therefore that these bands are due to N_2O.

these regions. It would appear that the correlation of long wave limits of continuous absorption with heats of dissociation must be carried out with great caution, for only in extremely fortunate circumstances would the relative positions of the Franck-Condon curves be such that an experimentally determined limit would have any theoretical significance. In addition, Boltzmann factors for the normal vibrations of N_2O, while small, do not exclude absorption from higher ground levels than the zero level, which further confuses the interpretation of a long wave limit. The "limit" for the next absorption region at longer wave-lengths was given as 1850A by Sen-Gupta. Here (at 7.3 mm 200 cm column) absorption extends visibly to 2068A.

We are unable to relate definitely the single observed excited state frequency (621) to the normal frequencies observed in the infrared It is probably a modification of 1285.4 ($\overleftarrow{N\ N\ O}$) or 589 ($\uparrow N\ N \downarrow\ O \uparrow$). If the molecule remains linear in the excited state, 621 is more probably a lowering of 1285 than a modification of 589, which is not totally symmetrical. If the molecule becomes bent in the upper state no decision could be made from symmetry considerations. Resolution of the rotational structure of the bands would, of course solve the problem, since one of these frequencies is $\parallel$ and the other $\perp$. These remarks apply also to a less complete set of bands farther in the ultraviolet where the frequency separations have comparable values.

The next electronic transition (*D*) farther in the ultraviolet shows no vibrational structure at the lowest pressures. It is first observed at a pressure of 0.002 mm, about 200 cm^{-1} wide, with a center at about 77,900 cm^{-1}. The region widens almost symmetrically until at 0.2 mm the limits are 82,221 − 73,724 cm^{-1}.

At the end of this region of absorption, a region of relatively high transmission begins. At 0.05 mm it extends from 82,300 to 83,700 cm^{-1}. At 0.2 mm it can still be seen though it is partly absorbed at this pressure.

Between 83,700 and about 93,000, where another transmission region begins, there are probably two electronic transitions. Corresponding to one there is a strong continuous region of absorption very similar to the transition called *D*. The center of this region is approximately 91,200 at the lowest pressure. This transition is called *F*. To the long wave-length side of this continuous region are five sharp bands which seem to be related to each other but not to the continuous absorption. There are also three other bands in this region which are more diffuse and weaker, at least in comparison with the continuous absorption. The first five bands are considered to belong to one electronic transition, called *E*. The last three bands 86,750, 87,439, and 88,241 could not be explained in any way, and may belong to still other electronic transitions. The two frequency differences between these three bands are so different that a classification with the *E* bands is not permitted. These three bands

may be seen faintly on Fig. 1, being almost lost in the continuum. The second member of the E bands 84,992 cm^{-1} is the strongest of all the ultraviolet absorption bands. As will be noted in Fig. 1 this is the only band appearing on the lowest pressure spectrum (b). The first band, 84,397, is much weaker and we believe that it comes from the level $v''=1$ of the normal electronic state. The difference between this and the strong band 84,992 is 595, which is equal, within our experimental error, to the fundamental perpendicular infrared frequency 589 cm^{-1}.[8] The other three bands of the E transition are 85,473, 85,880, and 86,125. The frequency differences resemble those in the C transition around 1500A, but are lower. The bands are shaded more definitely to the red than the C bands.

Below these bands a short transmission region (seen at the left of Fig. 1) extends to about 94,500 cm^{-1}. There are five bands of moderate intensity at shorter wave-lengths beyond this transmission region. There is also continuous absorption all over this region. Beyond the last band measured, 100,397 cm^{-1}, continuous absorption extends to the end of the plate, about 850A. The centers of four of these five bands, together with the lowest pressure centers of D and F fit into a Rydberg series with the following formula:

$$\nu=102{,}567-R/(n-0.92)^2 \quad (n=3,4,5\cdots).$$

There are probably a few vibrational transitions accompanying these electronic transitions, but they are too weak to measure with certainty. These bands with values calculated from the above equation are shown in Table II. The

TABLE II. *Rydberg series in N_2O.*

n	Calc.	Obs.	Calc.−obs.
3	77,202	77,900 (D)	−700
4	90,999	91,200 (F)	−200
5	95,975	95,852	+123
6	98,315	98,326	− 11
7	99,598	99,609	− 11
8	100,378	100,379	− 1

[8] E. K. Plyler and E. F. Barker, Phys. Rev. **38**, 1827 (1931).

TABLE III. *Summary of electronic states of N_2O.*

State	Description	Lowest pressure at which it appears (mm)
B	center about 1900A, 7.3 mm	between 0.5 and 7.3
C	discrete bands, origin 65,939	0.01
	max. intensity 68,224	
D	continuous, center 77,900	0.002
E	discrete bands, origin 84,992	0.001
F	continuous, center 91,200	0.01
G	single band 94,681	0.004
	Four others in Rydberg series (Table II)	

ionization potential obtained by extrapolating this series, 12.66 ev, is a "vertical" (Franck-Condon) ionization potential, since the most probable transition to the upper state is measured in all cases. This is the center of absorption at the lowest pressure at which any absorption can be observed. This value may be compared with the value 12.9±0.5 ev obtained by electron impact[9] and with the vertical I of $2p\pi$ of N(12.7 ev).[10]

Finally the electronic transitions which have been found are summarized in Table III. The band 94,681 cm^{-1} must represent a separate electronic transition, but no explanation can be given at present of its significance. In reference to Table III, the letter A is reserved for the absorption above 2100A[1-3] though this may prove to be a continuation of B.

The strongest objection to the Rydberg series above comes from the relatively low intensity of $n=6$ as compared to $n=5$ and $n=7$. This is however evident only when the three are compared at the lowest pressure. At pressures of 0.01 mm the intensities appear about the same. The strongest band in the whole spectrum does not fit into this Rydberg series. It does not fit with any other member into a series which converges to the first ionization potential. It is possible however, that it is the first member of a series converging to a higher ionization potential of this molecule, which perhaps lies at wave-length shorter than 850A.

The writer expresses his gratitude to the Warren Fund of the American Academy of Arts and Sciences for financial aid during the progress of this work.

[9] H. D. Smyth and E. C. G. Stueckelberg, Phys. Rev. **36**, 478 (1930).

[10] R. S. Mulliken, J. Chem. Phys. **3**, 736 (1935).

Kinetics of OH Radicals as Determined by Their Absorption Spectrum

I. The Electric Discharge Through Water Vapor

A. A. FROST AND O. OLDENBERG, *Research Laboratory of Physics, Harvard University*

(Received August 7, 1936)

(1) The order of the reaction causing the rapid disappearance of OH radicals after interrupting an electric discharge through H_2O vapor is measured by photometry of absorption spectra taken in snapshots. (2) These spectra are taken in time intervals of a few tenths of a second with a 21-foot grating and rotating interrupter and sector. (3) Relative concentrations of OH radicals are derived by comparing intensities of rotational lines within one branch of the 0→0 band of OH, the relative intensities being given by the theory of Hill and Van Vleck. (4) The decay of OH with time for various H_2O pressures and addition of He is given in diagrams and a table of rate constants. (5) A discussion of the kinetics leads to triple collisions consuming OH. (6) KCl covering the surface of the absorption tube materially increases the rate of the reaction. (7) The absorption spectrum of H_2O_2 investigated simultaneously showed that no appreciable H_2O_2 is formed in the reaction. (8) In the processes consuming OH radicals after interrupting the discharge through H_2O vapor in clean glass tubes, the triple collision $H+OH+M \rightarrow H_2O+M$ plays a predominant part.

I. PROBLEM AND PREVIOUS WORK

IN preceding papers[1] observations have been reported of the absorption spectrum of free OH radicals in a reacting gas at room temperature. In particular it was shown that OH as produced by the electric discharge through H_2O vapor could be observed to last for at least $\frac{1}{8}$ second after interrupting the discharge. It was concluded that the recombination process determining the disappearance of OH is not so fast that a bimolecular association has to be assumed, as had been suggested by other observations.[2]

The work here reported was carried out in order to obtain further information regarding this process, and consists in determining quantitatively relative values of the OH concentration and so obtaining the rate of disappearance of OH as a function of the composition of the reacting gas mixture.

II. EXPERIMENTAL

The apparatus was essentially that described previously, but improved in several respects in order to allow for more quantitative results. It consisted of:

(a) Source of continuous radiation
(b) Absorption tube
(c) Rotating sector and switch
(d) Spectrograph

The OH λ3064 band was to be observed in absorption. The carbon arc in nitrogen as used previously did not provide a sufficiently continuous radiation to be used as a source in quantitative work. However, the carbon arc burning in flowing helium was found to be satisfactory in this respect and was used in a number of experiments. This source was discarded later in favor of a particularly intense hydrogen discharge tube.[3] The latter carried a current of one to two amperes through a 1×5 mm capillary and was less intense by a factor of two to four, but was much easier to operate, and provided a radiation which was constant over long periods of time.

The absorption tube was 150 cm long and 4.7 cm in diameter and closed at each end with quartz windows. Large aluminum electrodes were placed in side tubes at a distance of about 20 cm from the absorption tube proper.

A synchronous motor operated a revolving sector which allowed light to pass to the spectrograph during the desired interval of time. On the same shaft with the sector was a sliding contactor which served to control the discharge through the gas in the absorption tube. At first this contactor was placed in series with the discharge and the secondary of a transformer, an arrangement which proved unsatisfactory because of the high potential involved. This

[1] O. Oldenberg, J. Chem. Phys. **2**, 713 (1934) and **3**, 266 (1935).
[2] W. H. Rodebush and M. H. Wahl, J. Chem. Phys. **1**, 696 (1933).
[3] Constructed by N. D. Smith, Thesis, Harvard University. To be published.

TABLE I.

Rotational Quantum Number	Relative Absorption Coefficient
$1\frac{1}{2}$	0.571
$2\frac{1}{2}$	0.725
$3\frac{1}{2}$	0.605
$4\frac{1}{2}$	0.390
$5\frac{1}{2}$	0.195
$6\frac{1}{2}$	0.081

problem was solved by putting the contactor in the grid circuit of a thyratron (FG–29) which regulated the current through the transformer primary.[4] 60-cycle a.c. 110 and 220 volts was used in the primary, the power varying from 2 to 4 kilowatts. One or four half-cycles were passed through the primary depending upon the gear system used with the synchronous motor. The shaft was rotated at 6 revolutions per second, or at $1\frac{7}{8}$ revolutions per second, different speeds being necessary in order to follow the reaction under widely differing conditions.

A high frequency discharge was used in several runs and was produced with the aid of a 250-watt power oscillator, the high frequency potential being applied between external electrodes running the full length of the absorption tube. The advantage of this arrangement was that a discharge could easily be obtained with much higher pressures of water vapor, up to 5 mm Hg.

For obtaining the weak band absorption, the second order of a 21-foot concave grating spectrograph was used. The high resolving power was necessary in order to observe the very narrow absorption lines of the band. To decrease the exposure time as much as possible a cylindrical lens was placed in front of the photographic plate.[5] This increased the intensity over the small spectral range to be observed by a factor of about 20 without affecting the resolving power. Eastman IV–O plates were used.

III. Evaluation of Relative OH Concentrations

The individual OH absorption lines being so very narrow (cf. the spectrum reproduced, reference 1, Fig. 2) it was not found possible to measure the intensity of absorption with the available microphotometer. However, the following method involving only visual comparison of absorption lines was found to be reasonably satisfactory. It so happens that instead of the conventional intensity marks, the individual lines of one branch of a band represent concentration marks since the relative concentrations of the rotational quanta for a given temperature and their absorption coefficients are theoretically predictable on the basis of the theory of Hill and Van Vleck.[6] Lines of the Q_1 branch were used because of their intensity and freedom from overlapping with lines of other branches. Assuming that the rotation of OH is in equilibrium at slightly above room temperature (300°K) the relative values of the absorption coefficients (Boltzmann factor×statistical weight×probability of transition) are given in Table I.

In order to obtain relative OH concentrations corresponding to two different exposures, the exposures were placed side by side in the field of view of a microscope and the absorption lines compared until one or more pairs of lines were found, the lines of each pair having nearly the same intensity of absorption.[7] In this comparison care must be taken to have equal intensity of the continuous background in the two exposures and to use the photographic plate in the linear portion of its characteristic. One exposure is taken as a standard furnishing an arbitrary unit pressure of OH. All measurements discussed in the following sections are expressed in the same standard units of OH pressure. Suppose the mth line of the unknown is paired with the nth line of the standard and let k_m and k_n be the respective values of the relative absorption coefficients found in Table I. Then the OH concentration for the unknown is k_n/k_m units. Several such concentration values may be obtained for a single exposure if interpolation of intensities between lines is made use of. Only the third, fourth, fifth and sixth lines and two or three gradations between each neighboring pair were used in the comparison. The available concentration range was about 1 : 100. A typical set of values of OH

[4] Following a suggestion by Dr. F. V. Hunt.

[5] O. Oldenberg, J. Opt. Soc. Am. **22**, 441 (1932).

[6] E. Hill and J. H. Van Vleck, Phys. Rev. **32**, 250 (1928). Calculations for the special case under discussion were carried out by L. T. Earls, Phys. Rev. **48**, 423 (1935). We appreciate the advice of Professor Van Vleck in the problem of intensities.

[7] An instrument was devised which enabled this comparison to be made without the need of cutting the plates up into their separate exposures.

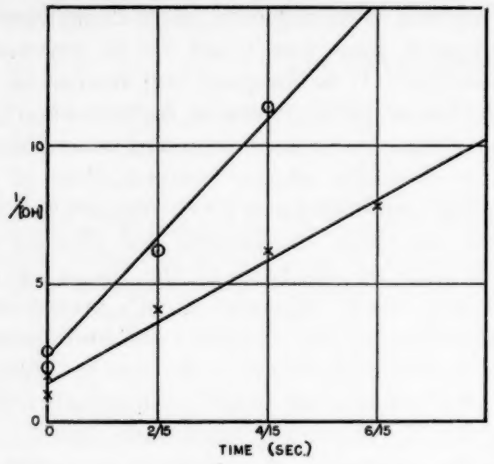

FIG. 1. Dependence of 1/[OH] upon time; ×, H_2O 1.1 mm; ○, H_2O 1.1 mm; He 3.7 mm; 1/[OH] in 1/standard pressure.

concentration obtained in this way for a single exposure is as follows: 0.64, 0.50, 0.50, 0.37, 0.46; average 0.49; mean deviation 12 percent. The results are not very precise but they are accurate enough for the present purpose of determining the order of the reaction.

IV. Experimental Results

As is shown in the next section it is expected that for any set of conditions there should be a linear relation between 1/[OH] and the time. That this is true within the experimental error is shown in Fig. 1, in which are plotted the results for typical cases. The slope of the straight line represents an experimental rate constant $\bar{k}$ for the particular conditions employed. Table II is a summary of the experimental results as expressed by values of $\bar{k}$ corresponding to different values of H_2O and He pressure.

V. Chemical Kinetics

The various possible processes leading to a long life of OH in the electric discharge through water vapor have been discussed at length in the preceding paper. For the present purpose we shall base our calculations on the following assumptions:

(a) The reacting mixture consists of H_2O, H and OH, with the addition of He in several runs. Ions will have recombined within a few thousandths of a second after the discharge. O atoms can be assumed to be present in negligibly small amounts if the current is not too high. The experimental arguments for this assumption have been summarized by Oldenberg. From the molecular structure it is plausible that the easiest dissociation process leads to H and OH, not to free O atoms.

(b) The probable reactions are:

(1) $H+H+M\rightarrow H_2+M$
(2) $H+OH+M\rightarrow H_2O+M$
(3) $OH+OH+M\rightarrow H_2O_2+M$

} Termolecular Processes where M is any third molecule

or instead of (2) and (3)

(2a) $H+OH\rightarrow H_2O$
(3a) $OH+OH\rightarrow H_2O_2$

} Bimolecular Processes

(c) H_2O is only to a small part dissociated so that $[M]$ will be approximately constant during the reaction.

For reactions (1), (2), (3) the rate of disappearance of OH is given by

$$-(d[\mathrm{OH}]/dt)=k_2[\mathrm{OH}][\mathrm{H}][M]+k_3[\mathrm{OH}]^2[M]$$

plus additional terms with different constants if more than one kind of molecule is effective as a third body. Since we assume the statement of Rodebush and Wahl that [H] and [OH] are the primary products, the reaction starts from equal concentrations [H] and [OH]. If we furthermore assume that H and OH disappear by triple collisions at not very different rates it follows that $[H]\backsimeq[OH]$ during the time through which

TABLE II.

Plate number	H_2O (mm Hg)	He (mm Hg)	$\bar{k}$ (standard pressure units^{-1} sec.$^{-1}$)
1	1.3	0	24
	2.6	0	24
	5.2	0	48
2	1.0	0	14
	2.0	0	17
	4.1	0	30
3	1.0	0	13
	1.0	7.2	31
4	1.45	0	17
	1.45	2.75	27
5	1.1	0	17
	1.1	3.7	31
6	0.75	0	18
	0.75	4.1	27

the reaction is observed. In this case the two terms may be combined and

$$-(d[\mathrm{OH}]/dt)=k[\mathrm{OH}]^2[M],$$

which may be integrated, M being constant with respect to the time:

$$(1/[\mathrm{OH}]_t)-(1/[\mathrm{OH}]_0)=k[M]t.$$

The corresponding treatment for OH reacting according to (2a) and (3a) would result in

$$(1/[\mathrm{OH}]_t)-(1/[\mathrm{OH}]_0)=k't.$$

The same equation would hold if the wall reaction is predominant. In any case there should be a linear relationship between $1/[\mathrm{OH}]$ and the time. This relationship has been used in the preceding section.

The experimental constant $\bar{k}$ is to be compared with the constants $k[M]$ or k' of the theory. If $\bar{k}$ is independent of the H_2O and He concentrations the reaction proceeds according to (2a), (3a). On the other hand, if $\bar{k}$ increases with the H_2O and He concentrations in such a way that

$$\bar{k}=k_{H_2O}[H_2O]+k_{He}[He],$$

then the reaction is termolecular according to (2) and (3). That the latter is the case may be seen at least qualitatively in Fig. 1 where it is noticed that the addition of He increases the rate of the reaction. The constant k_{H_2O} may be calculated directly from data on the reaction in the absence of He. Fig. 2 is a plot of $\bar{k}$ against H_2O pressure based on the experiments with a wide variation of H_2O up to 5.2 mm (plates 1 and 2 of Table II). The rate does definitely increase with increasing $[H_2O]$. The fact that the best straight line does not go through the origin seems to indicate the simultaneous occurrence of a slow bimolecular reaction, presumably at the surface. More evidence of a surface reaction is given in the next section.

The value of k_{H_2O} as given by the slope of the line of Fig. 2 is

$$k_{H_2O}=6.8;\quad H_2O \text{ in mm Hg.}$$

The constant k_{He} is most easily obtained by dividing the increase in the constant $\bar{k}$ due to the addition of He by the pressure of He added. The four last plates of Table II give the four values 2.5, 3.6, 3.8, 2.2, the average of which is

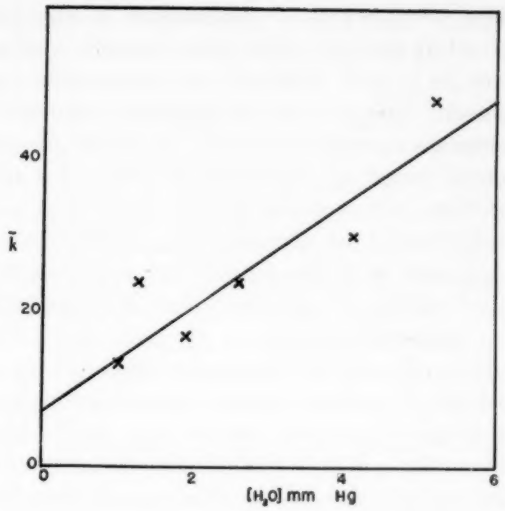

FIG. 2. Dependence of experimental rate constant $\bar{k}$ upon H_2O pressure; $\bar{k}$ in standard pressure units^{-1} $\times$sec.$^{-1}$.

$k_{He}=3.0$. These results for k_{H_2O} and k_{He} are based on the same "standard units" of $[\mathrm{OH}]$.

In order to determine whether or not these are reasonable values for triple collision rate constants the absolute concentration of OH must be known or estimated. If we assume that the maximum OH concentration obtained with the present apparatus, defined as a standard in section III, is about 0.1 mm so that the large majority of molecules is not dissociated, then the reaction constants are

$$k_{H_2O}=68 \quad \text{and} \quad k_{He}=30 \quad (\mathrm{mm^{-2}\ sec.^{-1}})$$

or $$k_{H_2O}=2.4\times10^{16} \quad \text{and} \quad k_{He}=1.1\times10^{16} \quad (\mathrm{cc^{-2}\ mole^{+2}\ sec.^{-1}}).$$

These values although being very approximate compare favorably with rate constants for similar third order reactions such as

$$H+H+M\rightarrow H_2+M^*$$

and

$$Br+Br+M\rightarrow Br_2+M^*$$

with values ranging from 10^{15}–10^{16}.

Obviously the problem remains of determining the *absolute* concentration of OH which in this argument is rather arbitrarily assumed. The only

[8] H. M. Smallwood, J. Am. Chem. Soc. **51**, 1985 (1929) and **56**, 1542 (1934).

[9] K. Hilferding and W. Steiner, Zeits. f. physik. Chemie **B30**, 399 (1935); E. Rabinowitsch, Zeits. f. physik. Chemie **B33**, 275 (1936).

method to apply is a comparison of the OH observed at the discharge with a known concentration as it was observed by Bonhoeffer and Reichardt[10] in water vapor partially dissociated at temperatures above 1150°C. An experimental difficulty turns up, however, in that the two absorption experiments to be compared are carried through at temperatures different by a factor 5 and pressures by a factor 1000, so that the line widths are quite different. But the total energy absorbed within a spectral line of a certain coefficient of absorption depends upon the width of the line—apart from the properties of the spectrograph. Hence the comparison requires a special study of the pressure broadening of the OH lines. For this purpose even the second order of the 21-foot grating is not adequate. An attempt will be made to solve this problem and so determine the absolute values of the reaction rate constants k_{H_2O} and k_{He}.

VI. Surface Reaction

The pressure effect reported definitely indicates a gas reaction. If the surface reaction were prominent He would decrease rather than increase the rate, contrary to the values of Table II. In the following experiments a potassium chloride surface was studied for various reasons. KCl is known not to catalyze the recombination of hydrogen atoms. Hence any positive effect in the discharge through water vapor must be due to the adsorption of OH radicals. A very strong effect of KCl was discovered by Pease[11] in the slow combustion of H_2 at temperatures of 520–550°C. This is known to be a chain reaction. When the glass walls are covered with KCl the rate is reduced by a factor of about 1000. Since chain reactions are easily broken by surface reactions removing one chain carrier, the effect of a KCl surface on radicals is of interest. Taylor and Lavin[12] observed the heating of thermometers covered with various substances in the flowing gases pumped out of the discharge through H_2O; they inferred adsorption and recombination of OH on a KCl surface.

The rate of disappearance of OH, observed by the decay of the absorption spectra, was compared for a glass surface carefully cleaned with cleaning solution, boiling water and distilled water, and on the other hand for the same surface covered with KCl. In both cases, of course, the surface was moist. The KCl surface increases the rate materially. While for the glass surface the absorption spectrum of OH is easily traced through 8/15 sec., it disappears completely for the KCl surface in the same time interval. Furthermore, since the discharge proper producing OH is not instantaneous but lasts through 1/15 sec. it is noticeable that, right after interrupting it, more OH is present in the case of the clean glass than in the case of the KCl surface.

The obvious interpretation of this experiment is that the KCl surface adsorbs OH radicals and so catalyzes their reaction, in agreement with the result of Taylor and Lavin.

The noticeable increase of the surface reaction caused by the KCl surface indicates that for clean glass the surface reaction is not predominant. Whether or not in the experiment of Pease the same effect takes place, i.e., whether OH is one of the chain carriers, remains uncertain. An endeavor will be made to obtain further evidence.

VII. Absorption Spectrum of H_2O_2

In section 5 it was shown that OH disappears largely by triple collisions. It remained uncertain whether H_2O or H_2O_2 is formed, that is, whether reaction (2) or (3) takes place. The results of Rodebush and Wahl seemed to indicate an overwhelming probability for the formation of H_2O_2 since concentrations of nearly 50 percent H_2O_2 were obtained in the gases pumped out of the discharge. It should be possible to measure a concentration as high as that by the absorption spectrum. Rodebush and Wahl failed in doing this. They explained that their failure was caused by lack of sensitivity of the experiment. Since the absorption spectrum of OH proved to be valuable for the study of kinetics, it seemed worth while to improve the sensitivity with which the absorption spectrum of H_2O_2 was to be observed.

[10] K. F. Bonhoeffer and H. Reichardt, Zeits. f. physik. Chemie **139**, 75 (1928).
[11] R. N. Pease, J. Am. Chem. Soc. **52**, 5106 (1930).
[12] H. S. Taylor and G. I. Lavin, J. Am. Chem. Soc. **52**, 1910 (1930).

According to Urey, Dawsey and Rice,[13] H_2O_2 has a continuous absorption spectrum extending from about λ3100 with increasing intensity to short waves beyond the range of the quartz spectrograph. No other molecule present in this experiment shows continuous absorption in the same range. In particular OH has the major intensity in the 0→0 band so that no continuous OH spectrum beyond a convergence limit of vibrational quanta is to be expected which might obscure the H_2O_2 spectrum. The difficulties of the two absorption experiments are entirely different. While for the absorption spectrum of OH because of the exceedingly narrow lines high resolving power is necessary, the absorption spectrum of H_2O_2 can be observed with any small quartz spectrograph because of its continuous nature. In order to detect small traces of H_2O_2 a very accurate measurement of the light intensity passing through the vapor is necessary, hence a very steady source of light is required.

In order to take advantage of the strong absorption at short wave-lengths, some experiments were made with an electric discharge through Cd vapor, the resonance line of which at λ2280 is rather isolated in its spectrum. However, the mercury line λ2537 emitted from an ordinary arc proved about as effective and easier to apply. Instead of using a monochromator in order to separate the line λ2537 from the intense long wave-length spectrum which is not absorbed by H_2O_2, a chlorine filter was applied, consisting of a layer of chlorine gas of 1 atmosphere, 30 cm long. The intensity of the light passing the H_2O_2 was measured by a photoelectric cell which indicates small changes of intensity much better than the photographic plate. A cadmium cell, argon filled, in a quartz bulb, made in this laboratory by Mr. H. W. Leighton, was used. The visible light transmitted by the chlorine filter has no effect on the cadmium cell since its long wave-length limit is λ3100. The current was amplified with a type 32 tube and measured with a microammeter. This system—lamp, chlorine filter, cadmium cell—was calibrated for its power to indicate the presence of H_2O_2 by H_2O_2 vapor of known concentration.[14] The calibration showed that in the same absorption tube of 150 cm length H_2O_2 of 1/100 mm could be detected.

We are interested as to whether or not in the electric discharge through water vapor the OH radicals when recombining form H_2O_2. The absorption experiment gave no trace of H_2O_2. This result indicates that the considerable amount of H_2O_2, frozen out in the experiment of Rodebush and Wahl in the liquid-air trap, is formed in the trap, not in a gas reaction.

The formation of H_2O_2 *in the trap* was mentioned as an alternative explanation by Rodebush and Wahl themselves. That this actually takes place was concluded by Campbell and Rodebush[15] from recent experiments. Their result has recently been confirmed by Geib,[16] who found hydrogen peroxide in the gases pumped out of the discharge tube only under conditions which according to his own experiments are favorable for the formation in the trap of H_2O_2.

In the interpretation of the experiments by Rodebush and Wahl the difficulty remains that the concentration of H_2O_2 observed in the trap does not appreciably change, while the time of flow between discharge bulb and trap (velocity of flow and distance) is varied. It must be concluded that no appreciable combination of OH+H takes place during the time of flow. This might be largely due to the fact that they worked with pressures as low as 0.1 or 0.2 in the discharge tube, hence still somewhat lower in the flowing system, so that triple collisions consuming the OH radicals are still less probable than in the experiments reported above. Furthermore the 50 percent yield of H_2O_2 reported in their experiments means the value relative to H_2O, not to the total gas content pumped out of the discharge. At any rate, their observation confirms the conclusion of section 6 that no fast combination of OH on a clean glass wall takes place since even the gas slowly flowing through long glass tubes shows the same yield of H_2O_2 in the trap.

VIII. Processes in the Discharge through H_2O

It remains to summarize the chemical processes taking place after interrupting the discharge

[13] H. C. Urey, L. H. Dawsey and F. O. Rice, J. Am. Chem. Soc. **51**, 1371 (1929).

[14] Concentrated H_2O_2 was made for other experiments which will be described in another paper.

[15] R. W. Campbell and W. H. Rodebush, J. Chem. Phys. **4**, 293 (1936).

[16] K. H. Geib, J. Chem. Phys. **4**, 391 (1936).

through water vapor or else in the gases pumped out of the discharge. We are not concerned with the discharge proper in which reactions may be caused by ions as discussed in detail by Brewer.[17]

Again we assume H and OH as primary products, since O is produced at a comparatively small concentration. The main result of the present paper is that the disappearance of OH is largely due to a termolecular gas reaction. From our failure to observe the absorption spectrum of H_2O_2 and from the results of Campbell and Rodebush and of Geib, $H+OH+M \rightarrow H_2O+M$ is to be assumed as the most plausible process. A wall reaction is certain not to play a predominant part for a clean glass surface but to become important at the KCl surface.

In addition it is possible that H_2O_2 is produced but rapidly decomposed so that no appreciable concentration builds up, since H atoms and OH radicals are both able to decompose it.[18]

[17] A. K. Brewer, J. Phys. Chem. **38**, 1051 (1934).

[18] Cf. K. H. Geib, Zeits. f. physik. Chemie **A169**, 161 (1934). Evidence for the decomposition process $OH+H_2O_2$ will be presented in another paper.

OCTOBER, 1936 JOURNAL OF CHEMICAL PHYSICS VOLUME 4

The Crystal Structure of Polonium by Electron Diffraction

M. A. ROLLIER,* *University of Milan*
AND
S. B. HENDRICKS AND LOUIS R. MAXWELL, *Bureau of Chemistry and Soils, Washington, D. C.*

(Received July 2, 1936)

Electron diffraction photographs ($\lambda=0.062$A) were obtained from about 10^{-7} g of polonium that had been volatilized in a stream of hydrogen and condensed over an area of about 3 mm² on a thin collodion film. Diffraction patterns were also obtained from bismuth and tellurium since it was expected that polonium would have a similar crystal structure. Analysis of these patterns shows that the structure of polonium closely resembles that of tellurium, the lattice being pseudohexagonal with $a=4.25$A, $c=7.06$A, or 14.12A, and the calculated density 9.39 assuming 3 Po in the pseudo unit of structure. The true lattice is probably monoclinic with $a=7.42$A, $b=4.29$A, $c=14.10$A and β quite close to 90°, a suggested value being $\beta=92°$; the calculated density for 12 Po in the unit of structure is 9.24. A structure, based upon the space group C_2^3-C2, in which each polonium atom has four nearest neighbors gives moderate agreement between observed and calculated intensities of reflection.

INTRODUCTION

POLONIUM is the superior homolog of tellurium in the periodic system of the elements and immediately follows bismuth in atomic number. It resembles both these elements in its chemical properties but, of course, differs from them in being radioactive. The crystal structure of the element could be expected to be similar to that of tellurium or bismuth.

Sufficiently large amounts of polonium have not yet been available for x-ray diffraction experiments and thus no information is available on its crystal structure or its density. A strong source of polonium for radioactive work contains *ca.* 10^{-6} g of material, which is quite sufficient to give electron diffraction photographs provided that it can be obtained as a thin film.

PREPARATION OF THE POLONIUM FILM

Pure polonium was prepared from old radon bulbs[1] under the supervision and with the constant help of Dr. L. R. Hafstad[2] who has developed a technique for the production of strong polonium sources after the method used by Mme. I. Curie.[3] According to this method

* On leave of absence from the University of Milan. I am particularly indebted to Professor Dr. G. Bruni, Dr. Charles L. Parsons, Dr. H. G. Knight and Dr. C. H. Kunsman for making arrangements necessary for the successful culmination of this work and for their many courtesies.

[1] We are indebted to Dr. C. F. Burnham and Dr. F. West of the Kelly Hospital, Baltimore, Maryland, for the liberal supply of old radon bulbs that they placed at our disposal. The purification of the polonium was carried out at the National Bureau of Standards. Successful completion of the work was due in a large part to the cooperation of Dr. Hafstad, of the Department of Terrestrial Magnetism, Carnegie Institution of Washington.

[2] L. R. Hafstad, J. Frank. Inst. **221**, 191 (1936).

[3] I. Curie, J. chim. phys. **22**, 471 (1925).

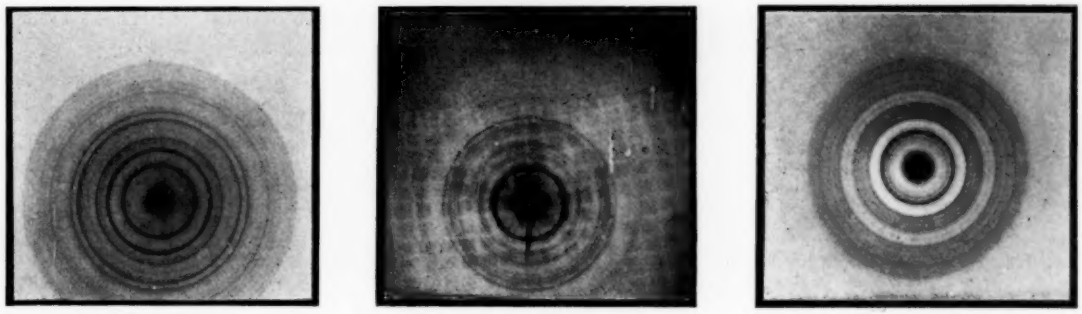

Bismuth
λ = 0.062A
plate dist. = 24.5 cm.

Polonium
λ = 0.0622A
plate dist. = 24.5 cm.

Tellurium
λ = 0.059A
plate dist. = 24.3 cm.

FIG. 1. Electron diffraction photographs of bismuth, polonium and tellurium (full size).

the polonium is separated from the solution containing salts of radium D and E by displacement on silver, complete separation is shown by absence of β-ray activity. The polonium was finally displaced from solution upon a cleaned and outgassed nickel disk. A film was obtained by evaporating the polonium from the nickel base in a stream of pure hydrogen and condensing the vapor on a very thin collodion film supported by a fine platinum gauze. The volatilizing apparatus used was similar to that described by Rona and Schmidt,[4] and Curie and Joliot.[5] During the evaporation process the nickel was maintained at a dull red heat which was sufficient to volatilize the polonium[6] without carrying over traces of nickel. A dark visible coating was obtained over an area of about 3 mm² on the collodion film.

Electron diffraction photographs were taken immediately after preparation of the sample since the radioactivity of the polonium soon destroyed the film. α-ray air ionization measurements taken after the film was destroyed showed the presence of about 1500 e.s.u. or 2.52×10^{-7} g of polonium remaining on the wire support. It is estimated that the original thickness of the polonium film was not less than 100A.

Electron Diffraction Apparatus

The apparatus used for electron diffraction has been described elsewhere.[7] Electrons with a de Broglie wave-length of about 0.06A were used with a film to plate distance of 245.6 mm. Preliminary tests were made with collodion films upon which lead, bismuth and tellurium had been volatilized in the apparatus mentioned above. The lead films were prepared from about 10^{-6} g of the element that had been deposited upon nickel. In all these cases the diffraction photographs obtained were in complete agreement with the crystal structure data for these elements. There was only slight evidence of scattering from collodion on any of the photographs.

Five electron diffraction photographs were obtained from polonium films at de Broglie wave-lengths between 0.0623 and 0.0627A. One of these is reproduced in Fig. 1 together with photographs from bismuth and tellurium. Average values of $Q=1/d^2=4\sin^2\theta/\lambda^2$ as measured on the polonium photographs are listed in Table I together with the estimated intensities of reflection.

The Lattice and Crystal Structure of Polonium

Diffraction rings of polonium can roughly be accounted for, as shown in Table I, on the basis of a hexagonal lattice having $a=4.254$A and $c=7.06$A. These lattice dimensions are the expected ones if the structure of polonium is similar to that of tellurium or bismuth. Moreover, as shown in Table II, the intensities are not greatly unlike those of tellurium. However, closer inspection shows that neither the above lattice nor the one having $c=14.12$A can be correct. It perhaps can be seen on the electron diffraction photograph of polonium reproduced

[4] E. Rona and E. A. W. Schmidt, Zeits. f. Physik **48**, 784 (1928).
[5] I. Curie and F. Joliot, J. chim. phys. **28**, 201 (1931).
[6] P. Bonét-Maury, Ann. de physique **11**, 253 (1929).
[7] S. B. Hendricks, L. R. Maxwell, V. L. Mosley and M. E. Jefferson, J. Chem. Phys. **1**, 549 (1933).

TABLE I. *Electron diffraction data from polonium interpreted according to a hexagonal lattice.*

Ring No.	Q Obs.	Q Calc.	Pseudo hexagonal indices	Intensity* (obs.)
1	0.0890 to 0.0940	0.0919	(10.1)	*vs*
2	0.1580	0.1520	(10.2)	*m*
3	0.1804	0.1805	(00.3)	*ms*
4	0.2175	0.2210	(11.0)	*w*
5	0.2481	0.2415	(11.1)	*mw*
6	0.2642	0.2522	(10.3)	*w*
7	0.3634	0.3730	(20.2)	*w*
8	0.370			*vw*
9	0.4068	0.3925	(10.4)	*m*
		0.4016	(11.3)	
10	0.4480			*m*
11	0.46	0.4732	(20.3)	*vw*
12	0.5310	0.5340	(21.1)	*s*
		0.5418	(11.4)	
13	0.7170	0.7216	(00.6)	*w*
		0.7221	(11.5)	
14	0.8000	0.7940	(20.5)	*vw*
15	0.8465	0.8436	(30.3)	*w*
16	0.8953	0.8840	(22.0)	*w*
		0.9040	(22.1)	
17	0.9920	0.9640	(22.2)	*mw*
		1.014	(20.6)	
18	1.149	1.136	(31.3)	*vw*
		1.177	(40.0)	
19	1.248	1.257	(40.2)	*vw*
20	1.473	1.456	(31.5)	*w*
		1.478	(32.2)	
		1.498	(40.4)	
21	1.627	1.624	(00.9)	*vw*
		1.627	(41.2)	

* The following abbreviations are used throughout this work; *vs*, very strong; *s*, strong; *ms*, medium strong; *m*, medium; *mw*, medium weak; *w*, weak; *vw*, very weak.

in Fig. 1 that the first ring is quite broad, as is also true for some of the other rings. The (8) and (10)–(11) rings cannot be accounted for by the hexagonal lattice and the agreement between observed and calculated values of $Q=4\sin^2\theta/\lambda^2$ is extremely poor for the (2), (7) and (10)–(11) rings. This lack of agreement is not changed by doubling the value of c.

Before continuing the direct structure argument for polonium it is best to point out some of the structural characteristics of the elements in the 5th and 6th subgroups of the periodic system; the pertinent facts are summarized in Table III. Both the bismuth and tellurium type structures can be considered as distortions of the mercury structure which is itself a deformation of a close-packed structure. Each mercury atom has six nearest neighbors; in bismuth the displacement is 0.15A along the c axis, leading to three nearest neighbors, and in tellurium 0.25A perpendicular to that axis such as to give two nearest neighbors. As the atomic number increases in either series the differences in distance between nearest and next nearest neighbors decreases. Now if the pseudo lattice of polonium is approximately correct and if the pseudo parameter values are those of tellurium then the distances to surrounding atoms are those shown in Table III.

The true lattice of polonium is probably a monoclinic one and it is logical to suppose that the space group is the monoclinic subgroup common to both $D_3^4-C3_12$ and $D_{3d}^5-R\bar{3}m$, namely C_2^3-C2. A strictly analogous situation is found for plaster of Paris, $2\,CaSO_4\cdot H_2O$, which as studied by x-ray powder diffraction methods[8] was found to have a structure based on the enantiomorphic space groups $D_3^4-C3_12$ and $D_3^6-C3_22$. Earlier and more thorough work on single crystals of $2\,CaSO_4\cdot H_2O$,[9] however, shows that the true lattice is monoclinic with $\beta=90°\ 38'$

TABLE II. *Diffraction results from tellurium.*

Q Obs.	Q Calc.*	Indices	Intensity* X-ray	Electron	Polonium
0.097	0.0966	(10.1)	*s*	*s*	*vs*
.184	.1840	(10.2)	*ms*	*ms*	*m*
.201	.2024	(11.0)	*m*	*m*	*w*
.231	.2315	(11.1)	*w*	*mw*	*mw*
.263	.2620	(00.3)	*w*	*w*	*ms*
.302	.2990	(20.1)	*m*	*m*	
.322	.3190	(11.2)	*vw*	*vw*	
	.3295	(10.3)			*w*
.396	.3860	(20.2)	*m*	*w*	*w*
.469	.4645	(11.3)	*m*	*m*	*m*
	.4722	(21.0)			
.496	.5013	(21.1)	*w*	*w*	*s*
.533	.5332	(10.4)	*w*	*w*	*m*
	.5318	(20.3)			

* The formula used was $Q=0.06746(h^2+k^2+hk)+0.02911l^2$ corresponding to a lattice having $a=4.445$ and $c=5.86$A, the value of c being slightly smaller than 5.91A as found by Bradley (Phil. Mag. **48**, 477(1924)) from x-ray diffraction.

TABLE III. *Structures of some elements of the 5th and 6th subgroups of the periodic table.*

Element	Space Group	Hexagonal Lattice Dimensions A: a	c	c/a	Neighboring Atoms: No.	Distance	No.	Distance
As	$D_{3d}^5-R\bar{3}m$	3.76	10.57	2.81	3	2.51	3	3.15
Sb	$D_{3d}^5-R\bar{3}m$	4.26	11.29	2.65	3	2.87	3	3.37
Bi	$D_{3d}^5-R\bar{3}m$	4.56	11.85	2.60	3	3.10	3	3.47
Se	$D_3^4-C3_12$	4.33	9.94	2.28	2	2.32	4	3.46
Te	$D_3^4-C3_12$	4.44	11.82	2.66	2	2.86	4	3.74
Pseudo polonium lattice		4.25	14.12	3.32	—	3.10	—	3.58

[8] W. A. Caspari, Nature **133**, 648 (1934).
[9] P. Gallitelli, Periodico di Mineralogia **4**, 132 (1933).

TABLE IV. *Electron diffraction data from polonium with suggested monoclinic indices.*

Ring No.	Observed Q	Intensity	Pseudo hexagonal indices	Q Calc.	Monoclinic indices	Q Calc.	Calculated values of $J \cdot S/F_{Po}^2$
1	0.0890	*vs*	(10.1)	0.0919	$(20\bar{2})$	0.0900	230
	−0.0940				$(11\bar{2})$	0.0911	10
					(112)	0.0927	460
					(202)	0.0950	10
2	0.1580	*m*	(10.2)	0.1520	$(20\bar{4})$	0.1471	20
					$(11\bar{4})$	0.1497	380
					(114)	0.1551	20
					(204)	0.1577	240
3	0.1804	*ms*	(00.3)	0.1805	(006)	0.1800	300
4	0.2175	*w*	(11.0)	0.2210	(020)	0.2176	70
					(310)	0.2173	250
			(11.1)	0.2415	(312)	0.2336	80
					(022)	0.2376	40
5	0.2481	*mw*			(312)	0.2414	20
			(10.3)	0.2522	$(20\bar{6})$	0.2444	60
					$(11\bar{6})$	0.2484	80
6	0.2642	*w*			$(11\bar{6})$	0.2564	40
					(206)	0.2604	4
			(20.1)	0.3129	$(40\bar{2})$	0.3043	0
					$(22\bar{2})$	0.3070	100
					(222)	0.3123	10
					(402)	0.3149	100
7	0.3634	*w*	(20.2)	0.3730	$(40\bar{4})$	0.3590	60
					$(22\bar{4})$	0.3642	100
8	0.370	*vw*			(224)	0.3750	300
					(404)	0.3802	10
			(11.3)	0.4016	$(31\bar{6})$	0.3853	100
9	0.4068	*m*			(026)	0.3973	150
					(316)	0.4093	460
			(10.4)	0.3925	(208)	0.4030	50
					(118)	0.3977	440
					$(11\bar{8})$	0.3870	40
					$(20\bar{8})$	0.3818	80
10	0.4480	*m*	(20.3)	0.4732	$(40\bar{6})$	0.4536	100
					$(22\bar{6})$	0.4616	90
11	0.46	*vw*			(226)	0.4776	60
					(406)	0.4856	10
12	0.5310	*s*	(21.1)	0.5340	$(51\bar{2})$	0.5202	70
					$(42\bar{2})$	0.5217	40
					$(13\bar{2})$	0.5256	50
					(132)	0.5282	170
					(422)	0.5321	140
					(512)	0.5336	200
			(11.4)	0.5418	$(31\bar{8})$	0.5213	80
					(028)	0.5373	110
					(318)	0.5533	100

and $a/b=1.744$ instead of 1.732 and that the space group is probably C_2^3-C2. This conclusion has recently been challenged[10] but the properties of the crystal, particularly the biaxial character, gives it strong support.

The quadratic form for a monoclinic lattice is:

$$Q=\frac{4\sin^2\theta}{\lambda^2}=\frac{h^2}{a^2\sin^2\beta}+\frac{k^2}{b^2}+\frac{l^2}{c^2\sin^2\beta}-\frac{2\cos\beta}{ac\sin^2\beta}hl.$$

Now if the lattice is pseudohexagonal about the c axis β must be near 90° and thus $\sin\beta$ must be approximately unity while $\cos\beta$ is very sensitive to deviations from 90°. The pseudohexagonal (00.3) becomes the monoclinic (006) and thus $c\sin\beta$ is 14.10A and c is very close to 14.10A. If the structure is pseudohexagonal the intensities of the reflections from the monoclinic $(hk0)$ should differ chiefly by the multiplicity factor. Thus both (020)(310)←(11.0) should have an appreciable intensity. If the limits of Q for the fourth line are taken as 0.2175 ± 0.035 then $b=4.29\pm0.04$A and $a=7.42\pm0.07$, giving $a/b=1.763$ to 1.700 and

$$Q=0.0181h^2+0.0544k^2+0.0050l^2 -0.0190\cos\beta hl.$$

In estimating the value of β it is noted that (1)

[10] W. A. Caspari, Proc. Roy. Soc. **A155**, 41 (1936). Note that the Laue photograph as reproduced *does not* have a threefold axis.

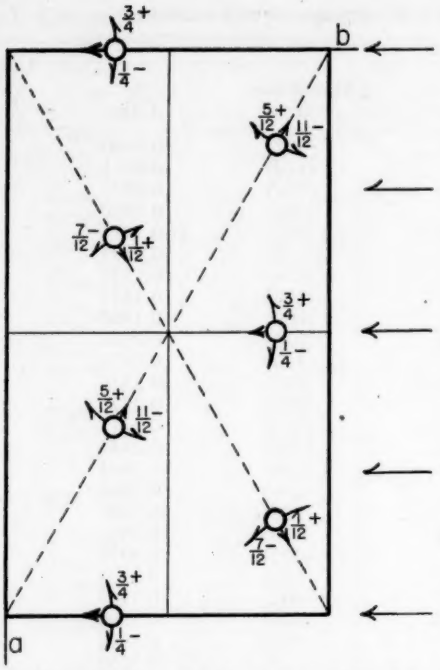

FIG. 2. A projection showing the relationship of the polonium structure to that of bismuth and tellurium as obtained by deformation from the mercury structure. The full arrows that are parallel to the *ab* plane represent deformation towards tellurium and the curved half arrows toward polonium. Bismuth positions are obtained by displacements along the normal to the *ab* plane.

is broad, that (2) does not agree well with the pseudohexagonal spacing, and that the agreement between observed and the calculated value of (10) for the pseudo lattice is poor (Table I). A suggested value of $\cos\beta$ is -0.035 which corresponds to $\beta=92°$. Values of Q calculated on the basis of this lattice for planes possibly contributing to the first twelve lines of the polonium diffraction pattern are listed in Table IV. The agreement between observed and calculated values of Q is quite satisfactory.

If the space group is $C_2{}^3-C2$ the polonium atoms are probably in three sets of general positions: xyz; $\bar{x}y\bar{z}$; $\frac{1}{2}+x, \frac{1}{2}+y, z$; $\frac{1}{2}-x, \frac{1}{2}+y, \bar{z}$.[11] Parameters corresponding to the hexagonal tellurium positions are

$x_1=0.00,$	$x_2=0.14,$	$x_3=0.36,$
$y_1=.27,$	$y_2=-.14,$	$y_3=.36,$
$z_1=.25,$	$z_2=.42,$	$z_3=.08.$

The intensity of the pseudohexagonal (10.3) which is present on the polonium photograph but absent for tellurium cannot be explained by use of these values, nor by considerable distortion of them with the symmetry of $C3_12$ tending to equalize the distances of nearest and next nearest neighbors.

Inspection of Table I further shows that the pseudohexagonal planes corresponding to the (13)–(21) lines either are $3n$ orders of (00.l) or usually have low values of l. The probable explanation for the latter fact is that the spacings of the monoclinic planes derived from a particular pseudohexagonal plane are grouped quite close together for low values of l. This is well illustrated by the strong (12) ring as shown in Table IV, there being eight possible contributing monoclinic forms. The high intensity of the (3) ring and the possible presence of reflections from (0012) and (0018) strongly suggests that the c parameters of polonium are quite close to those of tellurium.

After considerable work it was found that the following parameter values gave moderate agreement between observed and calculated intensities of reflection as perhaps can be seen by inspection of Table IV, column 8.

$x_1=0.05,$	$x_2=0.13,$	$x_3=0.35,$
$y_1=.27,$	$y_2=-.20,$	$y_3=.40,$
$z_1=.245,$	$z_2=.43,$	$z_3=.07.$

It is not considered that these particular parameter values are the correct ones but a deformation of this type from the tellurium structure is probably required by the data. They lead to the following approximate separations of the polonium atoms:

$x_1y_1z_1$ to $x_2y_2z_2$, 3.50A, 3.34A and 4.06A;
$x_1y_1z_1$ to $x_3y_3z_3$, 3.30A, 3.38A and 3.95A.

This distortion is in such a direction as to give four nearest neighbors at a distance of about 3.40A about a particular polonium atom.

A projection of the above structure on (001) is shown in Fig. 2 together with the indicated relationship to a similar projection of the bismuth and tellurium positions.

The density calculated, for the atomic weight 210, on the basis of the monoclinic lattice is 9.24 and for the pseudohexagonal lattice 9.39. The calculated atomic volume is 22.7 cc per mole, a value to be expected from a consideration of the atomic volume-atomic number relationships of the elements of high atomic weight.

[11] *Int. Tables for the Determination of Crystal Structures*, (Berlin, 1935), Vol. I.

The Photovoltaic Effect for Sodium

ROBERT B. GIBNEY AND MALCOLM DOLE, *Department of Chemistry, Northwestern University*

(Received June 29, 1936)

Attempts to produce a photovoltaic effect with reversible electrodes made of an active metal photoelectrically sensitive to visible light, such as sodium, and dipping into a solution containing ions of the metal, met with no success provided the solvent and salt which formed the electrolyte were carefully dried before preparing the cells. Slight photovoltaic effects of the order of 0.5 mv or smaller were observed in the case of two cells known to contain traces of water, but these effects were probably due either to the water present or to the compound electrode Na/Na_2O rather than to the pure metal. It is concluded that the energy supplied to the electrons by the visible light is not sufficient to bring about the transition of the electron from the metal to the solution.

CONVENTIONS AND DEFINITIONS

HUGHES and DuBridge[1] use the term "photovoltaic effect" to include "phenomena associated with the production of an electromotive force in a cell consisting of two similar electrodes, separated by a suitable electrolyte or other substance, when the electrodes are unsymmetrically illuminated." We shall define the photovoltaic potential as being positive when the potential of the illuminated electrode becomes more positive on illumination irrespective of the sign of the electrode potential in the dark. We believe that the use of the terms anode and cathode in the case of cells generating an e.m.f. is inadvisable and confusing if not entirely incorrect. The values and sign of the e.m.f. of the cells as given in this paper will always be the potential of the electrode which is illuminated or about to be illuminated in reference to the potential of the other electrode kept continually in the dark.

By *external* photoelectric effect we mean, as usual, the ejection of electrons from a metal to a vacuum by light. By *internal* photoelectric effect we signify the ejection of electrons by the light from one solid phase to another solid phase, the ejection of electrons from a layer of cuprous oxide to the underlying copper, for example.

INTRODUCTION

The interesting question regarding the extent to which light may affect the potential of a metal or metal coated with an insoluble salt in contact with an electrolyte has been investigated by a number of workers from the original discovery of Becquerel[2] in 1839 to the present day. Hughes and DuBridge[3] summarize papers published through 1929 while Audubert[4] and Athanasiu[5] have recently published extensive reviews. Photovoltaic potentials have been observed for a number of compound electrodes such as $Ag|AgI$, $Cu|Cu_2O$, etc., dipping into aqueous solutions, but these photopotentials largely disappear when the electrodes are carefully dried and then dipped into electrically conducting nonaqueous solutions, the photopotential of a cuprous oxide electrode, for example, drops from 120 mv to 3 mv on elimination of water from the system. Audubert explains the photovoltaic effects in the case of aqueous solutions by postulating that the light "photolyzes" water molecules which are adsorbed on the surface of the electrodes to form either hydrogen or oxygen which then enter into equilibria involving ions of the metal, thereby affecting the potential of the electrode. Consider, for example, the $Cu|Cu_2O$ electrode whose potential becomes more positive on illumination;[6] for this electrode the reaction

$$Cu^+ + \tfrac{1}{4}O_2 + \tfrac{1}{2}H_2O \rightleftarrows Cu^{++} + OH^-$$

is applicable. The incident light photolyzes the water, increasing the concentration of the oxygen and forcing the above equilibrium to the right.

[1] A. L. Hughes and L. A. DuBridge, *Photoelectric Phenomena* (McGraw-Hill Book Co., New York, 1932), p. 352.

[2] E. Becquerel, Comptes rendus **9**, 144, 561 (1839).

[3] Reference 1, Chap. IX.

[4] R. Audubert, J. de phys. et rad. (7) **5**, 486 (1934).

[5] G. Athanasiu, Ann. de physique (11) **4**, 377 (1935).

[6] At least in the case of cuprous oxide made in the dry way.

The resulting increase in the concentration of the cupric ion produces the positive photopotential. In support of this hypothesis may be cited the fact that in the case of the $Cu|Cu_2O$ electrode its positive photopotential is increased in reducing solutions and reduced in oxidizing solutions, is reduced by increased concentration of cupric ions and is reduced by increase of *p*H.

Athanasiu[5] has studied the influence of *p*H, temperature and wave-length on the photovoltaic effect. His results may be summarized as follows; decrease of *p*H favors the positive photoeffect, increase of temperature lowers the photopotential markedly, increase of wave-length of the incident radiation decreases the positive photopotential and may produce a negative photopotential. In the case of Ag|AgI electrode immersed in a neutral solution of KCl after a basic treatment the positive photopotential shows a maximum at 4200A and the negative photopotential a maximum at 4400A. The maximum of the spectral absorption coefficient of silver iodide, the maximum of its photoconductivity and the maximum of the photovoltaic effect all occur in the same wave-length range, about 4200A, but the threshold of the *external* photoelectric effect is below 4070A. Athanasiu concludes that the photovoltaic effect begins with an *internal* photoelectric effect of the light sensitive salt or oxide layer, followed by photochemical reactions in which the electrolyte may take part. In addition to a photochemical reaction there must also be a possibly reverse thermal reaction in order to account for the pronounced temperature coefficient of the photovoltaic effect.

The photopotential of pure metals has been investigated in the case of noble metals which may be assumed to be freer of oxide coating than more active metals like copper or zinc, although the presence of adsorbed layers of gases makes it impossible to assert that a pure metal surface has ever been studied for its photovoltaic effect. The photopotentials of the noble metals are much smaller than those discussed above and rather difficult to measure because of the instability of the electrode potentials in the dark; the electrodes probably acting as oxygen electrodes.

Audubert and Roulleau[7] studied the photovoltaic effect for selenium on platinum and found large photopotentials even in the absence of water. They used solutions of potassium iodide dissolved in a number of organic solvents, and found in contrast to the $Cu|Cu_2O$ electrode that the observed positive photopotentials were increased in oxidizing solutions. Very few experimental details were given, so that the purity of the selenium surface is open to question; the authors believe that a true photoelectric effect was concerned and that electrons were ejected into the solution by the action of the light.

In all previous work on the photovoltaic effect no investigations have been made to our knowledge on metals having low work functions like sodium. It would seem that if a true photoelectric effect existed, for the boundary metal|solution, it would be much more pronounced for active metals than for the relatively inert metals having high work functions. Accordingly we decided to investigate the photovoltaic effect for pure sodium surfaces in contact with a solution containing sodium ions. We hoped in this way to be dealing with electrodes giving reversible and stable potentials in the dark and with metal surfaces as clean as they could be when in contact with a liquid electrolyte. Sodium electrodes also have the advantage that there is no photosensitive oxide or insoluble salt layer which would make possible an internal photoelectric effect or photochemical reactions with the electrolyte.

Experimental

The general method of investigating the photovoltaic effect for sodium consisted in preparing a dry nonaqueous solvent, dissolving dry sodium iodide in it, pouring the solution onto sodium electrodes and finally measuring the e.m.f. between the two electrodes before and after the illumination of one of the electrodes. The cell used was $Na|NaI$ in $C_5H_{11}NH_2|Na$.

Sharples Solvent Company technical grade monoamylamine was selected as the solvent because it is conveniently a liquid at room temperature. It was dried by refluxing over liquid sodium-potassium alloy for three hours

[7] R. Audubert and J. Roulleau, Comptes rendus 198, 1489 (1934).

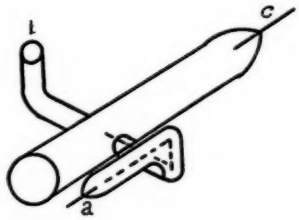

FIG. 1.

followed by repeated distillations in vacuum into flasks containing sodium mirrors until the solvent was so dry that a thin sodium mirror would no longer be removed. Connections between flasks were opened by breaking an inner bulb with a magnetic hammer; a large bulb was broken rather than a capillary tip in order to expedite the distillation of the solvent and later on the pouring of the solution from one flask to another. The iron magnetic hammer was encased in glass in order that iron rust would not catalyze the reaction between sodium and the amine to form hydrogen and an amide.[8] Various methods were tried in an attempt to dry sodium iodide recrystallized from water by fusion, but invariably a saturated aqueous solution of the resulting fused iodide was alkaline to phenolphthalein so that the drying was usually done by heating the salt at a pressure of 1 micron from room temperature to 100°C and then at 300°C at a pressure of 0.1 micron for ten hours. This process gave a neutral salt which on solution in dry amyl amine contained insufficient water to remove a thin sodium mirror. The solutions were made by distilling the solvent onto the salt, followed by shaking. The concentrations of the solutions were estimated roughly by evaporating the solvent from a weighed quantity of the solution and weighing the dry residue or by adding a known volume of liquid to a known weight of salt. A saturated solution of the salt contains approximately 27 percent of sodium iodide by weight.

The sodium for the electrodes and mirrors was melted in vacuum, filtered through a capillary tube to remove oxide and finally pushed by means of hydrogen or allowed to run by gravity through a second capillary tube into a flask or

[8] T. H. Vaughn, R. R. Vogt and J. A. Nieuwland, J. Am. Chem. Soc. **56**, 2120 (1934), have discovered that ferric nitrate dissolved in liquid ammonia catalyzes the amide-forming reaction between sodium and ammonia.

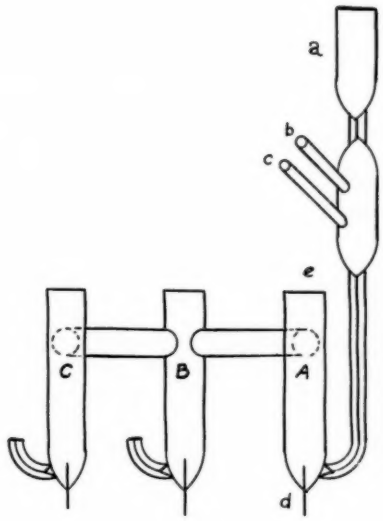

FIG. 2.

cell. The side arms containing the sodium reservoir and capillary tubes were removed after the sodium mirror had been formed. The cells, described below, were at first maintained at constant temperature, 25°, in an air bath; but later it was found that the actual temperature of the experiment was of no apparent importance so that the air in the bath was merely stirred vigorously, the essential precaution being that the two sodium electrodes be at the same temperature. An e.m.f. of 0.5 mv or higher could be produced by touching one side of a cell with the hand. The e.m.f. was measured usually to 0.01 mv with a type K-2 Leeds and Northrup potentiometer using a Leeds and Northrup type R galvanometer (sensitivity 5×10^{-10} amp. per mm scale deflection).

A 200-watt tungsten filament lamp with a liter flask filled with water or saturated copper sulfate solution as a condensing lens and heat filter was used in the first experiments, but later a mercury arc without any filter giving more intense light was constructed and used. The arc was enclosed in Pyrex glass so that light of wave-length below 3000A was cut off. The monoamylamine also begins to absorb strongly in the ultraviolet region below 3000A.[9]

The cells illustrated in Figs. 1 and 2 were of two types. Type *A*, Fig. 1, contained one sodium

[9] See J. Bielecki and V. Henri, Comptes rendus **156**, 1860 (1913).

electrode which could be illuminated while type *B*, Fig. 2, contained three sodium electrodes capable of illumination. In Fig. 1 at *a* and *c* are two tungsten electrodes sealed through the Pyrex glass, both of which were covered with sodium metal which was admitted through a capillary not shown in the figure. A sodium mirror was deposited on the inside walls of the cell around the electrode *c* by gently heating the sodium at *c*. Light entered through a thin Pyrex window of the type described by Sonkin,[10] at *d* while solution was poured into the cell at *b*. After the filling of the cell the side arm at *b* was sealed off. In Fig. 2 is illustrated a cell of type *B* and the auxiliary capillary tube for admitting the sodium is also pictured. In some cells of this type no sodium mirror was formed, the sodium electrodes simply consisting of a pool of sodium metal at the bottom of each arm of the cell.

The results of the investigation are collected in Table I which is self-explanatory but to which the following remarks should be appended. In all the cells except No. B-1 the electrodes were mirror electrodes, the electrodes of cell B-1 were formed of sodium in the bulk. After a zero photopotential had been observed for all the electrodes of cells B-1 and B-2 sodium was deposited electrolytically in the form of shiny white needles on one electrode of each of the cells, but no photopotential resulted. The electrical resistance of cells B-1, A-1, A-5, A-6, and A-7 was rather high due to the dimension of the cells or to the low concentration of the solution, preventing measurements to be made to 0.01 mv. Water was purposely added to cell A-8 causing gas evolution at the electrodes and producing an erratic e.m.f. but after the water present had combined with the sodium leaving a thick layer of hydroxide on the electrode surface an e.m.f. could be measured, however, no photopotential was observed. No photopotential was observed in the case of pure solvent in contact with the sodium electrode, cell No. A-6, but here the measurements were not very accurate due to the high internal resistance of the cell. Cell No. A-3 was deliberately opened to the air after preparation, a small photopotential was indicated by a slight motion of the galvanometer on illumination but it was not definite enough to measure. In the case of cell No. A-5 air was purposely admitted to the cell after the sodium mirror had been formed and before the solution was poured in, thereby making it probable that a thin layer of sodium oxide covered the mirror. No photopotential was observed, possibly because of the insensitivity of the measurements or because of the thickness of the oxide layer.

The only cell which showed a definite photovoltaic effect was cell No. A-2, but this cell contained some water since on standing the sodium covering one of the tungsten wires disappeared bringing the tungsten into direct contact with the solution and causing the dark e.m.f. to rise to 0.9 v. Before this happened, the e.m.f. of the cell in the dark changed gradually

TABLE I.

Cell No.	Concn. of Soln. in wt. percent	Light Source	No. of illuminated electrodes	Dark e.m.f. of electrode to be illuminated in reference to other electrode, millivolts	Photo e.m.f. millivolts
A-1	3.9	lamp	1	8	0
A-2	18.2	lamp	1	25.10−16.5	+0.5±0.05
B-1	27	arc	3	*B–A* 76.1	*A* 0±0.1
				C–A 16.0	*B* 0
				B–C 61.3	*C* 0
B-2	27	arc	2	*B–A* 0.20	*A* 0±0.01
					B 0
A-3	27	arc, lamp	1	−0.45	trace ±0.01
A-4	27	arc, lamp	1	−0.18	0±0.01
A-5	5	arc, lamp	1	−5.5	0±0.2
A-6	0	arc, lamp	1	±0.1 v	0±0.1 v
A-7	1	arc, lamp	1	26	0±1
A-8	27	arc, lamp	1	37	0

[10] S. Sonkin, J. Opt. Soc. Am. **19**, 65 (1929).

from +0.025 v to −0.0165 v while the photopotential amounted to 0.5 mv irrespective of the dark e.m.f., the illuminated electrode becoming more positive. This photovoltaic production of an e.m.f. occurred instantaneously on illumination as far as could be told, but it was probably due to a layer of oxide or hydroxide on the surface of the sodium since no photovoltaic effect was ever observed for a perfectly dry cell in which the sodium surface was apparently clean. $Cu|Cu_2O$ electrodes in the presence of water exhibit a large photovoltaic effect so it is reasonable to suppose that a $Na|Na_2O$ electrode would act similarly. Sodium iodide dried by fusion was used in the case of cells A-1, A-2 and A-7 and sodium iodide dried in a vacuum at 300° in the case of the remaining cells.

In summarizing the experimental results we can say that no measurable photovoltaic effect exists for a clean surface of sodium in equilibrium with an anhydrous solution of sodium iodide in monoamylamine. Sodium surfaces formed by electrolysis, by condensation from the vapor state and by solidification of the liquid metal behaved alike. Changing the concentration of the solution and the source of the illumination likewise produced no photovoltaic effect. We do not believe, therefore, that a pure metal in equilibrium with a solution of its ions and of such a nature that no photochemical reaction can occur will show a photovoltaic effect analogous to the photoelectric effect exhibited by metals in contact with a gas or evacuated phase.

Discussion

Having come to the conclusion that no observable photovoltaic effect exists for sodium, it is next of interest to consider what theoretical implications are inherent in this conclusion. In order to measure the e.m.f. to 0.01 mv a current of the order of magnitude 10^{-8} amp. must flow through the galvanometer; the galvanometer, however, is sensitive to currents of 5×10^{-10} amps. Currents measured usually in photoelectric experiments vary from 10^{-11} to 10^{-15} amp., but may become as great as 10^{-3} amp.,[11] depending on the conditions, intensity of light, activity and dimensions of metal surface, presence of gas, etc. In our case we can conclude that if a photovoltaic current was produced it must have been smaller than 10^{-9} amp.

The probable reasons for the absence of a photovoltaic effect are; first, the absence of any chemical reaction which might take place under the influence of light such as the photolysis of water postulated by Audubert and second, unfavorable energy relationships. When visible light, or light of shorter wave-length, falls on a sodium surface exposed to a vacuum, electrons are ejected into the vacuum because the energy of the light added to the energy of the electron in the metal produces electrons having high enough energy to escape into the vacuum. In our case it may be that the stable energy level, if indeed such a level exists, of an electron in monoamylamine solution is so high that electrons in the metal activated by the energy of the visible light are unable to make the transition metal to solution. The presence of the positive sodium ions in the solution complicates matters, however, since the energy relations of the electrons may be modified by sodium ion transitions between the metal and the solution; for this reason quantitative calculations are at present impossible, but it is evident that the presence of the sodium ions does not change the energy relationships sufficiently to produce a photovoltaic effect.

[11] Reference 1, p. 435.

Liquid Hydrogen Chloride. Electrical Conductance and Dielectric Constant

GEORGE GLOCKLER AND R. E. PECK,[1] *University of Minnesota*

(Received July 24, 1936)

Liquid hydrogen chloride has a specific electrical conductivity of 0.35×10^{-8} reciprocal ohms at $-85°C$. The temperature coefficient is negative: -0.65×10^{-10} in the range from $-84°C$ to $-64°C$. The molecular conductivity at infinite dilution is estimated to be 184 ($-85°C$) and 192 ($-53°C$). The ionization constant is 0.083×10^{-16} at $-78°C$ and 0.051×10^{-16} at $-68°C$. The change in heat content of the ionization reaction is:

$$(x+y+2)HCl \rightarrow (H_2Cl\cdot HCl_x)^+ + (Cl\cdot HCl_y)^-, \qquad \Delta H_{195} \doteq -3500 \text{ cal.}$$

INTRODUCTION

LIQUID hydrogen chloride has been studied as an ionizing solvent by various investigators[2] and for this purpose its dielectric constant, electrical conductivity and viscosity must be known. These quantities have been determined earlier.[3] We wish to report here new values for the first two properties since they differ considerably from the figures given in the literature.

The conductivity cells. Since we wished to determine the electrical properties of liquid hydrogen chloride in the temperature range from $-90°$ to about 15°C it was necessary to construct cells which would withstand pressures from 1 to 50 atmospheres. We constructed five different types of cells but found the first four designs undesirable for various reasons.[1] The final design which satisfied all our requirements is shown in Fig. 1. These all-glass cells withstood the pressure involved satisfactorily and it can be seen that the platinum electrodes (nonplatinized) are not affected by the pressure changes involved when the cells are placed in various temperature baths. The tungsten inseals were covered with glass along their full length so that the platinum wires only were exposed to the hydrogen chloride. The cells were washed with dilute hydrochloric acid and conductivity water. The cell constants were determined with 0.0125N hydrochloric acid and were 0.00373, 0.00321, 0.00451 and 0.00400 for the four cells used. The cylindrical electrodes were 14.0 cm long; the inner cylinder had a radius of 0.60 cm and the outer one 0.80 cm. The distance between the two electrodes was 0.1 cm. The cells were baked out at 415°C for four days and hydrogen chloride was distilled into them. They were heated between each run, having been flushed with liquid hydrogen chloride.

The cell constants should have been determined with a standard liquid of much lower specific conductance than the hydrochloric acid used in order to avoid the Parker effect.[4] However the conductivities to be measured were such low order that this correction appeared to be unnecessary.

Preparation and drying of hydrogen chloride. The gas was generated by dropping concentrated sulphuric acid onto solid sodium chloride in a thoroughly evacuated and flamed out system. Two drying agents were employed: Phosphorus pentoxide and a combination of calcium chloride and magnesium perchlorate.

While Fairbrother[5] has shown that phosphorus pentoxide is a satisfactory drying agent for hydrogen chloride gas, if the latter is not very wet, we find that it is unsatisfactory when the gas is to be liquefied and then used for the determination of the electrical conductivity of the liquid. The second drying agent mentioned gave a much better product for the purpose of conductivity measurements.

It should be noted that the hydrogen chloride did not come in contact with mercury surfaces after it was dried and fractionally distilled. Mercury vapor also was excluded from the

[1] This article is based upon a thesis presented to the faculty of the Graduate School of the University of Minnesota by R. E. Peck in partial fulfillment of the requirements for the degree of Doctor of Philosophy.

[2] P. Walden, *Ostwald-Drucker Handbuch der allgem. Chemie IV (1 and 2)*; Akad. Verlags G. m.b.H. (Leipzig, 1924).

[3] Reference 2 and I. C. Tables.

[4] Th. Shedlovsky, J. Am. Chem. Soc. **54**, 1411 (1932).

[5] F. Fairbrother, J. Chem. Soc. **2**, 1539 (1933).

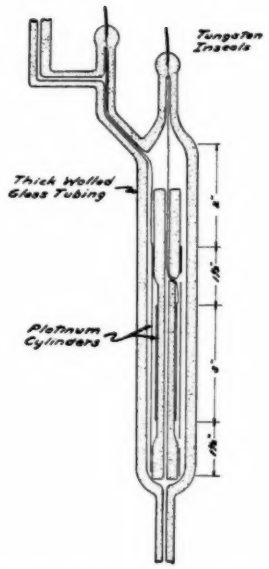

FIG. 1. Conductivity cell for liquefied gases. Pressures up to 30 atmospheres.

system by appropriate means. The reason for these precautions was the fact that we could not obtain consistent results unless mercury was excluded. The results of the conductance measurements are shown in Table I. The measurements marked "fresh" were made as soon as the cell had been removed from the liquid-air bath, where the gas was condensed, and allowed to warm up to the temperature of the cryostat (−85°C). Agitation and standing would increase the conductivity several fold. Similar observations have been made by others, for example in the case of water by Noyes.[6]

The dielectric constant of liquid hydrogen chloride. The above-mentioned measurements were carried out with two different resistance bridges: one a slide wire bridge actuated by a homemade oscillator (500 and 2200 cycles) and a two-stage amplifier and a Jones conductivity bridge[7] No. 260418 at 500, 1000 and 2000 cycles. With the latter instrument it was possible to determine the dielectric constant from the reading of the balancing condensers. The results are given in Table II.

[6] A. A. Noyes, *The Electrical Conductivity of Aqueous Solutions* (Carnegie Institute, Washington, D. C., 1907), page 206.

[7] P. H. Dike, Rev. Sci. Inst. **2**, 379 (1931).

Discussion of Results

The values of the specific conductivity of liquid hydrogen chloride reported here are lower than any found in the literature. It should be noted that the conductivity of freshly prepared hydrogen chloride is lower than that of the material after standing. In twenty-four hours the conductivity (at −85°C) changed from 0.7 to 5.4×10^{-8} mho (expt 10) and from 0.35 to 2.1×10^{-8} mho (expt 11). It seems that no better results can be obtained in glass-vessels and employing the usual methods of purification.

The temperature coefficient of the specific conductivity has been found to be negative (-0.065×10^{-9} mho/degree).

TABLE I. *The specific conductance of liquid hydrogen chloride (0.5, 1.0 and 2.0 kilocycles).*

Expt. No.	Drying Agent	Temp. Range t°C	L specific conductance at −85°C $\times10^{8}$ (mhos)	$\frac{-\Delta L}{\Delta t}\times10^{9}$	Remarks f. = fresh a.s. = after standing
1	P_2O_5	−80→−20	9.0	1.11	a.s.
2	"	" →+10	10.8	1.05	"
9	$CaCl_2$ and $Mg(ClO_4)_2$	−10→ "	6.8	0.47	"
10	"	−60→ "	5.4	0.48	"
11	"	−85→0	2.1	0.07	"
9	"		1.0		f.
10	"		0.7		"
11	"	−85→−60	0.35	0.065	"

TABLE II. *Dielectric constant of liquid hydrogen chloride (1.0 kilocycle).*

temp. t°C	Dielectric Const.	density (grams/cc)	Molar Polarization P (cc)
−85.0	10.10	1.191	23.0
−80.5	9.80	1.179	23.1
−66.5	8.92	1.141	23.6
−34.8	7.33	1.046	23.7
−19.0	6.55	0.993	23.9
−15.0	6.32	0.980	23.7
			Average P 23.5 cc.

TABLE III.

Solvent	t°C	η_∞	ϵ	x	λ_∞	Const.
H_2O	0	0.01780	88.1	3	264	0.160
"	18	.01060	80.8	"	379	.149
"	25	.00891	78.4	"	419	.143
C_2H_5OH	"	.01145	21.7	3.3	90	.157
CH_3OH	"	.00553	32.5	3.8	190	.123
NH_3	−34	.00256	22.0	1.2	1001	.134
HCl	−89.8	.00474	10.45	1.7	(182)	(.144)
"	−84.8	.00458	10.10	"	(184)	"
"	−73.0	.00423	9.50	"	(186)	"
"	−53.0	.00364	8.40	"	(192)	"
					Average const.	.144

TABLE IV. *$K_{i.p.}$ and K_i for the ionization of liquid hydrogen chloride.*

Temperature: °C	−88	−83	−78	−73	−68	Remarks
$L\times10^9$ (mho)	3.70	3.36	3.05	2.72	2.38	Run 11(*f*)
C (moles/liter)	32.90	32.55	32.15	31.80	31.42	
$(\lambda=1000L/C)\times10^7$	1.123	1.032	0.948	0.855	0.757	
λ_∞	182	184	186	187	188	Table III
$(\alpha=\lambda/\lambda_\infty)\times10^9$	0.617	0.562	0.508	0.456	0.402	
$(K_{i.p.}=(H^+)(Cl^-))\times10^{16}$	4.20	3.30	2.67	2.03	1.59	
$(K_i=(H^+)(Cl^-)/(HCl))\times10^{16}$	0.125	0.103	0.083	0.066	0.051	

The dielectric constant decreases with increasing temperature (Table II). If we assume that the usual expression for molar polarization[8] holds for liquids then we find the molecular polarization for liquid hydrogen chloride to be 23.5 cc. Smyth and Hitchcock[9] report 23.1 cc at −112°C.

The equivalent conductance. It is possible to calculate the equivalent conductance of liquid hydrogen chloride from the specific conductance and density. The latter has been obtained by Maass and Wright.[10] If we could obtain the equivalent conductance of hydrogen and chloride ions at infinite dilution, we could calculate the ionization constant and the ion product constant for the ionization of liquid hydrogen chloride. It is possible to obtain a very reasonable estimate for the equivalent conductance (λ_∞) of hydrogen chloride at infinite dilution in liquid hydrogen chloride by the use of a relation established by Walden[2]

$$\lambda_\infty\cdot\eta_\infty\cdot x=\epsilon\cdot\text{const.},$$

where η_∞ = the absolute viscosity of the solvent in poises, x = the association factor obtained from the temperature variation of the molar surface energy and ϵ = the dielectric constant of the solvent (see Tables III and IV).

The values of the ionization constant at various temperatures enable us to calculate the temperature coefficient of its logarithm (−0.02) and by means of the well-known relation

$$(d\log K_i)/(dT)=\Delta H/2.3RT^2$$

we find

$$\Delta H_{195}=-4.6\times0.02\times(195)^2=-3500\text{ cal.}$$

This value is the heat absorbed for the ionization act of HCl in liquid hydrogen chloride

$$(x+y+2)\text{HCl}\rightarrow(\text{H}_2\text{Cl}\cdot\text{HCl}_x)^+ + (\text{Cl}\cdot\text{HCl}_y)^-,\qquad \Delta H_{195}\doteq-3500\text{ cal.}$$

Several weak acids have been shown by Harned and Embree[11] to have negative heats of ionization especially at higher temperatures. These calculations are based on the lowest values of the conductivity of freshly prepared liquid hydrogen chloride and since these conductivities are very low and hence difficult to measure, it must be realized that the ionization constant, the ion product constant and the heat of ionization are not determined to a high degree of accuracy. It is clear that the calculation just given has significance only in the case that the measured conductance is really due to the conductivity of liquid hydrogen chloride and not due to some impurity. The three following facts cause us to believe that we have measured the conductivity of liquid hydrogen chloride: (1) The method of purification involved several (three to seven) fractional distillations; (2) The fresh material used for the measurements was kept at low temperatures (−180° to −60°C), where solubility rates of impurities are slow; (3) The conductivity rose on agitation and standing.

[8] C. P. Smyth, *Dielectric Constant and Molecular Structure*. (Chem. Catalog Co. N. Y., 1931.)

[9] C. P. Smyth and C. S. Hitchcock, J. Am. Chem. Soc. **55**, 1830 (1933).

[10] O. Maass and C. H. Wright, J. Am. Chem. Soc. **43**, 1098 (1921).

[11] H. S. Harned and N. D. Embree, J. Am. Chem. Soc. **55**, 1050 (1934).

Absolute Rates of Four-Atom Reactions

WM. ALTAR AND H. EYRING, *Frick Chemical Laboratory, Princeton University, Princeton, New Jersey*

(Received June 15, 1936)

Equipotential surfaces such as one encounters in valence problems and particularly in the calculation of absolute rates, are discussed in a "bond space" instead of configuration space, with much simplification resulting both in the general aspects and in the practical handling of such problems. The exchange part, as well as the so-called coulombic part, of the bond energies is seen to obey a simple vector addition rule. A complete treatment of a four-atom reaction without symmetry ($H_2+ICl \rightarrow HI+HCl$) is carried out and results are compared with the existing experiments.

INTRODUCTION

THE simultaneous interaction of more than two atoms with each other is a complicated theoretical problem. Insofar as it manifests itself in chemical exchange reactions it can be described on the following four assumptions:

I. When an atom is joined by at least sufficiently many bonds to saturate its valence the lower potential energies will correspond to configurations which makes additional bonds to this atom as small as is possible without weakening the main bonds.

IIa. The energy of interaction of more than two atoms can be expressed as a function of single bond additive and exchange energies. Here we are using the word "bond" in a somewhat wider sense than usual, meaning electron pair energy which two atoms at any particular distance would exhibit in the absence of other atoms.

IIb. The interaction energy a of a pair of atoms consists of two parts: one part A arising from "classical" forces, which is purely additive, and a second α arising from quantum-mechanical electron exchange. This latter part is not simply additive and is responsible for the valence properties of atoms.

III. In the approximation considered here, the addition law for the latter type of binding is taken to be that following from perturbation theory calculations. For the case of three and four atoms the following well-known formula is obtained:[1]

$$E=A+B+C-(\tfrac{1}{2}[(\alpha-\beta)^2+(\beta-\gamma)^2+(\gamma-\alpha)^2])^{\frac{1}{2}}, \quad (1)$$

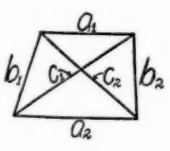

FIG. 1.

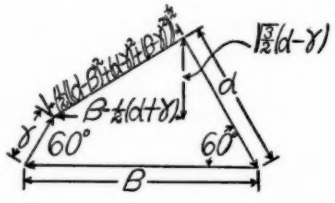

FIG. 2. Vector addition of exchange binding.

[1] F. London, Zeits. f. Elektrochemie **35**, 552 (1929); Eyring and Polanyi, Zeits. f. Physik **B12**, 19 (1931).

where $a=A+\alpha$, $b=B+\beta$, $c=C+\gamma$, are the bonds in the case of three atoms, while for four atoms (see Fig. 1),

$$a=a_1+a_2, \quad b=b_1+b_2. \quad c=c_1+c_2$$
$$A=A_1+A_2, \text{ etc.},$$
$$\alpha=\alpha_1+\alpha_2, \text{ etc.}$$

IV. The actual amounts of additive and of exchange energy for each pair are taken to be constant fractions of the total interaction energy as represented by its Morse curve.

$$\begin{aligned} A_1&=\lambda a_1, & \alpha_1&=(1-\lambda)a_1, \\ B_1&=\lambda b_1, & \beta_1&=(1-\lambda)b_1, \\ C_1&=\lambda c_1, & \gamma_1&=(1-\lambda)c_1. \end{aligned} \quad (2)$$

The assurance with which these four assumptions can be accepted probably decreases in the order in which they are quoted. It will naturally be very interesting to see to what extent these assumptions, taken separately, can be justified or improved upon by comparison with experiment. Even the most specific assumption IV has not been shown to be in disagreement with experiment for configurations near the activated state though for interatomic distances less than the equilibrium distance of two atoms the fraction λ certainly decreases with decreasing distance. When more experimental information is available we may find it desirable to replace the assumption of a percentage λ not varying with distance, by more general relations. There is nothing in our present procedure that would not be equally well adapted to such a generalization. We shall find that assumptions I and II, together with very much less specific assumptions than III and IV, permit us to draw conclusions based only on the potential curves of the atom pairs and on geometrical relations. In view of the semi-empirical basis of (1) it is desirable to carry the more firmly established assumptions to their farthest logical conclusions before making more specific assumptions about (1). For example, the

conclusions that activated complexes for three monovalent atoms should be linear and that activated complexes of four monovalent atoms are planar or more generally that configurations are more stable the smaller the exchange binding between the atoms not paired in the ordinary chemical sense rest on a more general basis than III and IV and yet these conclusions are sufficient to enable us to find the "best reaction surface" in bond space as we shall see.

We propose to describe the potential function E of a three or four-particle system in bond space instead of the usual configuration space. That is, we shall represent our system by using the three bond energies a, b, c as orthogonal coordinates. That this is possible for four atoms depends on the fact that the three pairs of bonds a_1 and a_2, b_1 and b_2, c_1 and c_2 enter into (1) only through their sums. Apparently it is generally true that the interaction energy of an even numbered particle system, $2n$, involves no more linearly independent combinations of bonds to express the energy than does the one for $(2n-1)$ atoms.

By abandoning the configuration space one sacrifices the foremost advantage of that treatment, namely that the configurational changes of the system in a reaction may be represented by a mass point subjected to the known potential E and obeying the laws of ordinary mechanics. But such a representation turns out to be not feasible for more than three particles, quite apart from the complications in visualizing which arise from the many dimensions.

The success and the simplicity of the new treatment depend on the following fact: In general, of the six parameters specifying a configuration of four particles in space, only two, say a and b, need be considered as actually independent and as determining a surface B which will include the best reaction path. This surface will be considered in detail later. A reaction may be described by saying that the system starts from a configuration where a has its maximum value and $b=c=0$, and proceeds to a final state where b is a maximum and $a=c=0$. By the "best reaction path" is meant that sequence of configurations by which this transition is accomplished in a way most economical of potential energy. Thus each of these configurations must have a minimum potential energy in all directions except the one in which the reaction proceeds. The point of highest potential energy along this path represents the activated configuration. It is clearly true that for this point—a saddle point—the energy is stationary in all directions, a fact of fundamental importance in that it allows us to use the theory of small vibrations for setting up the partition function of the activated state. Mathematically, the activated configuration is thus determined as the point with the highest potential along the best reaction path for which $dE=0$.

It is characteristic of the theory of reaction rates that the original and the activated configuration are the only ones whose physical properties determine the rate of reaction. Only in the case of two saddle points of nearly equal heights is it necessary to consider both.

Since we propose to describe the progress of a reaction in bond space we must consider how points in bond space and in configuration space correspond to each other. In the case of three atoms, the three bonds are just sufficient to determine the configuration, except for a certain ambiguity which is readily disposed of.[2] In the case of four atoms, however, the situation is complicated by the fact that it takes six parameters to determine a configuration so that there exist in general ∞^3 configurations for a point (a, b, c). On the other hand there are regions in bond space which are not attainable by a particular system owing to the obvious restriction on the greatest absolute value a bond can take, and also owing to the geometrical restrictions which prevail among the six distances between four atoms. It so happens that in spite of this general situation the best reaction path, because of the conditions on c, always lies on the boundary surface between the physically attainable and the unattainable region, and for this surface B there does exist a point to point correspondence between bond and configuration space.

We now show that the best reaction path lies completely on the boundary surface. We start

[2] This ambiguity arises in the case of four, three and even two-atom systems, from the fact that two different distances are always associated with every negative value of E occurring in the diatomic potential curve. No complication arises from this fact since the reaction path never involves configurations where an interatomic distance is contracted beyond the equilibrium distance for that pair.

out by finding for every given pair of values, a, b, the smallest possible value of $|c|$ which is attainable by our system under its geometrical restrictions. The surface so defined in bond space will clearly be a boundary surface for the attainable region. Its equation can be set down as

$$d(c_1+c_2)_{a,\,b}=0. \tag{3}$$

On the other hand, if we restrict our attention to all those points (a, b, c) which for given values a, b, have their minimum value of E, then the surface so obtained must completely contain the best reaction path. But this condition can be written

$$(dE)_{a,\,b}=(\partial E/\partial c)(dc_1+dc_2)=0. \tag{4}$$

It should be borne in mind that the differentials dc_1 and dc_2 occurring in (3) and (4) are related to each other in a way depending upon the geometry of the system, i.e., on the specific values assigned to a_1, a_2, b_1, b_2, and also involve the Morse curves of the individual atom pairs. But from (4) it follows that a stationary value of E corresponds to a stationary value of c, ignoring the unimportant singular cases where $\partial E/\partial c=0$. Whether a minimum of E corresponds to a minimum or a maximum of c, is determined by the sign of $\partial E/\partial c$, which in the particular case of the London formula can be written as:

$$\partial E/\partial c=\lambda-(1-\lambda)(c-\tfrac{1}{2}(a+b))\times[\tfrac{1}{2}(a-b)^2+(a-c)^2+(b-c)^2)]^{-\frac{1}{2}}. \tag{5}$$

This is negative if $|c|$ is the smallest of the bonds, as it is for the comparatively small values which λ assumes for nonmetallic elements. Thus we have shown that, to make E as low as possible for a given a and b, the value $|c|$ must be made a minimum, and thus the best reaction path lies in the boundary surface. Equations exactly similar to (3) and (4) can be discussed for a and b. If $|a|$ happens to be the largest of the three, then $\partial E/\partial a$ is positive so that a minimum value of E will now go with a maximum value for $|a|$. In some cases it is found more convenient to use this latter relationship. In the intermediate case where $|b|$ say, is neither the largest nor the smallest of the three $|b|$ should be made a minimum or a maximum depending on whether $\partial E/\partial b\lesseqgtr 0$. A mechanical device which enables one easily to satisfy condition (3) will be described in a later section.

A Vector Addition Rule for Bond Energies

After this more or less kinematical discussion of configurations in bond space we now turn to the question of the interaction energy of a system of atoms. In particular we shall consider the nature of the equipotential surfaces defined by (1) and (2). We now prove that the law of combination of exchange energies as expressed by the square root in (1) is equivalent to the following simple vector addition:

$$E_{ex}=(\tfrac{1}{2}[(\alpha-\beta)^2+(\beta-\gamma)^2+(\gamma-\alpha)^2])^{\frac{1}{2}}=|\alpha+\omega\beta+\omega^2\gamma|, \tag{6}$$

where ω and ω^2 are third roots of unity. This situation is also represented by the vector diagram Fig. 2 in terms of which the following simple proof can be given: If we plot the bond energies α, β, γ end-on making angles of 60° with each other as in Fig. 2, then the resultant has the horizontal and vertical components $(\beta-\frac{1}{2}(\alpha+\gamma))$ and $\frac{1}{2}\times 3^{\frac{1}{2}}(\alpha-\gamma)$. Thus its length turns out to be just E_{ex}. The existence of such a simple vector addition rule for bonds in three and four particle systems is significant and suggests the possibility of similar relations in more complicated cases. Its practical importance lies in the avoidance of practically all calculations in obtaining potential energies from the individual bonds, especially since the 60° triangular paper on the market is ideally suited for such purposes.

The equipotential surfaces in bond space likewise turn out to be strikingly simple. Transforming to new orthogonal coordinates by means of a rotation of the a, b, c axes,

$$\begin{aligned} x&=1/\sqrt{2}(a-b),\\ y&=1/\sqrt{6}(a+b-2c),\\ z&=1/\sqrt{3}(a+b+c), \end{aligned} \tag{7}$$

we find the expression for the energy of the system using (1) and (2) becomes:

$$E=\sqrt{3}(\lambda z-(1-\lambda)(\tfrac{1}{2}(x^2+y^2))^{\frac{1}{2}}=\sqrt{3}[\lambda z-((1-\lambda)/\sqrt{2})r]. \tag{8}$$

Thus it is seen that the equipotential surfaces are circular cones with their axes along the z axis, and with their apex angle $2\tan^{-1}\lambda/(1-\lambda)$ depending only on the ratio of additive to exchange binding. The relation exhibited by (8) that E_{ex} is simply proportional to the distance r

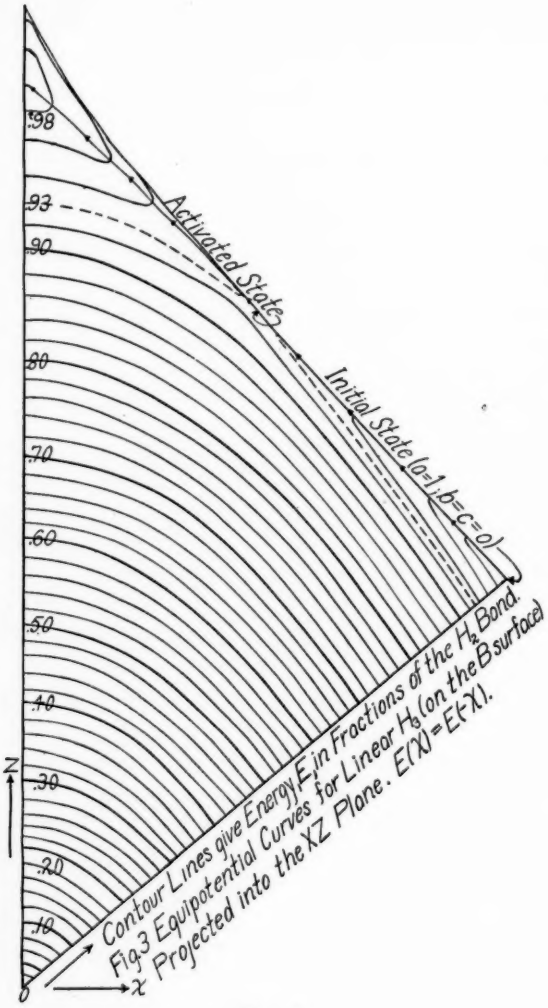

FIG. 3.

from the z axis provides an alternative proof of our previously given vector addition rule since the three valence bonds α, β, γ when plotted along their axes, a, b, c appear to make just the angles used in Fig. 2 to an observer looking down the z axis. The equipotential surfaces in bond space together with the boundary surface B determine completely the best reaction path: The intersection of the equipotentials with B traces a system of equipotential lines on B of much the same character as the system of equipotential lines found in the usual plots of a potential surface in configuration space for a three-atom problem.

In many triatomic reactions the smallest bond, c, remains very small throughout so that the surface B can be approximated by the plane $c=0$. In this case the equipotential curves on B are simply a system of confocal ellipses generated by the intersection of the ab plane with the cones. The reaction path is then the line where either a or b has its most negative value, c being zero.

The other extreme where $|c|$ assumes comparatively large values for three-atom reactions is typified by the case of three H atoms. In Fig. 3 we have given the equipotential curves plotted on the B surface as they appear looking along the y direction in bond space. This particular projection was chosen because of the ease with which the construction can be carried out.

The potential diagram for $c=0$ is practically identical with the one for 3 H atoms in the region lying below the best reaction path indicated by arrows in Fig. 3.[3] It has seemed desirable to give this brief discussion of two typical three-atom cases since the general features are just the same as for four-atom reactions.

LOCATING THE ACTIVATED CONFIGURATION OF FOUR ATOMS

It is in the application to four-atom reactions that the use of bond space instead of configuration space proves to be of real advantage. Even in the presentation of a symmetric case such as H_2+I_2, the method of finding the activated state as well as the representation of the potentials in configuration space becomes extremely laborious. With the present method, a four-atom system with no symmetry at all such as H_2+ICl has been investigated and the reaction rate calculated with no unreasonable hardships.

A mechanical device for selecting configurations which, for a given pair of values a, b, have the smallest possible $|c|$ to go with it, is pictured in Fig. 4. Scales are provided on which the six interatomic distances between four atoms H, H, I, Cl are marked with their respective bond

[3] As pointed out in reference 2, we are ignoring throughout configurations involving "contracted" bonds. However, if one wants to extend the B surface into this region, it results in making multiple-valued the present allowed portion of the B surface in the case when $c=0$. In the case $c\neq 0$, the extended B surface bends over completely in the direction of the z axis, crosses it and finally departs in the direction of infinite positive z.

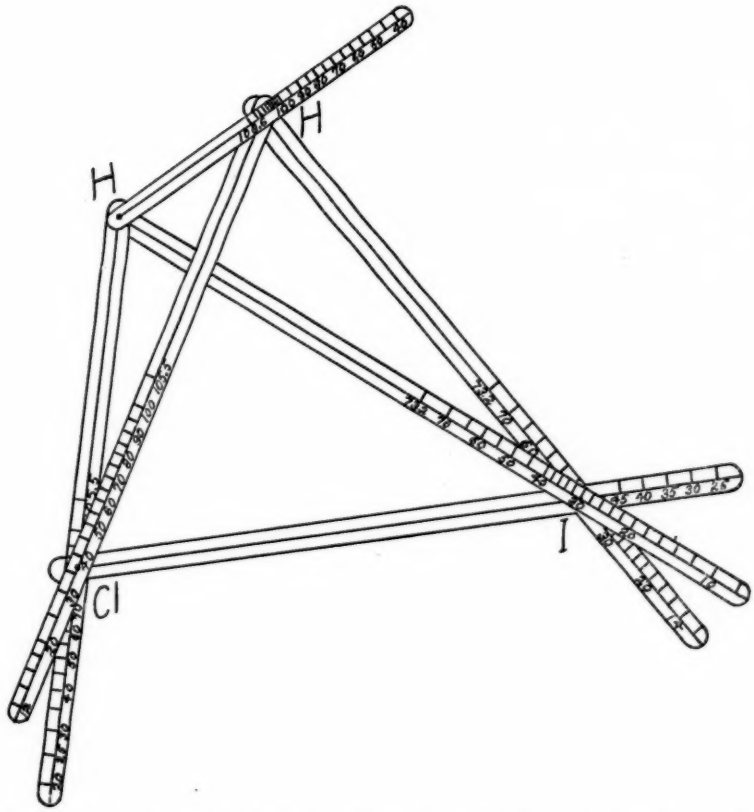

FIG. 4. Device for rapidly finding configurations which lie on the boundary surface, i.e., having the lowest sum, c, for the diagonal bonds for a given a and b. The activated configuration is the one shown.

energies and the scales so obtained attached to each other so as to present a model of the plane configurations of these four atoms. The scales are hinged by means of thumb-tacks in such a way that, without varying four of the six distances, the remaining two, let us say the diagonal ones, can be adjusted until the sum of their energies (absolute values) as read directly from their scales is a minimum. In doing this one must of course try various combinations of a_1 and a_2 which add up to the same a, and also various combinations for b, until an absolute minimum for $|c|$ is obtained. By way of emphasis we should like to point out that this method of variation leads to a unique configuration for fixed values of a and b thus establishing our previous statement that there exists a point-to-point correspondence between those points in three-dimensional bond space which lie on the surface B, and the points on the corresponding surface in six dimensional configuration space.

A point of the B surface can be found in a few minutes with the use of this device. A sufficient number of such combinations (a, b, c) must be found to map out the potential diagram on the B surface. A very pleasant feature of this procedure is that it enables us to describe the essential aspects of the potential surface in two-dimensional diagrams in spite of the fact that the number of parameters of the dynamical problem is six. The plot for the reaction, $H_2+ICl \rightarrow HI+HCl$ is given in Fig. 5, showing the projection on the ab plane of the intersections of the boundary surface with the equipotential curves. An alternative way which is sometimes more satisfactory is to plot the xy projection.

Since the B surface does not depend on a particular potential law, the points (a, b, c) determined in the way described may be used for

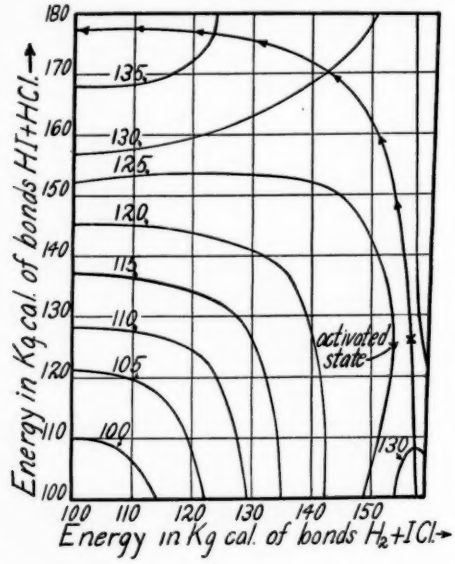

FIG. 5. Projection on the *ab* plane of the intersections of the equipotentials with the boundary surface *B* for the reaction $H_2+ICl \rightarrow HI+HCl$.

different fractions λ of additive binding and indeed for different laws of interaction and the results compared with experiment. In this particular case we have located the activated point and determined the activation energy for 14, 17 and 20 percent of additive binding, with results given later in Table II.

The constants used in the Morse curves for the various bonds are given in Table I where the Morse curve is given by

$$E=D'[e^{-2a(r-r_0)}-2e^{-a(r-r_0)}].$$

TABLE I.

	r_0 (A°)	ω_0 (cm^{-1})	D (kcal.)	D' (kcal.)	a
H−H	0.74	4375	102.4	108.6	1.941
I−Cl	2.310	384.6	49.4	49.95	1.871
H−Cl	1.282	2840.8	101.5	105.5	1.781
H−I	1.616	2233	70.0	73.2	1.700

There is nothing in our procedure which limits us to the constant percentage rule as expressed by the constant λ in Eq. (2). We might equally well have replaced each of the energy scales in our model by a double scale giving the additive and the exchange part of the bond as separate functions of the distance.

The accuracy with which the activated configuration can be found using this easily improvised mechanical model (of a size no larger than is convenient) is more than sufficient for all practical purposes. But if greater accuracy is required, a rapidly converging mathematical procedure can be devised which renders the question of attainable accuracy merely one of how much numerical computation one is willing to bestow on the solution. Suppose that from the mechanical model we have obtained a configuration close enough to the activated one so as to make all the first derivatives $\partial E/\partial q_i$ small, and suppose that we are in possession of a complete set of second derivatives $\partial^2 E/\partial q_i \partial q_k$, taken with respect to all five "plane" coordinates q_i, for this configuration. Knowledge of these second derivatives is necessary anyway for the calculation of the characteristic vibrations, and the method for obtaining them will be described later in that connection. Denoting by Δq_i the differences of the coordinates of the true activated configuration minus the ones for the approximate one which was found, we can expand the first derivatives $\partial E/\partial q_i$ in the neighborhood of the activated point where $(\partial E/\partial q_i)_{q_i=0}=0$, as follows:

$$(\partial E/\partial q_i)_{q_i=-\Delta q_i}=\sum_k(\partial^2 E/\partial q_i \partial q_k)(-\Delta q_k). \quad (9)$$

Solving this set of inhomogeneous linear equations for the quantities Δq_k and using five arbitrary quantities λ_k as multipliers, we can express our solution in a particularly condensed form as follows:

$$D\equiv\begin{vmatrix} -\sum\lambda_k\Delta q_k & \partial E/\partial q_1 & \partial E/\partial q_2 & \cdots & \partial E/\partial q_5 \\ \lambda_1 & \partial^2 E/\partial q_1\partial q_1 & \partial^2 E/\partial q_1\partial q_2 & \cdots & \partial^2 E/\partial q_1\partial q_5 \\ \lambda_2 & \cdot & \cdot & \cdot & \cdot \\ \cdot & \cdot & \cdot & \cdot & \cdot \\ \cdot & \cdot & \cdot & \cdot & \cdot \\ \lambda_5 & \partial^2 E/\partial q_5\partial q_1 & \cdot & \cdots & \partial^2 E/\partial q_5\partial q_5 \end{vmatrix}=0. \quad (10)$$

TABLE II.

	Config.*	H—H r_1	I—Cl r_2	H—Cl r_3	H—I r_4	H—Cl r_5	H—I r_6	$\partial E/\partial q_1$	$\partial E/\partial q_2$	$\partial E/\partial q_3$	$\partial E/\partial q_4$	$\partial E/\partial q_5$
17%	1	.8033	2.335	1.597	2.264	2.214	2.475	2.966	−4.022	−3.831	−1.519	.795
	2	.8048	2.354	1.597	2.200	2.195	2.460	.395	− .399	.158	.200	− .513
20%	1	.791	2.346	1.564	2.372	2.166	2.548	1.071	.229	−1.050	−4.143	−1.415
	2	.792	2.345	1.564	2.330	2.190	2.508	.037	− .06	.80	.48	.06
14%	1	.830	2.39	1.61	2.08	2.24	2.41					

* 1 and 2 refer to the preliminary and the improved configuration. Distances are given in A units.

From (10) a particular Δq_ρ is determined by putting the corresponding $\lambda_\rho = 1$ and all the other λ's equal to 0. For practical computation it is very convenient to first reduce the determinant D to diagonal form except for the first row and the first column, thus obtaining all quantities Δq_i at once. These five quantities define a certain change in the originally assumed configuration, a change which can be carried out graphically with great ease and precision. For this new configuration the first derivatives $\partial E/\partial q_i$ may be recalculated and the improvement obtained in locating the activated point may be judged by the decreases simultaneously obtained in all five derivatives. The process has been applied to the activated configurations of H_2+ICl both for $\lambda = 17$ percent and 20 percent, with results tabulated in Table II. The simultaneous decrease of all five derivatives by approximately a factor 0.10 must be very striking to anyone who tries to improve the approximate configuration in a less systematic fashion. The activation energies E_c (see Fig. 6) for 14 percent and for 20 percent were found to be 41.2 and 24.9 kcal., respectively. By linear interpolation a percentage of 17 was indicated as giving $E_c = 33$. The experimental value of E is approximately 34 kcal.[4] The activated point for 17 percent was then actually determined and gave an activation energy $E_c = 32.8$ kcal. The activated configuration for 14 percent was not determined with the same accuracy as for the other two cases. Sherman and Li[5] have calculated a value of 24.6 kcal. using 14 percent additive binding in agreement with the value given here.

THE VIBRATIONS OF THE ACTIVATED STATE (VIBRATIONS OF PLANE CONFIGURATIONS OF FOUR UNLIKE ATOMS)

Six of the twelve modes of motion of four atoms arranged in a plane involve a change in the relative positions of the atoms while the other six amount to rigid translations or rotations of the whole molecule, and proceed without change in the potential energy. Of the "internal" motions, five preserve the plane arrangement of the four atoms whereas the sixth involves displacements different in sign for adjacent atoms and at right angles to the plane of equilibrium. Since this plane is obviously a plane of symmetry for the molecule, this last mode belongs to a symmetry class different from the rest and the secular equation will split into two factors of first and fifth degree, respectively. There are no other symmetry conditions imposed on the activated configuration as there is in reactions of the type $H_2+I_2 \rightarrow 2HI$ where the secular equation decomposes into 1+2+3 degrees of freedom.[6]

We consider first the vibrations where the plane arrangement is preserved but ignore translational motions in this plane by keeping the center of gravity fixed at the origin. Tentatively we introduce 6 parameters the meaning of which is apparent from Fig. 7 and the following remarks: q_3 is the distance between the two centers of gravity of m_1 with m_2 and m_3 with m_4. One of these centers of gravity separates q_1 into

[4] Bonner, Gore and Yost, J. Am. Chem. Soc. **57**, 2723 (1935).

[5] Sherman and Li, J. Am. Chem. Soc. **58**, 690 (1936).

[6] Wheeler, Topley and Eyring, J. Chem. Phys. **4**, 178 (1936).

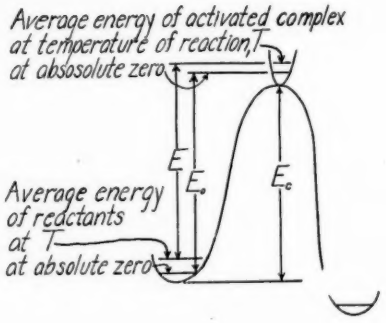

FIG. 6. Activation energies: E is the usual difference in average energies at temperature of reaction; E_0 = activation energy at absolute zero; E_c = "classical" activation energy at absolute zero. All are useful quantities in the theoretical treatment of reaction rates.

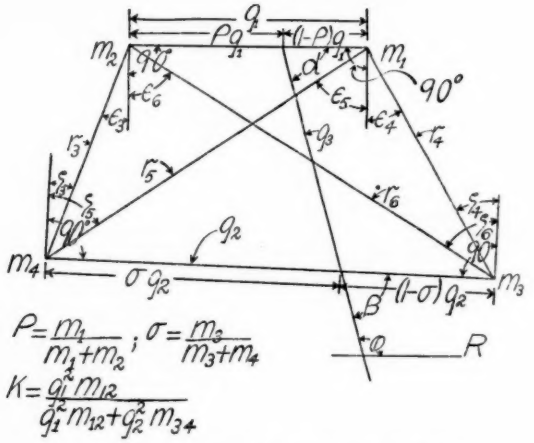

FIG. 7. Notation used in treating four atoms.

two parts in the ratio $\rho : (1-\rho)$ and the other separates q_2 in the ratio $\sigma : (1-\sigma)$. These six coordinates not only describe the relative positions of the four particles but also the angular position φ of the whole system relative to a reference line R fixed in the plane. Thus the kinetic energy, when expressed in all six parameters, includes a part arising from rotations in the plane which can be separated from the rest because such a motion involves no changes in the potential energy.

The final coordinates were chosen in such a manner as to give a sum of square terms for the kinetic energy. This determines the coordinates, of course, only to within an orthogonal transformation, but the rotational coordinate Φ is uniquely determined by the requirement that it be normal to all the other coordinates none of which can involve the parameter φ.

The expression for the kinetic energy in terms of the parameters defined in Fig. 7 is easily calculated to be:

$$2K = m_{12}\dot{q}_1^2 + m_{34}\dot{q}_2^2 + m_{1234}\dot{q}_3^2 + a\dot{\varphi}^2 + b(2\dot{\varphi}\dot{\alpha} + \dot{\alpha}^2) + c(2\dot{\varphi}\dot{\beta} + \dot{\beta}^2), \tag{11}$$

where m_{12}, m_{34} and $m_{12\,34}$ are reduced masses of m_1 with m_2, m_3 with m_4, m_1+m_2 with m_3+m_4 respectively, and where a, b, c stand for

$$a = \sum_1^4 m_i R_i^2, \quad b = q_1^2 m_{12}, \quad c = q_2^2 m_{34}.$$

The R's measure distances from the center of gravity of the system. The last three terms of (11) are easily transformed into a sum of squares if we substitute

$$\dot{u} = \dot{\varphi}(a-b-c)^{\frac{1}{2}}, \quad \dot{v} = b^{\frac{1}{2}}(\dot{\alpha}+\dot{\varphi}), \quad \dot{w} = c^{\frac{1}{2}}(\dot{\beta}+\dot{\varphi}),$$

which property is preserved under any orthogonal transformation, in particular the following one:

$$\begin{aligned} U &= a^{-\frac{1}{2}}((a-b-c)^{\frac{1}{2}}u + b^{\frac{1}{2}}v + c^{\frac{1}{2}}w), \\ V &= [(a-b-c)/(a(b+c))]^{\frac{1}{2}}[-(b+c)/(a-b-c)^{\frac{1}{2}}u + b^{\frac{1}{2}}v + c^{\frac{1}{2}}w], \\ W &= (b+c)^{-\frac{1}{2}}(c^{\frac{1}{2}}v - b^{\frac{1}{2}}w). \end{aligned} \tag{12}$$

Substituting for these variables in terms of the original parameters φ, α, β and also for a, b, c we obtain:

$$2K = m_{12}\dot{q}_1^2 + m_{34}\dot{q}_2^2 + m_{1234}\dot{q}_3^2 + \left[q_1^2 m_{12} + q_2^2 m_{34} - \frac{(q_1^2 m_{12} + q_2^2 m_{34})^2}{\sum m_i R_i^2}\right]\dot{q}_4^2 + \frac{q_1^2 q_2^2 m_{12} m_{34}}{q_1^2 m_{12} + q_2^2 m_{34}}\dot{q}_5^2 + \frac{\dot{\Phi}^2}{\sum m_i R_i^2}, \tag{13}$$

where $q_4=k\alpha+(1-k)\beta=(q_1^2m_{12}\alpha+q_2m_{34}\beta)(q_1^2m_{12}+q_2^2m_{34})^{-1}$, $q_5=\alpha-\beta$,

$$\dot{\Phi}=\sum m_iR_i^2\dot{\varphi}+q_1^2m_{12}\dot{\alpha}+q_2^2m_{34}\dot{\beta}. \tag{14}$$

The newly defined coordinates q_4 and q_5 do not involve the angle φ and are thus orthogonal to the rotations of the system as a whole. The rotational coordinate is thus Φ; since it does not enter into the potential function for the system, it may be omitted from further consideration.

As was stated previously there exists but one internal degree of freedom which carries the four particles out of their plane of equilibrium $z=0$. Indeed, of the four independent motions involving displacements z_i at right angles to the equilibrium plane we may choose two as the rotations r_x and r_y, and a third as the translation t_z, and represent them by the following coordinates:

$$r_x=\sum m_iz_ix_i=q_1m_{12}\sin\alpha(z_1-z_2)+q_2m_{34}\sin\beta(z_3-z_4),$$

$$r_y=\sum m_iz_iy_i=(q_3/\sum m_i)\{-(m_3+m_4)(m_1z_1+m_2z_2)+(m_1+m_2)(m_3z_3+m_4z_4)\},$$

$$t_z=\sum m_iz_i.$$

The internal motion is then completely determined by the requirement that its coordinate q_6 be orthogonal to r_x, r_y, t_z. Let q_6 be a linear function of the z displacements $q_6=\sum_i\sigma_iz_i$, then the following relations must hold among the σ's:

$$\sum_{i=1}^{4}m_i\sigma_ix_i=0,\quad \sum_{i=1}^{4}m_i\sigma_iy_i=0,\quad \sum_{i=1}^{4}m_i\sigma_i=0.$$

Thus we find by a simple elimination process, that q_6 is proportional to:

$$q_6\sim\begin{vmatrix} z_1 & z_2 & z_3 & z_4 \\ q_1m_{12}\sin\alpha & -q_1m_{12}\sin\alpha & q_2m_{34}\sin\beta & -q_2m_{34}\sin\beta \\ q_1m_{12}\cos\alpha-m_1q_3\dfrac{m_3+m_4}{\sum m_i} & -q_1m_{12}\cos\alpha-m_2q_3\dfrac{m_3+m_4}{\sum m_i} & q_2m_{34}\cos\beta+m_3q_3\dfrac{m_1+m_2}{\sum m_i} & -q_2m_{34}\cos\beta+m_4q_4\dfrac{m_1+m_2}{\sum m_i} \\ m_1 & m_2 & m_3 & m_4 \end{vmatrix}.$$

One possible way of describing the internal motion connected with q_6 is the following:

$$\begin{aligned} \Delta z_1&=\Delta q_6\left[\frac{\cot\alpha-\cot\beta}{q_3(m_1+m_2)}+\frac{1}{q_1m_1\sin\alpha}\right],\quad \Delta z_3=\Delta q_6\left[\frac{-\cot\alpha-\cot\beta}{q_3(m_3+m_4)}-\frac{1}{q_2m_3\sin\beta}\right], \\ \Delta z_2&=\Delta q_6\left[\frac{\cot\alpha-\cot\beta}{q_3(m_1+m_2)}-\frac{1}{q_1m_2\sin\alpha}\right],\quad \Delta z_4=\Delta q_6\left[-\frac{\cot\alpha-\cot\beta}{q_3(m_3+m_4)}+\frac{1}{q_2m_4\sin\beta}\right]. \end{aligned} \tag{15}$$

The displacements (15) comply with the three conditions:

$$\sum m_ix_i\Delta z_i=0,\quad \sum m_iy_i\Delta z_i=0,\quad \sum m_i\Delta z_i=0,$$

as can be readily established. Thus they are orthogonal to the three rigid motions (Δr_x, Δr_y, Δt_z), and of course also to the other modes which do not involve z_i. Using (15), the kinetic energy K_6 associated with q_6 is then

$$2K_6=\dot{q}_6^2\left[\left(\frac{\cot\alpha-\cot\beta}{q_3}\right)^2\left(\frac{1}{m_1+m_2}+\frac{1}{m_3+m_4}\right)+\left(\frac{1}{q_1\sin\alpha}\right)^2\frac{1}{m_{12}}+\left(\frac{1}{q_2\sin\beta}\right)^2\frac{1}{m_{34}}\right].$$

The next problem is the computation of the force constants of the activated configuration. Since the activated configuration, like a stable configuration of atoms, has a stationary value of the interaction energy, it is actually in stable equilibrium in all degrees of freedom except the one along which

the reaction proceeds. That means that all first derivatives $\partial E/\partial q_\alpha$ are 0 and that for small displacements from the activated configuration the energy function can be expanded:

$$dE=\sum_{\alpha\beta}\frac{\partial^2 E}{\partial q_\alpha \partial q_\beta}dq_\alpha dq_\beta. \tag{16}$$

The second derivatives in (16) are force constants for small displacements from equilibrium. When transformed into a sum of squares, only one force constant in (16) will exhibit a negative sign.

It has been preferable here to follow an explicit analytical procedure in deriving numerical values for the force constants rather than the previously followed methods which though applicable in simpler cases become excessively laborious for more degrees of freedom. One other fact should be borne in mind. The present method of second derivatives gives the force constants for infinitesimal vibrations so that in case of considerable anharmonicities they may not give the correct frequencies of finite vibrations.

Formulas necessary for the calculation of the second derivatives are presented in Tables III, IV and V. Formulas in IV and V are of course perfectly general and depend only on the geometry of the quadrilateral (Fig. 7). They give only first derivatives since tabulation of all second derivatives would require too much space; however, calculation of the second derivatives $\partial^2 r_i/\partial q_\alpha \partial q_\beta$ from IV, V requires no further consideration of Fig. 7.

The second derivative $\partial^2 E/\partial q_6^2$ remains to be calculated. We have

$$\frac{\partial^2 E}{\partial q_6^2}=\sum_{ij}\frac{\partial^2 E}{\partial r_i \partial r_j}\frac{dr_i}{\partial q_6}\frac{dr_j}{\partial q_6}+\sum_i\frac{\partial E}{\partial r_i}\left\{\frac{\partial^2 r_i}{\partial z_i^2}\left(\frac{\partial z_i}{\partial q_6}\right)^2+\frac{dr_i}{dz_i}\frac{\partial^2 z_i}{\partial q_6^2}\right\}, \tag{17}$$

which reduces to

$$\frac{\partial^2 E}{\partial q_6^2}=\sum_i\frac{\partial E}{\partial \alpha_i}\frac{\partial \alpha_i}{\partial r_i}\frac{1}{r_i}\left[\frac{d}{dq_6}(z_{i2}-z_{i1})\right]^2 \tag{18}$$

since all the derivatives $\partial r_i/\partial q_6$ are zero on account of the symmetry character of this mode of motion (all the r's are minima in the plane arrangement) and since

$$\frac{\partial^2 z_i}{\partial q_6^2}=0 \quad \text{and} \quad \frac{\partial^2 r_i}{\partial z_i^2}=\frac{1}{r_i}.$$

Here the z_i in (17) refer to the z projections of the distances r_i and the quantities z_{i1} and z_{i2} in (18) refer to the two end-points of the interatomic distances r_i. Thus the force constant is given by (18) and all the mixed derivatives involving q_6 vanish identically.

The Vibration Frequencies for the Reaction $H_2+ICl\rightarrow HI+HCl$

In evaluating the terms for the kinetic and the potential energy using 17 percent additive binding we are led to the following secular equations for the five normal vibrations in a plane:

$$\begin{vmatrix} (402.82-.25X) & 5.29 & 93.30 & 107.33 & .87 \\ 5.29 & (246.10-13.86X) & 5.72 & 34.54 & 7.78 \\ 93.30 & 5.72 & (-62.70-.9879X) & -78.64 & -20.12 \\ 107.33 & 34.54 & -78.64 & (112.37-3.99X) & 39.50 \\ .87 & 7.78 & -20.12 & 39.50 & (29.86-.161X) \end{vmatrix}=0.$$

The twisting vibration out of the plane is given by the equation $272.88-1.5788X=0$. Here the force constants are in units of kcal. per mole A^{-2} and in the kinetic energy mass is expressed in molecular weights and distance in angstroms (where distance occurs). The six characteristic frequencies ν_i for

TABLE III.

$$E=\lambda(a+b+c)-(1-\lambda)R.$$

Here $R=[\frac{1}{2}((a-b)^2+(b-c)^2+(c-a)^2)]^{\frac{1}{2}}$ and $a=a_1+a_2,\quad b=b_1+b_2,\quad c=c_1+c_2$

$$\frac{\partial^2 E}{\partial q_\alpha \partial q_\beta}=\sum_i \frac{\partial E}{\partial r_i}\frac{\partial^2 r_i}{\partial q_\alpha \partial q_\beta}+\sum_{ik}\frac{\partial^2 E}{\partial r_i \partial r_k}\frac{\partial r_i}{\partial q_\alpha}\frac{\partial r_k}{\partial q_\beta} \qquad \frac{\partial E}{\partial a_1}=\frac{\partial E}{\partial a_2}=\lambda-\frac{3}{2}\frac{(1-\lambda)}{R}a+\frac{1}{2}\frac{(1-\lambda)}{R}(a+b+c)$$

$$\frac{\partial E}{\partial r_i}=\frac{\partial E}{\partial \alpha_i}\frac{\partial \alpha_i}{dr_i}=\frac{\partial E}{\partial a_i}\frac{da_i}{dr_i} \qquad \frac{\partial^2 E}{\partial a_1^2}=\frac{\partial^2 E}{\partial a_2^2}=\frac{\partial^2 E}{\partial a_1 \partial a_2}=-\frac{3}{4}\frac{1-\lambda}{R^3}(b-c)^2$$

$$\frac{\partial^2 E}{\partial r_i \partial r_k}=\frac{\partial^2 E}{\partial a_i \partial a_k}\frac{da_i}{dr_i}\frac{da_k}{dr_k}+\delta_{ik}\frac{\partial E}{\partial a_i}\frac{\partial^2 a_i}{\partial r_i \partial r_k} \qquad \frac{\partial^2 E}{\partial a_i \partial b_i}=-\frac{3}{4}(1-\lambda)\left[\frac{(a-b)^2}{R^3}-\frac{1}{R}\right]=\frac{\partial^2 E}{\partial c_i^2}+\frac{3}{4}\frac{(1-\lambda)}{R} \quad i=1,2.$$

TABLE IV. *Formulas $\partial r_i/\partial q_j$ valid for any configuration of four atoms in a plane. Notation as in Fig. 7.*

	q_1	q_2	q_3	q_4	q_5
r_1	1	0	0	0	0
r_2	0	1	0	0	0
r_3	$-\rho \sin \epsilon_3$	$\sigma \sin \zeta_3$	$\sin(\alpha-\epsilon_3)$	$q_3\cos(\alpha-\epsilon_3)$	$-\rho(1-k)r_1\cos\epsilon_3-\sigma k r_2\cos\zeta_3$
r_4	$-(1-\rho)\sin\epsilon_4$	$(1-\sigma)\sin\zeta_4$	$\sin(\alpha+\epsilon_4)$	$q_3\cos(\alpha+\epsilon_4)$	$(1-\rho)(1-k)r_1\cos\epsilon_4+(1-\sigma)kr_2\cos\zeta_4$
r_5	$(1-\rho)\sin\epsilon_5$	$\sigma\sin\zeta_5$	$\sin(\alpha-\epsilon_5)$	$q_3\cos(\alpha-\epsilon_5)$	$(1-\rho)r_1(1-k)\cos\epsilon_5-\sigma k r_2\cos\zeta_5$
r_6	$\rho\sin\epsilon_6$	$(1-\sigma)\sin\zeta_6$	$\sin(\alpha+\epsilon_6)$	$q_3\cos(\alpha+\epsilon_6)$	$-\rho(1-k)r_1\cos\epsilon_6+(1-\sigma)kr_2\cos\zeta_6$

TABLE V. *Derivatives of ϵ_i, α and β with respect to the coordinates q_k.*

	q_1	q_2	q_3	q_4	q_5
ϵ_3	$-\frac{\rho}{r_3}\cos\epsilon_3$	$\frac{\sigma}{r_3}\cos\zeta_3$	$-\frac{1}{r_3}\cos(\alpha-\epsilon_3)$	$\frac{q_3}{r_3}\sin(\alpha-\epsilon_3)$	$\frac{1}{r_3}[\rho r_1(1-k)\sin\epsilon_3+\sigma r_2 k\sin\zeta_3]+1-k$
ϵ_4	$-\frac{1-\rho}{r_4}\cos\epsilon_4$	$\frac{1-\sigma}{r_4}\cos\zeta_4$	$\frac{1}{r_4}\cos(\alpha+\epsilon_4)$	$-\frac{q_3}{r_4}\sin(\alpha+\epsilon_4)$	$-\frac{1}{r_4}[(1-\rho)r_1(1-k)\sin\epsilon_4-(1-\sigma)r_2 k\sin\zeta_4]$ $-1+k$
ϵ_5	$\frac{1-\rho}{r_5}\cos\epsilon_5$	$\frac{\sigma}{r_5}-\cos\zeta_5$	$-\frac{1}{r_5}\cos(\alpha-\epsilon_5)$	$\frac{q_3}{r_5}\sin(\alpha-\epsilon_5)$	$-\frac{1}{r_5}[(1-\rho)r_1(1-k)\sin\epsilon_5+\sigma r_2 k\sin\zeta_5]+1-k$
ϵ_6	$\frac{\rho}{r_6}\cos\epsilon_6$	$\frac{1-\sigma}{r_6}\cos\zeta_6$	$\frac{1}{r_6}\cos(\alpha+\epsilon_6)$	$-\frac{q_3}{r_6}\sin(\alpha+\epsilon_6)$	$\frac{1}{r_6}[\rho r_1(1-k)\sin\epsilon_6-(1-\sigma)r_2 k\sin\zeta_6]-1+k$
α	0	0	0	1	$1-k$
β	0	0	0	1	$1-k$

The corresponding derivatives for the angle ζ_i follow from the same table as the ϵ_i by use of the identities: $\epsilon_i-\zeta_i=\pm(\alpha-\beta)$ $i=3, 4, 5, 6$, where the plus sign goes with $i=3, 5$ and the minus sign goes with $i=4, 6$. The geometrical significance of the symbols is given in Fig. 7.

TABLE VI.

Activated configuration for	Moments of Inertia (gram atom, A^2)			Frequencies of char. vibrations				(cm^{-1})		Act. Energy E_c (kcal.)
	A_3	B_3	C_3	ν_1	ν_2	ν_3	ν_4	ν_5	ν_n	
17%	152.95	5.81	158.76	4391.	1580.	1426.	481.	435.	i1128	32.8
20% additive binding	158.54	6.00	164.54	4696.	1522.	1344.	550.	442.	i933	24.9

17 percent additive binding are given in Table VI in wave numbers. They are obtained from the six roots X_i of the secular equations by the simple relationship $\nu_i = 108.46X^{\frac{1}{2}}$.

The corresponding secular equations for 20 percent additive binding are:

$$\begin{vmatrix} (465.07-.25X) & -2.48 & 76.26 & 81.46 & -2.11 \\ -2.48 & (252.68-13.86X) & 11.65 & 38.50 & 6.60 \\ 76.26 & 11.65 & (-47.14-.9878X) & -46.41 & -19.00 \\ 81.46 & 38.50 & -46.41 & (148.57-3.99X) & 34.62 \\ -2.11 & 6.60 & -19.00 & 34.62 & (26.96-.1565X) \end{vmatrix} = 0$$

and $250.08 - 1.631X = 0$.

THE RATE OF REACTION

The general expression for the rate of a reaction of this type has been given.[7, 6] Thus we have the equation

$$k_1 = \kappa\left(\frac{m_3'}{m_1'm_2'}\right)^{\frac{3}{2}} \frac{\sigma_1\sigma_2}{\sigma_3} \frac{5.785\times10^{14}}{T} \frac{(A_3'B_3'C_3')^{\frac{1}{2}}}{I_1'I_2'} \frac{\left(2\sinh\frac{h\nu_1}{2kT}\right)\left(2\sinh\frac{h\nu_2}{2kT}\right)}{\prod_{i=1}^{5}\left(2\sinh\frac{h\nu_i}{2kT}\right)} \times\left(1-\frac{1}{24}\left(\frac{h\nu_n}{kT}\right)^2\right)\exp\left(-\frac{E_c}{kT}\right). \quad (19)$$

Here the subscripts 1 and 2 refer to the hydrogen and iodine chloride molecules, respectively, and 3 to the activated complex. κ, m_i', σ_i and ν_i refer to the transmission coefficient which we take equal to unity, the mass of the ith molecule, the rotational symmetry number and the frequency respectively. $A_3B_3C_3$ are the three principal moments of inertia of the activated complex and I_1' and I_2' the moments of inertia of the hydrogen and iodine chloride molecules respectively. ν_n is the imaginary mode of vibration normal to the barrier. The primes indicate that masses are to be taken in molecular weight units and lengths in angstroms in which case k_1 is given in the units cc moles^{-1} sec.$^{-1}$.

If, as is usual we define the energy of activation as

$$E = kT^2 d\log(k/T^{\frac{1}{2}})/dT$$

we have $$E = E_0 + \sum_{i=1}^{5}\frac{h\nu_i}{\exp(h\nu_1/kT)-1} - \frac{h\nu_1}{\exp(h\nu_1/kT)-1} - \frac{h\nu_2}{\exp(h\nu_2/kT)-1} - \frac{3}{2}kT$$

and $$E_0 = E_c + \sum_{i=1}^{5}\tfrac{1}{2}h\nu_i - \tfrac{1}{2}(h\nu_1 + h\nu_2).$$

[7] Eyring, J. Chem. Phys. **3**, 107 (1935), Eq. (7).

We thus obtain for 17 percent additive binding $E_c=32.8$; $E_0=37.85$ and $E=36.62$ at 503.2°. For 20 percent additive binding $E_c=24.9$; $E_0=30.29$; $E=29.04$. Now defining three A's by the following equations

$$k=A_ce^{-E_c/kT}=A_0e^{-E_0/kT}=Ae^{-E/kT}$$

we obtain Table VII.

TABLE VII.

% additive	T	k	$A_c\times10^{10}$	$A_0\times10^{13}$	$A\times10^{12}$
17	478.2	7.44×10^{-5}	7.36	1.50	4.11
17	503.2	5.12×10^{-4}	9.06	1.46	4.16
17	513.2	1.03×10^{-3}	9.64	1.37	4.09
20	478.2	2.28×10^{-4}	5.51	1.60	4.30
20	503.2	1.01	6.61	1.46	4.17
20	513.2	1.79	7.26	1.43	4.21

These values are to be compared with the experimentally obtained specific reaction rate of Bonner, Gore and Yost.[4] We change k from their units to cc mole^{-1} sec.$^{-1}$ and so obtain $k=.52=1.64\times10^{15}e^{-33,900/k478.2}$; $2.8=1.49\times10^{15}e^{-33,900/k503.2}$ and $5.8=1.60\times10^{15}e^{-33,900/k513.2}$

By inspection of Table VII we see that A is independent of whether 20 percent or 17 percent additive binding is used. This is important since this means it is uniquely fixed by the potential function and depends on no arbitrary constant. If the percentage additive binding were raised to a fraction over 20 percent E would be lowered by a calorie to 28 kcal. and k would then agree rather well with the experimental values. The theoretical k would, however, not increase with temperature as fast as the experimental value does. Thus, if Bonner, Gore and Yost are, as they believe, actually measuring the reaction rate here calculated and if their values of k are dependable then our calculated A is too small by a factor of ≈350. A would be increased by this amount if the three lowest frequencies are actually around 50 wave numbers instead of the calculated values. Such a change would also reduce the excess (E_0-E_c) of the zero-point energy in the activated state over that in the initial state to practically zero. More experiments seem necessary before any of these quantities can be assigned from experiment with assurance. The corresponding isotopic reactions will also be useful in calculating E_0-E_c. Extensive accurate data on reactions of this type will be particularly valuable in determining the accuracy and in suggesting methods for improving the calculation of potential functions of activated complexes.

OCTOBER, 1936 JOURNAL OF CHEMICAL PHYSICS VOLUME 4

The Diamagnetic Anisotropy of Aromatic Molecules

LINUS PAULING, *Gates Chemical Laboratory, California Institute of Technology, Pasadena**

(Received July 11, 1936)

Values of the diamagnetic anisotropy of benzene and other aromatic hydrocarbon molecules are calculated on the basis of the assumption that the p_z electrons (one per aromatic carbon atom) are free to move from carbon atom to adjacent carbon atom under the influence of the impressed fields. When combined with the assumed values for the contributions of the other electrons (-2.0×10^{-6} for hydrogen, -4.5×10^{-6} for aromatic carbon, -6.0×10^{-6} for aliphatic carbon) these lead to principal diamagnetic susceptibilities of molecules in approximate agreement with the available experimental data. The diamagnetic anisotropy of graphite is also discussed.

CERTAIN diamagnetic crystals, such as bismuth and graphite, show pronounced diamagnetic anisotropy, the susceptibility being of normal magnitude in the basal plane and abnormally large in the direction perpendicular to this plane. A similar phenomenon is shown by crystals of aromatic substances. It has been pointed out by Krishnan and his collaborators[1] that the magnitudes and orientations of the principal axes of the susceptibility ellipsoid of

* Contribution No. 555.

[1] (a) K. S. Krishnan, Proc. Ind. Sci. Cong., Madras Session, January, 1929; (b) K. S. Krishnan, B. C. Guha and S. Banerjee, Phil. Trans. Roy. Soc. **A231**, 235 (1933); (c) K. S. Krishnan and S. Banerjee, ibid. **A234**, 265 (1935).

such a crystal are determined by the values of the principal susceptibilities of the molecules of the aromatic substance and by the orientations of the molecules relative to the crystal axes. The susceptibility ellipsoids of the aromatic molecules are found to be approximately prolate ellipsoids of revolution, with the long axis normal to the plane of the ring system. As a result of the valuable investigations of Krishnan and his collaborators this phenomenon has been made the basis of an important auxiliary method for determining the structure of crystals.[1, 2]

A qualitative explanation of these abnormally large diamagnetic susceptibilities as arising from the Larmor precession of electrons in orbits including many nuclei[3] has come to be generally accepted. With the aid of simple assumptions, I have now developed this idea into an approximate quantitative treatment, described below.

Benzene

The Hamiltonian function for an electron in a constant magnetic field of strength H parallel to the z axis is[4]

$$\mathcal{H} = \mathcal{H}^0 + \mathcal{H}' + \mathcal{H}'', \tag{1}$$

in which $\mathcal{H}^0$ is the Hamiltonian function for zero field strength,

$$\mathcal{H}' = -(He/2mc)(xp_y - yp_x), \tag{2}$$

and

$$\mathcal{H}'' = (H^2e^2/8mc^2)(x^2+y^2). \tag{3}$$

The contribution of the electron to the diamagnetic susceptibility of the system can be calculated by the methods of quantum-mechanical perturbation theory, a second-order perturbation treatment being needed for the term in $\mathcal{H}'$ and a first-order treatment for that in $\mathcal{H}''$. In case that the potential function in $\mathcal{H}^0$ is cylindrically symmetrical about the z axis, the effect of $\mathcal{H}'$ vanishes, and the contribution of the electron to the susceptibility (per mole) is given by the Pauli expression, resulting from $\mathcal{H}''$,

$$\chi = -(Ne^2/4mc^2)(\rho^2)_{av}, \tag{4}$$

in which $(\rho^2)_{av}$ is the mean square of the distance of the electron from the z axis. This expression is valid for atoms and monatomic ions, the z axis being passed through the nucleus. It is not applicable (without correction for the term in $\mathcal{H}'$) to molecules. For most molecules a satisfactory approximate treatment can be used which consists in assigning electrons to the nearest nucleus, Eq. (4) being applied to the electrons about each nucleus.

Of the forty-two electrons of the benzene molecule, twelve (the carbon K electrons) make no appreciable contribution to the magnetic susceptibility. Twenty-four of the L electrons (which may be considered to be involved in electron-pair bonds between adjacent atoms) are in orbitals which are symmetric with respect to reflection in the plane of the nuclei. It is probable that the contribution of these to the magnetic susceptibility is normal. The remaining six L electrons, which give to benzene its characteristic electronic structure and properties,[5] occupy orbital wave functions which are antisymmetric with respect to reflection in the plane of the nuclei. The probability distribution function for these electrons is large only in two ring-shaped regions, one above and one below the carbon hexagon. We may well expect that in these regions the potential function representing the interaction of an electron with the nuclei and other electrons in the molecule would be approximately cylindrically symmetrical with respect to the hexagonal axis of the molecule, the electron, some distance above or below the plane of the nuclei, passing almost imperceptibly from the field of one carbon atom to that of the next. Under these conditions the contribution of each of these six electrons to the susceptibility with the magnetic field normal to the plane of the nuclei would be given by Eq. (4), with ρ measured from the hexagonal axis of the molecule, and it would hence be very large. On the other hand, because of the nodal plane of the wave functions these electrons would make only a very small contribution to the susceptibility

[2] S. Bhagavantam, Proc. Roy. Soc. **A124**, 545 (1929); S. Banerjee, Ind. J. Phys. **4**, 557 (1930); K. S. Krishnan, Nature **130**, 313, 698 (1932); K. S. Krishnan and S. Banerjee, ibid. **131**, 653 (1933); **132**, 968 (1933); Zeits. f. Krist. **91**, 173 (1935); K. Lonsdale, Nature **137**, 826 (1936); N. Ganguli, Zeits. f. Krist. **93**, 42 (1936).

[3] P. Ehrenfest, Physica **5**, 388 (1925); Zeits. f. Physik **58**, 719 (1929); C. V. Raman, Nature **123**, 945 (1929); **124**, 412 (1929); C. V. Raman and K. S. Krishnan, Proc. Roy. Soc. **A113**, 511 (1927).

[4] See, for example, J. H. Van Vleck, *Electric and Magnetic Susceptibilities* (Oxford University Press, 1932).

[5] E. Hückel, Zeits. f. Physik **70**, 204; **72**, 310 (1931); L. Pauling and G. W. Wheland, J. Chem. Phys. **1**, 362 (1933).

with the field in the nuclear plane. There would thus arise a large diamagnetic anisotropy of the molecule. If we use for $(\rho^2)_{av}$ the value R^2, in which R is the distance from the axis to the carbon nuclei, 1.39A, the anisotropy is calculated to have the value $\Delta K = -49.2\times10^{-6}$, which is in reasonably good agreement with the experimental value for benzene,[1b] $\Delta K = -54\times10^{-6}$.

A more detailed consideration may be given this argument by evaluating the terms corresponding to $\mathcal{H}'$ and $\mathcal{H}''$ with the use of assumed expressions for the wave functions. Using hydrogen-like $2p_z$ wave functions, the term corresponding to $\mathcal{H}''$ (Eq. (4)) has the value -49.2×10^{-6} for large values of the effective nuclear charge, the absolute value increasing with decrease in the effective nuclear charge, as a result of the greater contribution of large radii to $(\rho^2)_{av}$. The term in $\mathcal{H}'$ can be represented by means of the approximate second-order perturbation theory[6] as

$$\chi' = [(xp_y - yp_x)^2]_{00}/((W_m)_{av} - W_0), \quad (5)$$

in which the numerator represents the diagonal matrix element for the normal state under consideration, W_0 the energy of this state, and $(W_m)_{av}$ an average energy for significant excited states. It is found on evaluating this expression that it is small for reasonable values of the effective nuclear charge. However, this expression as well as that of Eq. (1) are rather sensitive to changes in the assumed wave functions, and there is little prospect at present of carrying out an accurate theoretical calculation of the susceptibility.

Condensed aromatic ring systems

We may now calculate the magnetic anisotropy of other aromatic hydrocarbons in the same way as for benzene, making the assumption that the $2p_z$ electrons are free to move under the influence of the impressed fields from carbon atom to adjacent carbon atom. Our problem is equivalent to that of calculating the magnetic effect of the currents induced in a conducting network. In benzene we have assumed the induced current to flow from atom to atom along circular arcs. In large condensed ring systems, such as graphite, the current would be assumed to flow along straight lines between adjacent atoms. In order to simplify the calculation we shall first consider rectilinear hexagonal nets, and then make a small correction by replacing the outermost lines by circular arcs. We assume in all cases that the electrons are uniformly distributed along the segments of the network, the linear density of electrons being σ.

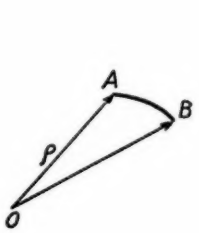

FIG. 1.

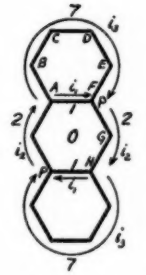

FIG. 2. Induced currents in anthracene.

FIG. 3. Assumed path of induced currents in anthracene.

Let us consider anthracene as an example. One solution of Maxwell's equations corresponding to a magnetic field parallel to the z axis, with strength increasing linearly with the time, involves an electric field acting in a direction in the xy plane at right angles to the radius vector ρ measured from the z axis and with strength proportional to ρ. The integrated ponderomotive force for a segment AB of a conductor is accordingly proportional to the area swept out by the radius vector ρ, in this case OAB. Using as our unit the area of one-sixth of a carbon hexagon, the integrated ponderomotive forces for anthracene (Fig. 2) are $P_1=1$ (for the segment AF), $P_2=2$ (for FGH), and $P_3=7$ (for $ABCDEF$), with values for the other segments given by the center of symmetry of the molecule and field. In addition we must introduce an auxiliary potential at the junction F (relative to A) represented by the symbol p. The effective resistances of the circuits, arising from the inertia of the electrons, are proportional to the lengths of the segments, and have the values $R_1=1$, $R_2=2$, and $R_3=5$. We thus obtain the equations

$$\begin{aligned} i_1 &= 1-p, \\ 2i_2 &= 2+p, \\ 5i_3 &= 7-p \end{aligned}$$

for the currents i_1, i_2, and i_3, together with the conservation equation

[6] L. Pauling and E. B. Wilson, Jr., *Introduction to Quantum Mechanics*, Sec. 27e.

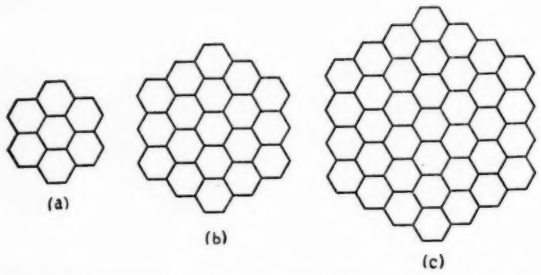

FIG. 4. The aromatic hydrocarbons (a) $C_{24}H_{12}$, (b) $C_{54}H_{18}$, and (c) $C_{96}H_{24}$.

$$i_2=i_1+i_3.$$

The values found on solution of these equations are $i_1=3/17$, $i_2=24/17$, and $i_3=21/17$. These correspond to a completed circuit i_1 about one hexagon and another completed circuit i_3 about three hexagons, the strength of the equivalent magnetic dipole being 66/17. A similar calculation for a benzene hexagon gives the value 1; the quantity $k=66/17$ accordingly represents the relative strengths of the induced magnetic dipoles for the anthracene network of three hexagons and the benzene circuit of one hexagon, difference in the linear electron density σ being neglected.

To obtain the susceptibility difference ΔK we make the following calculation. For naphthalene and higher aromatic hydrocarbons the average C−C distance[7] is 1.41A, corresponding to $\Delta K=-38.0\times10^{-6}$ for a six-electron hexagon. In general we write for ΔK the expression

$$\Delta K=-38.0\times10^{-6}\times k\sigma f, \qquad (6)$$

in which σ is the electron density per C−C bond and f a correction factor described below. Values of σ as well as of k are included in Table I; for anthracene, for example, σ has the value 14/16, there being 14 p_z electrons and 16 C−C segments in the network. The factor f is designed to correct for the assumption that the electrons move along rectilinear paths between the carbon atoms. In benzene we assumed the transit from atom to atom to be along circular arcs. For the condensed ring systems we may correspondingly replace the outermost rectilinear segments by circular arcs, as shown in Fig. 3 for anthracene. This introduces a correction[8] of 23 percent ($f=1.23$), leading to $\Delta K=-159\times10^{-6}$ for anthracene. Table I includes the results of a similar treatment of several hydrocarbons.

In order to predict approximate values of the principal susceptibilities K_1 $(=K_2)$ and K_3 $(=K_1+\Delta K)$ of these substances we may adopt the following empirical procedure. The molal susceptibility of H_2 is -4.00×10^{-6}; we accept -2.00×10^{-6} for H bonded to C. The atomic susceptibility of diamond is -6.00×10^{-6}; we accept this for aliphatic carbon. Now in the aliphatic carbon atom there are four L electrons contributing to the susceptibility in all directions, whereas in the aromatic carbon atom only three remain to be considered, the fourth being involved in the calculation of ΔK. For aromatic carbon, aside from the p_z electron, we accordingly assume the atomic susceptibility -4.5×10^{-6}. The principal susceptibilities of a hydrocarbon are thus given by the approximate expressions

$$K_1=K_2=-(2.0\,n_H+6.0\,n_{C\,al}+4.5\,n_{C\,ar})\times10^{-6} \qquad (7)$$

and

$$K_3=K_1+\Delta K, \qquad (8)$$

[7] L. Pauling, L. O. Brockway and J. Y. Beach, J. Am. Chem. Soc. **57**, 2705 (1935).

[8] The error introduced by using the values of relative currents for rectilinear segments is small.

TABLE I.

	σ	k	$-\Delta K\times10^6$	$-K_1\times10^6$	$-K_3\times10^6$
Benzene, C_6H_6	1	1	49	39	88
Naphthalene, $C_{10}H_8$	10/11	12/5	104	61	165
Anthracene, phenanthrene, $C_{14}H_{10}$	7/8	66/17	159	83	242
Pyrene, $C_{16}H_{10}$	16/19	84/13	237	92	329
Naphthacene, chrysene, etc., $C_{18}H_{12}$	6/7	156/29	214	105	319
Triphenylene, $C_{18}H_{12}$	6/7	60/11	217	105	322
Perylene, $C_{20}H_{12}$	5/6	111/13	314	114	428
Picene, dinaphthanthracene, etc., $C_{22}H_{14}$	11/13	227/33	268	127	395
$C_{24}H_{12}$	4/5	52/3	572	132	704
$C_{54}H_{18}$	3/4	2667/29	2770	279	3050
$C_{96}H_{24}$	8/11	67333/227	8200	480	8680

TABLE II.

	Observed			Calculated	
	$-K_1\cdot10^6$	$-K_2\cdot10^6$	$-K_3\cdot10^6$	$-K_1(K_2)\times10^6$	$-K_3\cdot10^6$
Benzene, C_6H_6	37	37	91	39	88
Durene, $C_{10}H_{14}$	77	86	141	79	128
Hexamethylbenzene, $C_{12}H_{18}$	101	103	164	99	148
Hexaethylbenzene, $C_{18}H_{30}$	165	165	231	159	208
Biphenyl, $C_{12}H_{10}$	67	67	175	74	172
Terphenyl, $C_{18}H_{14}$	98	98	260	109	256
Quaterphenyl, $C_{24}H_{18}$	129	129	345	144	340
1,3,5-Triphenylbenzene, $C_{24}H_{18}$	131	131	347	144	340
Fluorene, $C_{13}H_{10}$	73	73	194	80	178
Naphthalene, $C_{10}H_8$	39	43	187	61	165
Anthracene, $C_{14}H_{10}$	46	53	273	83	242
Phenanthrene, $C_{14}H_{10}$	74	74	240	83	242
Pyrene, $C_{16}H_{10}$	81	81	303	92	329
Chrysene, $C_{18}H_{12}$	88	88	306	105	319
1,2; 5,6-Dibenzanthracene, $C_{22}H_{14}$	110	110	358	127	395

in which n_H, $n_{C\ al}$, and $n_{C\ ar}$ represent the numbers of atoms of these kinds in the molecule.[9] Values calculated in this way are included in Tables I and II.

The hydrocarbons $C_{24}H_{12}$, $C_{54}H_{18}$, and $C_{96}H_{24}$ included in the table have the hexagonal symmetry D_{6h}, as shown in Fig. 4. It is interesting to note that the shape of the molecule has a large effect on the susceptibility; ΔK for the nearly circular molecule $C_{24}H_{12}$ is over twice that for the long molecules picene, etc. ($C_{22}H_{14}$), although the molecules differ only a little in composition. Pyrene (compared with naphthacene) shows the same effect. Aside from this, the configuration of the molecule is of little significance, the susceptibilities for isomers such as anthracene and phenanthrene being the same. Branching of the chain of benzene residues has a small effect (compare naphthacene and triphenylene).

Comparison with experiment

In Table II there are given the available experimental values of the principal susceptibilities of aromatic hydrocarbon molecules, from the papers of Krishnan and his collaborators.[1b, 1c, 10] It should be mentioned that in some cases the values have been obtained from crystal susceptibilities in a straightforward manner, with the use of the results of x-ray investigations of molecular orientations, but that in other cases the values given depend on various assumptions (such as that K_3-K_1 for phenyl and phenylene groups has the value found for benzene). It is seen that with certain exceptions mentioned below the observed and calculated values agree to within about 10 percent, the disagreement probably being due in part to experimental error and in part to theoretical inaccuracy.

The largest differences between calculated and observed values are shown by naphthalene and anthracene. I feel confident that the differences are due to errors in the reported experimental values, especially since good agreement between experiment and theory is found for phenanthrene.

The principal susceptibilities of graphite, per mole of carbon atoms, are reported[11] as $K_1=-5\times10^{-6}$ and $K_3=-275\times10^{-6}$. It is to be noted that the value of K_1 is less than for diamond (-6×10^{-6}), and agrees with our assumed value -4.5×10^{-6} to within the accuracy of its determination. The very large magnetic anisotropy of graphite shows that the p_z electrons are free to move over large areas of the hexagonal network of carbon atoms in the crystal. Extrapolating from the values of Table I, we find that molecules about 40A in diameter would have an anisotropy equal to that observed for graphite. It is interesting that the anisotropy and the average susceptibility of graphite are decreased by decreasing the size of the crystal grains.[12]

[9] The expressions could probably be made more accurate by the introduction of various constitutive correction terms (such as corresponding to Pascal's system). At present it does not seem worth while to attempt to refine the simple and straightforward treatment given above.

[10] The values for hexaethylbenzene are those given by N. Ganguli, Zeits. f. Krist. **93**, 42 (1936), and for 1,2; 5,6-dibenzanthracene those given by K. S. Krishnan and S. Banerjee, Zeits. f. Krist. **91**, 173 (1935).

[11] K. S. Krishnan, Nature **133**, 174 (1934).

[12] S. Paramasivan, Ind. J. Phys. **4**, 139 (1929); K. S. Krishnan and N. Ganguli, Current Science **3**, 472 (1935).

The Free Energy of Electron Gas

A. R. GORDON, *Chemistry Department, University of Toronto*

(Received July 14, 1936)

The energy and free energy of a semi-degenerate gas obeying the Fermi statistics are computed as functions of temperature and concentration. The significance of the deviation of the free energy from the limiting high temperature value is illustrated by calculating the degree of thermal ionization of potassium vapor under conditions of high electron concentration.

IT has long been known that the translational partition function for a gas obeying either the Bose-Einstein or the Fermi statistics approaches asymptotically with increasing temperature the limiting value given by the Sackur-Tetrode equation. In general this approach is to all intents complete within a few degrees of absolute zero, but in the case of an electron gas (owing to the small mass of the particle) the deviation from the classical value persists to much higher temperatures. Sommerfeld[1] in a well-known paper has derived expressions defining the translational energy, free energy, entropy etc. of a gas obeying the Fermi statistics, with special consideration of the case in which, owing to high concentration and moderate temperature, the deviations from the classical values are particularly great ("complete degeneracy"); and Mott[2] has recently computed the energy, heat capacity and magnetic susceptibility for a few points in the "semi-degenerate" range. In dealing with the equilibria involved in problems of thermal ionization, however, it is the free energy that is of primary importance, and the present paper deals with the calculation of this and related thermodynamic quantities for an electron gas when temperature and concentration are not such as to permit the conventional Sackur-Tetrode expression to be used.

Sommerfeld has shown that for a gas containing $N=6.06\times10^{23}$ electrons in V cc at $T°$K,

$$N=2\pi VG\cdot\frac{(2mkT)^{\frac{3}{2}}}{h^3}\cdot\int_0^\infty\frac{u^{\frac{1}{2}}\cdot du}{e^{\alpha}\cdot e^{u}+1}, \qquad (1)$$

where G (the spin weight of the electron) $=2$, $\alpha=-F/RT$, F is the free energy of one "mole" of the gas, m is the mass of the electron, and the other symbols have their conventional meanings. Eq. (1) can be written

$$Q^*=e^{\alpha}/I_{1/2}(\alpha), \qquad (2)$$

where Q^*, the classical expression for the partition function, is equal to

$$(2\pi MkT)^{3/2}\cdot VG/N^{5/2}h^3$$

$M=Nm=1/1838$, and $I_m(\alpha)$ is defined by

$$I_m(\alpha)=\int_0^\infty\frac{u^m\cdot du}{e^{u}+e^{-\alpha}}\Big/\Gamma(m+1). \qquad (3)$$

Similarly, the energy of one mole of the gas is given by

$$E=(3/2)NkT\cdot I_{3/2}(\alpha)/I_{1/2}(\alpha), \qquad (4)$$

while $pV/NkT=I_{3/2}(\alpha)/I_{1/2}(\alpha)$. For large values of α, i.e., large T or V, it is easily verified that both $I_{1/2}(\alpha)$ and $I_{3/2}(\alpha)$ approach unity, i.e., $\alpha(=-F/RT)=\ln Q^*$, etc.

Table I gives the values of $I_{1/2}(\alpha)$ and of $I_{3/2}(\alpha)$ for $-1<\alpha<6$, and Table II gives α as a function of $\ln Q^*$ for $-0.4<\ln Q^*<8.0$. For $\alpha\geqslant0.3$, $I_m(\alpha)$ was computed by the obvious relation

$$I_m(\alpha)=\sum_{n=0}^{\infty}(-1)^n\cdot e^{-n\alpha}/(n+1)^{m+1}. \qquad (5)$$

For $\alpha<0.3$, the range of integration was split; for $0<u<0.3$, e^u was expanded and the integrand reduced to a power series in which could be integrated term by term. For $0.3<u<2.0$, the integrals were evaluated by tabular integration, while for $2.0<u<\infty$, the contribution to $I_{1/2}(\alpha)$ was computed by the rapidly converging series

[1] Sommerfeld, Zeits. f. Physik **47**, 1 (1928).
[2] Mott, Proc. Camb. Phil. Soc. **32**, 108 (1936).

TABLE I.

$$I_{1/2}(\alpha)=\frac{2}{\sqrt{\pi}}\cdot\int_0^\infty\frac{u^{\frac{1}{2}}\cdot du}{e^u+e^{-\alpha}};\qquad I_{3/2}(\alpha)=\frac{4}{3\sqrt{\pi}}\cdot\int_0^\infty\frac{u^{\frac{3}{2}}\cdot du}{e^u+e^{-\alpha}}.$$

α	$I_{1/2}(\alpha)$	$I_{3/2}(\alpha)$	α	$I_{1/2}(\alpha)$	$I_{3/2}(\alpha)$
−1.0	0.57965	0.73659	+0.8	0.87138	0.93126
0.9	.59976	.75206	0.9	.88154	.93702
0.8	.61968	.76704	1.0	.89104	.94236
0.7	.63935	.78152	1.2	.90815	.95185
0.6	.65871	.79547	1.4	.92292	.95990
0.5	.67769	.80886	1.6	.93556	.96669
0.4	.69624	.82169	1.8	.94631	.97240
0.3	.71431	.83395	2.0	.95539	.97718
0.2	.73184	.84562	2.2	.96303	.98116
−0.1	.74880	.85670	2.4	.96942	.98447
0	.76515	.86720	2.6	.97475	.98721
+0.1	.78085	.87712	2.8	.97919	.98948
0.2	.79588	.88646	3.0	.98286	.99135
0.3	.81022	.89524	3.5	.98950	.99472
0.4	.82386	.90347	4.0	.99359	.99678
0.5	.83679	.91116	4.5	.99610	.99804
0.6	.84901	.91835	5.0	.99763	.99881
+0.7	0.86054	0.92504	5.5	.99856	.99928
			+6.0	0.99913	0.99956

$$\frac{2}{\sqrt{\pi}}\int_2^\infty\frac{u^{\frac{1}{2}}\cdot du}{e^u+e^{-\alpha}}=e^\alpha\sum_{n=1}^\infty(-1)^{n+1}\cdot e^{-n\alpha}\left[2\left(\frac{2}{\pi}\right)^{\frac{1}{2}}\cdot\frac{e^{-2n}}{n}+\frac{P(2n)}{n^{\frac{1}{2}}}\right],\quad(6)$$

where $$P(t^2)=(2/\sqrt{\pi})\cdot\int_t^\infty e^{-y^2}\cdot dy,$$

with a similar relation for $I_{3/2}$.

In dealing with electron concentrations, it is convenient to define a fictive pressure P^* such that $P^*V=NkT$; in terms of this new quantity, $\ln Q^*=-14.239+\ln T^{5/2}/P^*$ where P^* is measured in atmospheres. It is evident from Table II, that for $\ln Q^*>3.6$, i.e., $(5/2)\log T-\log P^*>7.75$, F may be replaced by $-RT\ln Q^*$ without introducing an error greater than $0.01RT$; Table II shows that in this case $P=P^*$ within one-half of one percent or less. This condition implies that T must be greater than 1250° for $P^*=1$ atmosphere, and greater than 20,000° for $P^*=1000$ atmospheres.

TABLE II.

$\ln Q^*$	α	$\ln Q^*$	α	$\ln Q^*$	α
−0.4	−0.9169	+0.7	+0.5256	+2.6	+2.5738
0.3	0.7686	0.8	0.6421	2.8	2.7785
0.2	0.6247	0.9	0.7571	3.0	2.9824
−0.1	0.4849	1.0	0.8706	3.5	3.4893
0	0.3488	1.2	1.0940	4.0	3.9935
+0.1	0.2160	1.4	1.3131	4.5	4.4961
0.2	−0.0862	1.6	1.5288	5.0	4.9976
0.3	+0.0408	1.8	1.7417	5.5	5.4986
0.4	0.1652	2.0	1.9522	6.0	5.9991
0.5	0.2874	2.2	2.1609	7.0	6.9997
+0.6	+0.4074	+2.4	+2.3680	+8.0	+7.9999

For smaller values of $\ln Q^*$, however, the use of such approximations may introduce appreciable errors. To take an extreme case (selected from Russell's tables[3] of metal ionization in stellar atmospheres) consider the ionization of potassium at 5000°K under an electron concentration such that $P^*=1000$ atmospheres; $\ln Q^*$ is then $+0.1462$, $\alpha=-0.1557$, and $P=(J_{3/2}/J_{1/2})P^*=1150$ atmospheres. From spectroscopic data,[4] it follows that if x be the fraction of potassium ionized, $\log x=-4.76$; had the Sackur-Tetrode approximation to the free energy of the electrons been used, the result would have been $\log x=-4.63$.

[3] Russell, Astrophys. J. **75**, 337 (1932).

[4] Bacher and Goudsmit, *Atomic Energy States* (1932), p. 245. In computing the State Sum for neutral potassium, only the low lying states up to and including ^2F were taken into account.

The Exchange of Energy Between Organic Molecules and Solid Surfaces

Part I. Accommodation Coefficients and Specific Heats of Hydrocarbon Molecules*

OTTO BEECK, *Shell Development Company, Emeryville, California*

(Received August 17, 1936)

A molecular beam method primarily devised for the investigation of heterogeneous thermal decomposition of hydrocarbon-molecules (to be published later) was used to determine the accommodation coefficients of various hydrocarbon molecules at 20°C on an ordinarily clean nickel surface at 140°C and at pressures in the region of 10^{-6} mm Hg. The absolute values of the accommodation coefficients were obtained by relative measurements with the help of the following simple relation that was found to exist for paraffin hydrocarbons between the accommodation coefficient α, the specific heat per mole at constant pressure for the ideal gas state C_{v_0}, and the molecular weight M,

$$\alpha(C_{v_0}+R/2)/M=\text{constant}=0.352,$$

where R is the gas constant per mole. This equation supports a further relation which can be set up for the mean specific heat between 20° and 140°C for the paraffins by using a few reliable C_{v_0} values: $C_{v_0}=0.352M+1.80$. A combination of both relations gives the simple equation for α of the paraffins:

$$\alpha=c_1M/(c_1M+c_2),$$

where $c_1=0.352$ and $c_2=1.80+R/2$. The accommodation coefficient for hydrogen was found to be 0.310, in excellent agreement with earlier experimental values. The accommodation coefficients of ethane and ethylene whose specific heats are known from normal frequencies were found to be equal within a few tenths of a percent; acetylene was found to be 3 percent lower. Specific heats have been calculated for paraffin gases and vapors up to *n*-heptane by a combination of the results of this work and the specific heat of ethane from the normal frequencies. The specific heats are given to 300°C. Under the assumption of equal accommodation coefficients for paraffins and corresponding olefines based on the accommodation coefficient measurements of ethane and ethylene and on their specific heats, specific heats are given for propylene and *n*- and isobutylene to 300°C. It was found that the absolute difference between the specific heats of a paraffin and the corresponding olefine decreases with the chain length. The C_{v_0} values of the following pairs were found to be equal within the experimental error of one percent: *n*- and isobutane, *n*- and isobutylene, methyl acetylene and allene. Approximate values for the mean specific heats between 20° and 140 C are given for methyl acetylene and allene. A discussion is given of the relationship of the present work to spectroscopic work in the field.

INTRODUCTION

THIS paper is part of a broader investigation that is chiefly concerned with an examination of the heterogeneous thermal decomposition of organic molecules by a molecular beam method. During the course of the investigation it was necessary, in order to facilitate the analysis of hydrocarbon mixtures and mixtures of hydrocarbons with hydrogen at pressures of some 10^{-6} mm Hg by the hot wire method, to study the relative accommodation coefficients of various hydrocarbon molecules. This study has disclosed an interesting relationship between the accommodation coefficient α, the molar heat at constant volume for the ideal gas (zero pressure) C_{v_0}, and the molecular weight M for paraffin hydrocarbons which makes it possible to determine the true accommodation coefficient of any gas from relative measurements only.

THEORY OF HEAT CONDUCTION AT LOW PRESSURES

According to M. Knudsen,[1] in agreement with M. v. Smoluchowski,[2] that part of heat transfer between two surfaces which is due to conduction by the gas molecules at low pressures, provided the mean free path is large compared with the relevant dimensions of the apparatus, may be written for monatomic gases

$$Q=\frac{4}{3(6\pi)^{\frac{1}{2}}}n\bar{\omega}C_v(T_2-T_1)=\frac{2}{(6\pi)^{\frac{1}{2}}}n\bar{\omega}R(T_2-T_1), \quad (1)$$

where Q is the heat transfer per unit area per second, n the number of mols per cm^3, $\bar{\omega}$ the mean molecular velocity, $C_v=(3/2)R$, the specific heat per mole at constant volume and (T_2-T_1) the temperature difference of the two surfaces.

Analogously we may write for polyatomic molecules according to Knudsen

* Presented in part before the American Physical Society at Seattle (Washington), June, 1936.

[1] M. Knudsen, Ann. d. Physik (4) **34**, 593 ff (1911).
[2] M. v. Smoluchowski, Ann. d. Physik (4) **35**, 990 (1911).

$$Q=\frac{4}{3(6\pi)^{\frac{1}{2}}}n\bar{\omega}(T_2-T_1)\left[\frac{3}{2}R+\frac{3}{4}\left(C_v-\frac{R}{2}\right)\right],$$
$$Q=\frac{1}{(6\pi)^{\frac{1}{2}}}n\bar{\omega}\left(C_v+\frac{R}{2}\right)(T_2-T_1), \tag{2}$$

where the expression in brackets is equal to the sum of the translational part of the specific heat plus $\frac{3}{4}$ of the internal specific heat. The factor $\frac{3}{4}$ expresses the fact that, under the assumption of independent Maxwell distributions of translational and internal energy, a molecule with high translational energy contributes more to the energy transfer than a slow molecule.

Eqs. (1) and (2) hold only if there is no temperature jump between the surfaces and the mean temperature of the gas molecules leaving the surface, i.e., if the temperature difference $(T_2'-T_1)$ of the gas before and after leaving the surface is equal to the difference of temperatures (T_2-T_1) of the surface and the gas before the collision. Otherwise we have to write, more generally,

$$(T_2'-T_1)=\alpha(T_2-T_1).$$

The coefficient α was called by Knudsen the accommodation coefficient. Since the present measurements, like most of the earlier work, have been done with a heated wire the dimensions of which are very small compared with the surrounding colder glass tube, the gas acquires the temperature of the outer tube and we may write Eqs. (1) and (2), by introducing the accommodation coefficient α between the heated wire and the gas,

$$Q=\frac{2}{(6\pi)^{\frac{1}{2}}}n\bar{\omega}R\alpha(T_2-T_1) \tag{3}$$

for monatomic gases and

$$Q=\frac{1}{(6\pi)^{\frac{1}{2}}}n\bar{\omega}\alpha\left(C_v+\frac{R}{2}\right)(T_2-T_1) \tag{4}$$

for polyatomic gases.

Experimental

As stated in the introduction, the apparatus was not primarily designed for the investigation of accommodation coefficients. The molecular beam method proved, however, to be so appropriate for the measurement of accommodation coefficients at extremely low pressures that it may very well be adopted for measurements of this type in the future.

The beam was produced in agreement with the specifications outlined in three important papers on the molecular beam method by O. Stern and collaborators.[3] The source aperture was a short channel 0.50 mm long and 0.528 mm in diameter. The image orifice, 26.2 mm away from the source, was a channel ~1 mm long and 0.900 mm in diameter. In line with these two orifices was the receiver canal, 62.2 mm away from the entrance to the image orifice. The canal had a conical shape for better definition of the beam although this is not essential for the present part of the investigation. The entrance orifice had a diameter of 0.795 mm, the end of the canal a diameter of 1.60 mm. The canal was 11.96 mm long. Its Knudsen resistance was 5.19 times larger than the resistance of an ideal aperture of the diameter of the entrance orifice, if the latter resistance is taken as

$$R_s=\frac{(2\pi)^{\frac{1}{2}}}{\pi r^2} \text{ and the former as } R_c=\frac{3}{8}\left(\frac{2}{\pi}\right)^{\frac{1}{2}}\int_0^L\frac{dl}{r^3},$$

r being the radius and L the length of the canal.[4]

The maximum gas pressure in the reservoir from which the gas effused was of the order of 0.1 mm Hg and was measured with an accuracy of 0.3 percent by a special manometer previously described.[5] The two spaces between the three apertures were evacuated by two high speed high vacuum oil diffusion pumps charged with Apiezon oil *B*. The fore vacuum for these two pumps was provided by another oil diffusion pump and finally by a "Cenco Megavac" rotating oil pump. With a reservoir pressure of 0.1 mm Hg, a vacuum of about $2\cdot10^{-5}$ mm Hg could be maintained in the first space and better than $1\cdot10^{-5}$ mm Hg in the second space. A molecular beam entering an otherwise closed

[3] O. Stern, Zeits. f. Physik **39**, 751 (1926); Knauer and Stern, ibid., p. 764; Knauer and Stern, ibid. **53**, 766 (1929). See also the excellent monography on *Molecular Rays* by Ronald G. J. Fraser (The Macmillan Company, 1931), The Cambridge series of Physical Chemistry.

[4] M. Knudsen, Ann. d. Physik **28**, 76 (1909); see also v. Smolocł owski, ibid. **33**, 1559 (1910).

[5] O. Beeck, Rev. Sci. Inst. **6**, 399 (1935).

vessel behind the receiver canal will set up a maximum stationary pressure:

$$p_\infty = (pa/\pi r^2)k \qquad (5)$$

if p is the reservoir pressure, a the area of the source aperture, r the distance of the source aperture from the entrance of the receiver channel and $k=(R_c+R_s)/R_s$, where R_c, R_s are, respectively, the Knudsen resistances of the canal, and of an ideal aperture of the same cross section as the entrance to the canal. Eq. (5) is correct only if the source aperture is ideal (infinitesmally thin), if source and receiver are at the same temperature, and if the molecules in the beam suffer no collisions in the two spaces between the apertures. The first and the last assumptions cannot be realized in practice. We see from Eq. (5) that, under ideal conditions, the pressure p_∞ is independent of the molecular weight of the gas and of the cross section of the canal. A careful and critical study of all the errors involved led us to the conclusion that a pressure $p=0.1$ mm Hg in the reservoir produced on the average a maximum stationary pressure $p_\infty = 1\cdot 10^{-6}$ mm Hg in the receiver vessel, which is about 10 times lower than would be expected under ideal conditions. This relationship also varies from gas to gas due to several factors, such as the resistance of the tube leading from the reservoir to the source orifice, the pumping speed, etc., all depending essentially on the mean free path of the gas under consideration. The pressure set up in the receiver vessel by the molecular beam was measured by a highly sensitive Pirani manometer of the type used by Knauer and Stern.[3] An exact counterpart of this manometer was placed beside the measuring manometer in the same constant temperature bath. The opening of this manometer led into the same space as the beam manometer. Thus it was subject to the same temperature and pressure fluctuation as the beam manometer. The manometers formed two arms in a balanced sensitive Wheatstone Bridge. The bridge is unbalanced when the molecular beam enters the beam manometer, and the observed galvanometer deflection is for small pressures proportional to the pressure change. The sensitivity of the arrangement used was approximately $2\cdot 10^{-8}$ mm Hg pressure change per mm deflection of the galvanometer for the monatomic gas argon. The sensitivity was of course very much higher for large polyatomic molecules.

Let us, for purposes of simplification, introduce the relative sensitivity S which is the galvanometer deflection in cm produced by a reservoir pressure of 0.1 mm Hg. The sensitivity is specific for a given gas. However, it also depends on the reservoir pressure since, as has been pointed out above, the conditions are not ideal. These difficulties have been overcome by measuring the sensitivity S as a function of the reservoir pressure for all gases under consideration. By extrapolation of these sensitivity curves the sensitivity S_0 for the reservoir pressure zero may be obtained. Except for the possibility of a small error due to vapor pressures of the sealing materials used in the apparatus, which might scatter the various gases in the beam by different amounts, the values for S_0 should obey Eq. (5), i.e., the values for S_0 are independent of the pressure p in the reservoir, and the pressure p_∞ is independent of the molecular weight of the gas.

Thus the values of S_0 may be used directly to find the relative accommodation coefficients of the gases investigated by combining them with Eq. (3) or (4) in which $\bar{\omega}$ is inversely proportional to $\sqrt{M}$. One may write, for instance,

$$\frac{(S_0)_{\text{gas}}}{(S_0)_A} = \frac{\alpha_{\text{gas}}(M_A)^{\frac{1}{2}}[(C_v)_{\text{gas}}+R/2]}{\alpha_A(M_{\text{gas}})^{\frac{1}{2}}2R},$$

where the subscript A refers to the monatomic gas argon. Then

$$\frac{\alpha_{\text{gas}}}{\alpha_A} = \alpha' = \frac{(S_0)_{\text{gas}}(M_{\text{gas}})^{\frac{1}{2}}2R}{(S_0)_A(M_A)^{\frac{1}{2}}[(C_v)_{\text{gas}}+R/2]}, \qquad (6)$$

α' being the accommodation coefficient relative to argon.

Fig. 1 shows the sensitivity S as a function of the reservoir pressure p for all gases and vapors investigated (for hydrogen see Fig. 2). It is evident that the extrapolation of the sensitivity curves to $p=0$ is permissible only if the individual accommodation coefficients do not change in the pressure interval in which the curve has been established. Reasonable as this assumption may seem because the pressure range is not more than twenty-fold and because the pressure

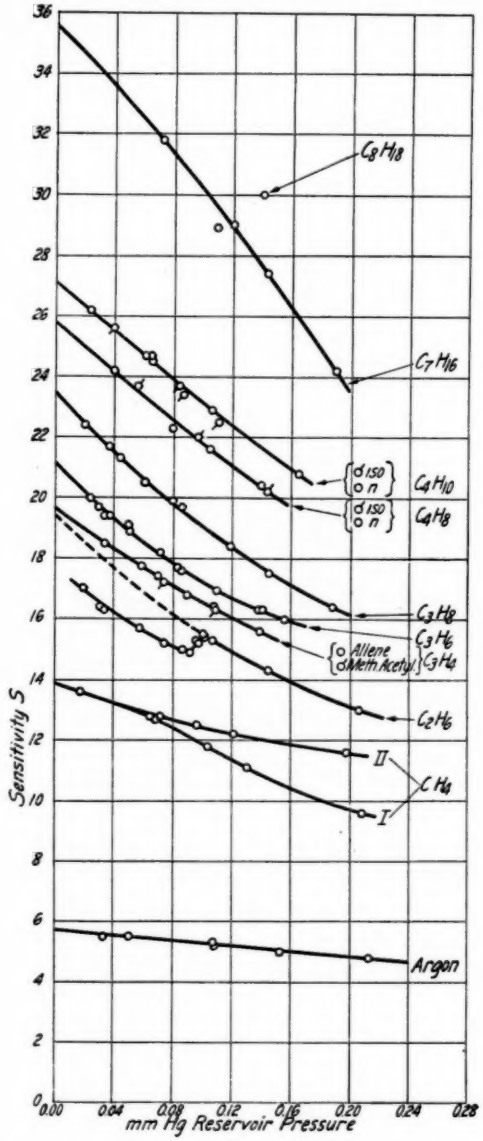

FIG. 1. Sensitivity S (i.e., galvanometer deflection per 0.1 mm Hg gas pressure in the reservoir) plotted against the reservoir pressure.

independence of the accommodation coefficient has been well established in higher pressure regions for various gases by several investigators,[6] the sensitivity curve of ethane shows a distinct break at a reservoir pressure of about 0.1 mm Hg which corresponds to a pressure rise of about $1 \cdot 10^{-6}$ mm Hg in the manometer vessel, caused by the entering beam. To this must be added an initial pressure which varies also with the reservoir pressure and is probably of the same order of magnitude. The sudden change in the accommodation coefficient of ethane is undoubtedly due to a sudden change of the surface conditions (type of adsorption layer) of the manometer wire. This change is evidently a function of the pressure of the surrounding gas.

Fig. 2 shows the sensitivity curve of ethane on a larger scale together with the sensitivity curves of ethylene and acetylene and two points for hydrogen. While there is no sharp break in the two latter curves, a discontinuity is readily observed in the case of ethylene, and acetylene also follows the same trend. This discontinuity is unique for these three gases. No other gas has shown a similar behavior. It seems that the pressure region was particularly favorable for such an effect with ethane, ethylene and acetylene. The same effect might be expected to occur for larger molecules at still lower pressures or higher temperatures of the manometer wire since the boiling points of these substances are higher. Consequently we have used the extrapolation of that part of the ethylene curve which belongs to the higher reservoir pressures. This extrapolation is in excellent agreement with the general relations derived from our measurements and discussed below.

The influence of the pumping speed on the sensitivity curves is illustrated in the case of methane (Fig. 1). Here two sensitivity curves have been taken with different pumping speeds; curve I with a lower speed than II. Both fall together as expected at low reservoir pressures.

It was found that for paraffins with the exception of methane the values for S_0 are, as shown in Table I, proportional to the square root of the molecular weight to a surprising degree of accuracy.

In combining this result with Eq. (4) and in setting Q proportional to S_0, i.e., proportional to $\sqrt{M}$, and $\tilde{\omega}$ inversely proportional to $\sqrt{M}$, we arrive at the simple equation:

$$\alpha(C_v+R/2)/M=\text{const.} \qquad (7)$$

In order to evaluate Eqs. (6) and (7) the specific heat C_v of the polyatomic gases under investigation must be known. To obtain high sensitivity, the temperature of the gauge wire

[6] See for instance: Rowley and Bonhoeffer, Zeits. f. physik. Chemie **B21**, 84 (1933).

was chosen considerably higher than the temperature of the gauge wall. We therefore have to consider the mean specific heat of the gas molecules between these two temperatures. The mean temperature of the wire itself was measured by its resistance, the temperature dependence of which had been established by a special calibration. This calibration was made by placing the gauge in constant temperature baths of various temperatures and measuring its resistance in a high-sensitive bridge with the lowest possible current passing through the bridge. By varying the current slightly, a curve was established whose extrapolation to zero current gave the correct resistance for the temperature of the bath.

Throughout the investigation the gauge wires were operated at a mean temperature of 140°C and the gauge walls were kept at 20°C. The gauges were Pyrex glass tubes about 12 cm long and 1 cm internal diameter, each containing a nickel ribbon 20 cm long, 50μ wide and 3μ thick. The nickel was shown by conductivity measurements to be almost pure. Its surface was brilliant like that of a platinum wire. The wire was not handled, and was cleaned only with alcohol and distilled water to remove the flux used in soldering the wire to its terminals. The wire was not heated above the operating temperature of 140°C. We may call the nickel surface "ordinarily clean." The mean specific heat between 20° and 140° was calculated from the normal frequencies[7] for methane, ethane, ethylene and acetylene, by the Planck-Einstein function. A value for butane at 80°C was taken from a recent investigation by Sage and Lacey.[8] A value for propane by the same authors was discarded because of its uncertainty.

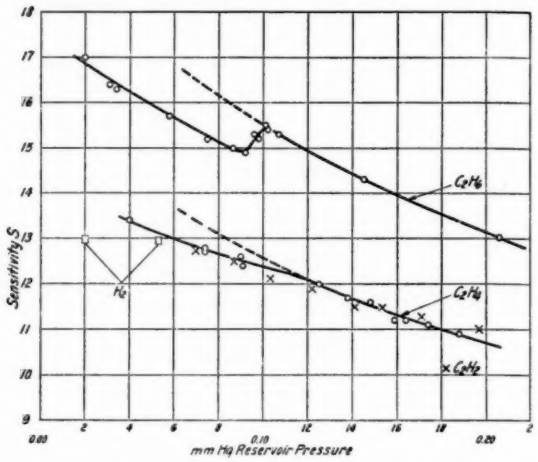

FIG. 2. Sensitivity S (i.e., galvanometer deflection per 0.1 mm Hg gas pressure in the reservoir) plotted against the reservoir pressure.

Remembering that Soddy and Berry,[9] Knudsen[1] and others have shown previously that on ordinarily clean surfaces the accommodation coefficient rapidly approaches unity with increasing molecular weight, we see from Eq. (7) that the increase of C_v must be proportional to M for high molecular weight paraffins. This proportionality, which is demanded by Eq. (7) is in fact approximately true for the specific heat of the three available lower paraffins, methane, ethane and butane and has also been observed by Lewis and McAdams.[10] It is needless to say that since we are concerned with specific heats at extremely low pressures, we are dealing essentially with C_{v_0} values, i.e., with specific heats of the ideal gases. Calculation from normal heat at 80°C, we have chosen for butane the true specific heat value at 80°C for reference in order not to depend on the slope of the line which fits the experimental points far better in the neighborhood of 80°C than at lower temperatures.

TABLE I.

	S_0	$\sqrt{M}$	$S_0/\sqrt{M}$
CH_4	13.9	4.00	3.48
C_2H_6	19.5	5.48	3.56
C_3H_8	23.5	6.64	3.54
C_4H_{10}	27.1	7.63	3.55
C_7H_{16}	35.6	10.01	3.56

[7] The following normal frequencies expressed in wave numbers were used:

CH_4	C_2H_2	C_2H_4	C_2H_6
1304(3x)	600(2x)	730	750(2x)
1520(2x)	729(2x)	950	827(2x)
2915	1975	1097	993
3020(3x)	3277	1110	1370
	3370	1160	1460(3x)
		1342	1480(2x)
		1444	2890(2x)
		1623	2899(2x)
		2990	2955
		3019	3020
		3110	
		3240	

For references on this subject see: A. Eucken and A. Bertram, Zeits. f. physik. Chemie **B13**, 361 (1936), and E. Teller and B. Topley, J. Chem. Soc. London, 885 (1935).

[8] B. H. Sage and W. N. Lacey, Ind. Eng. Chem. **27**, 1484 (1935). The authors give a straight line between 60° and 220°F. Since in case of ethane the mean specific heat between 20° and 140°C is very close to the true specific

[9] F. Soddy and A. J. Berry, Proc. Roy. Soc. **A83**, 254 (1910); ibid. **A84**, 576 (1911).

[10] W. K. Lewis and W. H. McAdams, Chem. and Met. Eng. **36**, 336 (1929). See also p. 689 of this paper.

frequencies give C_{v_0} values directly. The C_{v_0} value for butane was calculated from Sage and Lacey's measurements by means of Berthelot's equation of state. The almost perfect proportionality of the increase with M of those three values for C_{v_0} is at least a good support for the deductions made from Eq. (7). We feel, however, that there are good reasons for believing the methane value to be slightly lower (see discussion below). The equation for C_{v_0} was set up, therefore, by use of the ethane and butane values only. Thus we arrive at an equation representing the mean specific heat of the paraffins, between 20° and 140°C, in terms of the molecular weight.

$$C_{v_0}=0.352M+1.80. \tag{8}$$

Next α' has been calculated according to Eq. (6) for all cases in which the specific heat is known or can be calculated from Eq. (8). The values for α' are given in Table II.

By introducing the values for α' and for C_{v_0} into Eq. (7) we find for paraffins the relation

$$(C_{v_0}+R/2)\alpha'=0.388M. \tag{9}$$

and by combining Eqs. (8) and (9)

$$\alpha'=0.388M/(0.352M+1.80+R/2).$$

For large M, we obtain

$$\lim_{M\to\infty}\alpha'=0.388/0.352$$

and since this value must be identical with the true accommodation coefficient $\alpha=1$, we obtain $\alpha=(0.352/0.388)\alpha'$,

$$\text{or}\quad \alpha=\frac{0.352}{0.388}\left(\frac{0.388M}{0.352M+1.80+R/2}\right)$$

$$=\frac{0.352M}{0.352M+1.80+R/2}.$$

TABLE II.

Gas	α'	α
Argon	1	0.90_7
Hydrogen	0.34_2	0.31_0
Methane	0.73_7	0.66_9
Ethane	0.87_3	0.79_2
Ethylene	0.87_2	0.79_1
Acetylene	0.84_4	0.76_5
Propane	0.93_4	0.84_7
n-Butane, Isobutane	0.97_2	0.88_2
n-Heptane	1.02_3	0.92_8

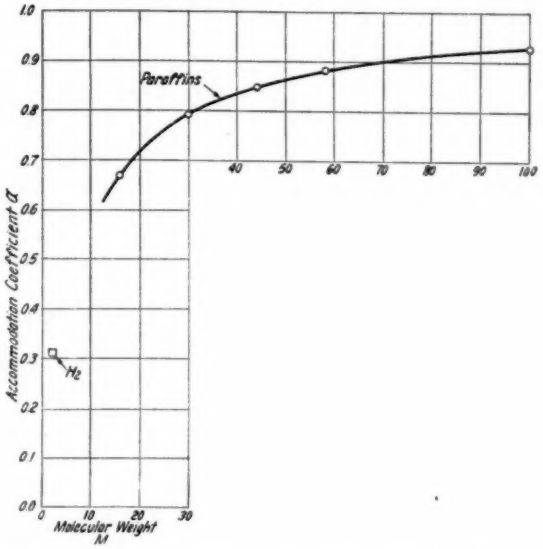

FIG. 3. The accommodation coefficients of the paraffins and of hydrogen plotted against the molecular weight.

The values for α are given in Table II. In Fig. 3, α for the paraffins is plotted against the molecular weight. α for hydrogen is added for comparison.

SPECIFIC HEATS

In examining Table II we find equal accommodation coefficients for *iso*- and normal butane and for ethane and ethylene. The former was derived from the fact that the sensitivity curve (Fig. 1) is the same for both gases. Strictly speaking, this only means that in both cases the product $\alpha\cdot(C_{v_0}+R/2)=$constant. If, therefore, we assume α to be the same for *iso*- and *n*-butane, we must conclude that C_{v_0} is also the same. In view of the fact that ethane and ethylene have been shown to have the same accommodation coefficient, equality of accommodation coefficients of the isomers of butane seems almost certain. Furthermore, the assumption seems justified that corresponding paraffins and olefines have the same accommodation coefficient. Again, since isobutylene and normal butylenes[11] lie on the same sensitivity curve, their accommodation coefficients and specific heats are presumably equal. The same sensitivity curve has been observed for allene and for methyl acetylene. Their absolute value, however,

[11] A mixture of 25 percent α-butylene and 75 percent β-butylene was used.

may not be obtained with the same certainty as the absolute values of the olefines, because we do not feel justified in setting their α equal to that of propane and propylene due to the fact that the accommodation coefficient of acetylene is about 3 percent lower than that of ethane and ethylene. The discrepancy will probably be less in the case of higher molecular weights and an approximate value of the specific heat of methyl acetylene and allene may be obtained by setting their accommodation coefficient equal to that of propane and propylene. In Table III are given the mean specific heats between 20° and 140°C at constant volume for the ideal gas state of all gases and vapors investigated.

This, however, is not the only information on specific heats that may be gained from these observations. In case of the paraffins, Eqs. (7) and (8) have been established for mean specific heats between 20° and 140°C. It follows therefore that the increase of the true specific heats at any temperature in this temperature interval must also be proportional to the molecular weight. Knowing accurately from spectroscopic data, in the case of ethane the relation of specific heat to temperature we are able to calculate true specific heats of all other paraffins at any temperature. Assuming that the laws established in the temperature region between 20° and 140°C will hold likewise at higher temperatures, we have calculated the specific heats of the paraffins up to 300°C, using ethane as reference. Furthermore, the specific heat of ethylene being known from spectroscopic data, we find by comparison of the curves for ethane and ethylene, that their ratio stays almost constant. At 300°C the ratio differs only 2 percent from its value at 0°C. Such a discrepancy necessarily will be smaller for larger paraffin molecules and their respective olefines.

Using Eq. (5) we arrive at the specific heat of the paraffins at any temperature by means of the relation

$$C_t=((C_t'-1.80)/(C'_{20\text{ to }140}-1.80))\times(C_{20\text{ to }140}-1.80)+1.80, \quad (10)$$

where C_t is the specific heat per mole of the gas considered, at zero pressure and at the temperature t, and C_{20-140} is the mean specific heat between 20° and 140°C of the same gas; C' refers to ethane, the reference gas, and 1.80 is an experimental constant. The values for the olefines are obtained by using the experimental ratio of paraffins and their respective olefines found for the mean specific heats between 20° and 140°C.

In Table IV are given the C_{v_0} values for C_nH_{2n+2} up to $n=7$, and also ethylene, propylene and acetylene. Further values for paraffins may be calculated from Eqs. (8) and (10) using the corresponding ethane value as standard.

Table V gives the specific heat C_p at constant pressure (one atmosphere) calculated with the help of Berthelot's equation of state. This equation is known to hold well for hydrocarbon vapors at pressures sufficiently below the critical pressure, which is true for all vapors under consideration. From Berthelot's equation we derive:

$$C_p=C_{v_0}+R+(81/32)R(T_c/T)^3p/p_c,$$

where T_c and p_c are the critical temperature and the critical pressure.

Discussion

Paraffins

A discussion of the theoretical aspects of the law governing the accommodation coefficients of the paraffins will be postponed until data for various gas temperatures and various surface temperatures have been completed.

Hydrogen

The value for the accommodation coefficient α of hydrogen is in excellent agreement with values recently obtained by other investigators on various surfaces, especially with the value obtained

Table III.

Gas	C_{v_0} mean 20° to 140°C	Remarks
CH_4	7.17	from normal frequencies
CH_4	7.25	this investigation (Eqs. (7) and (8))
C_2H_6	12.35	from normal frequencies (reference value)
C_3H_8	17.25	this investigation (Eq. (8))
n-C_4H_{10}	22.2	Sage and Lacey[8] (reference value)
iso-C_4H_{10}	22.2	assuming equal accommodation coefficient for n- and *iso*-C_4H_{10}
n-C_7H_{16}	37.0	this investigation (Eq. (8))
C_2H_4	9.55	from normal frequencies
C_3H_6	15.09	assuming equal accommodation coefficient for C_3H_8 and C_3H_6
n-, *iso*- C_4H_8	20.5	assuming equal accommodation coefficient for n-C_4H_{10} and *iso*- and n-C_4H_8
C_2H_2	9.50	from normal frequencies
allene, methyl acetylene C_3H_4	13.5	assuming equal accommodation coefficient for C_3H_8 and C_3H_4

TABLE IV.

	C_{v_0} in cal./mole °C			
t°C	0	100	200	300
CH_4	6.34	7.38	8.76	10.19
C_2H_6	9.86	12.98	16.06	18.78
C_2H_4	7.70	10.05	12.32	14.32
C_2H_2	8.15	9.78	10.89	11.73
C_3H_8	13.59	18.16	22.70	26.69
C_3H_6	11.89	15.89	19.82	23.30
C_4H_{10}	17.37	23.40	29.34	34.60
C_4H_8	16.04	21.61	27.09	31.95
C_5H_{12}	21.12	28.60	35.98	42.51
C_6H_{14}	24.87	33.80	42.62	50.42
C_7H_{16}	28.63	39.01	49.27	58.32

TABLE V.

	C_p (at 1 atmos.) in cal./mole °C			
t°C	0	100	200	300
CH_4	8.37	9.39	10.75	12.18
C_2H_6	11.99	15.02	18.07	20.78
C_2H_4	9.80	12.08	14.33	16.32
C_2H_2	10.29	11.83	12.91	13.73
C_3H_8	15.86	20.26	24.74	28.71
C_3H_6	14.14	17.98	21.86	25.31
C_4H_{10}	19.89	25.59	31.43	36.64
C_4H_8	18.61	23.82	29.19	34.00
C_5H_{12}	23.93	30.93	38.19	44.57
C_6H_{14}	27.93	36.26	44.89	52.51
C_7H_{16}	32.07	41.56	51.53	60.46

by Rowley and Evans[12] on an ordinarily clean iron surface at the same temperature as was used in this investigation. Their value is 0.31. Rowley and Evans by comparing their results with others came to the conclusions that they had measured the accommodation coefficient on an iron surface covered with adsorbed hydrogen. This conclusion was based on the fact that approximately the same value was found by other investigators on various materials. It seems most likely that at a surface temperature of 140°C a gas layer was present on the nickel used in this investigation or on the iron used by Rowley and Evans. Since this layer should not be affected by the hydrogen pressure at a moderately high temperature of the surface, it is not astonishing that the value found in this investigation with hydrogen pressures of some 10^{-6} mm Hg is in agreement with the value of Rowley and Evans at approximately 0.025 mm Hg. Earlier work of Rowley and Bonhoeffer, for instance, has shown the accommodation coefficient of hydrogen on platinum to be independent of the pressure between 0.03 and 0.3 mm Hg.

It must be emphasized that a direct measurement of the accommodation coefficient at pressures of 10^{-6} mm Hg would lead to great experimental difficulties since the energy radiated from the surface at 140°C is about 10^4 times larger than that resulting from the collision of the gas molecules. By means of the relations found for the paraffin series, the true accommodation coefficient for hydrogen or any other gas at 10^{-6} mm Hg was found by relative measurement only.

[12] H. H. Rowley and W. V. Evans, J. Am. Chem. Soc. **57**, 2059 (1935).

Specific heats and spectroscopy

The observed proportionality between the increase of C_{v_0} and M for the paraffins suggests at once a simple relationship of infrared and Raman spectra in the paraffin series. A glance at the graphic presentation of the Raman lines from *n*-butane to *n*-dodecane reveals indeed striking similarity and comparative simplicity. This agreement is not only true for frequencies assigned to C−H bonds and C−H deformations which lie above 1100 cm^{-1}, but is surprisingly good in the range of the chain oscillations proper. Propane and ethane show a much simpler Raman spectrum. The intimate relation between ethane, propane and *n*-butane, however, may be readily shown by an empirical summation rule of Kohlrausch and Barnés,[13] as applied to the C−C frequencies. This rule is applicable also to cyclopropane, isobutane and neopentane (tetramethylmethane). The rule is given by the equation:

$$\bar{\nu} = ((1/(s-1))\sum \nu_i^2)^{\frac{1}{2}},$$

where $\bar{\nu}$ is a frequency characteristic for C−C chains. In making the summation, frequencies of 2 or 3 fold degeneracy must be taken 2 or 3 times. s–1 is the number of similar valency bonds. Kohlrausch and Köppl found that the gases named above satisfy the rule with an error of one percent.

A few remarks are necessary in respect to methane. In spite of the fact that Eqs. (8) and (9) seem to hold for methane within a few percent, there are good reasons for believing that the methane value is slightly lower.

[13] K. W. F. Kohlrausch and D. Barnés, Ann. Soc. Españ. Fis. Quim. **30**, 733 see also: K. W. F. Kohlrausch and F. Köppl, Zeits. f. physik. Chemie **B26**, 209 (1934), especially p. 218 ff.

At 0°C the contribution of the oscillatory degrees of freedom to the specific heat is very small in the case of methane, and although this contribution still decreases towards lower temperatures, it is almost constant in the close neighborhood of $6R/2$. Towards lower temperatures the methane value is therefore too high and Eq. (8) must break down completely in the case of methane. At higher temperatures the value for the specific heat of methane which satisfies Eq. (8) is slightly greater than the value calculated from normal frequencies. In Fig. 4 are given curves for ethane and methane as calculated from normal frequencies and the curve for methane given by Eq. (8). It is readily seen that below 0°C. Eq. (8) breaks down entirely. As to the discrepancy at higher temperatures the following explanation may be offered without going into the details of this complex problem. Let us consider only the C−H frequencies and the C−H deformation frequencies. If the specific heat of the paraffins is proportional to M, we may assume that the contribution of the C−H frequencies and the C−H deformation frequencies is additive within the limit of error of our investigation. This can only mean that these oscillations are well localized and practically independent of the chain length, or in other words that we have a constant binding force. The group of C−H valence frequencies and deformation frequencies in the Raman spectra is indeed remarkably constant, especially from butane upwards.

There are two frequency regions of C−H deformation frequencies for paraffin molecules from ethane upwards, one region at about 750 cm^{-1} and the other about 1400 cm^{-1}. The frequency 750 cm^{-1} seems definitely to be associated with a bond angle that only occurs when two or more carbon atoms are present, probably the angle C−C−H.

Any attempt, therefore, to extrapolate to methane the measurements with higher paraffins would include the consideration of the deformation frequency at about 750 cm^{-1}. The number of frequencies depending on the bond angle C−C−H decreases according to: 10 for butane, 7 for propane, 4 for ethane, which would give the extrapolated value 1 for methane. The true value for methane is, however, zero. The contribution

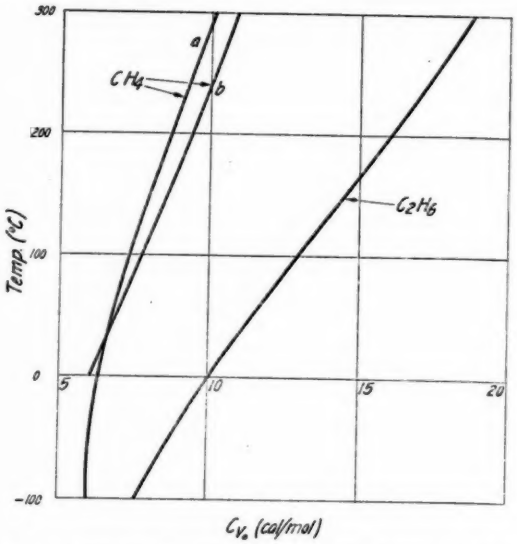

FIG. 4. The specific heat in cal. per mole and °C for the ideal gas state calculated for ethane and methane (curve *a*) from the normal frequencies and the values for methane (curve *b*) calculated from Eq. (8).

of this excess frequency to the specific heat is in rough agreement with the discrepancy between the values from normal frequencies and the value obtained by Eq. (8), the latter value being too high. This shows clearly that Eq. (8) must not be expected to hold for methane.

It is noteworthy that the absolute value of the difference between the specific heat of a paraffin and the respective olefine becomes smaller with increasing molecular weight. This indicates a definite effect of the chain length on the double bond. The only (and an apparently safe assumption), in obtaining the C_{v_0} value for the olefines is that of equality of the accommodation coefficients for paraffins and respective olefines; no other errors are possible. A similarly pronounced effect cannot be observed in Raman and infrared spectra, but this might be due to the fundamentally different method of excitation.

Special mention should also be made to the equality of C_{v_0} for the following pairs: *iso* and normal butane, *iso* and *n*-butylene, methyl acetylene and allene. In the latter case two double bonds are substituted for one single and one triple bond without altering the specific heat within the limits of the experimental error of one percent.

While it is realized that this discussion is incomplete from the spectroscopic standpoint, it is,

nevertheless, hoped that the specific heats and their simple relationships now presented will contribute considerably to the proper assignment of fundamental frequencies to the higher paraffins and by so doing will provide the foundation for a correct direct calculation from the normal frequencies of the specific heat of many higher hydrocarbons at higher temperatures.

Sources of error

Apart from the fact that the limit of error of the molecular beam measurements has been found to be one percent, thus establishing the proportionality of $\alpha(C_{v_0}+R/2)$ with M to within one percent, the actual equation for C_{v_0}, Eq. (8), has been set up by the use of the specific heat value of ethane (from normal frequencies)[7] and n-butane (Sage and Lacy).[8] Inasmuch as the value of Sage and Lacey may be slightly in error, all other derived values may show about the same relative error. We have, however, confidence in their value for n-butane since it was obtained by an adiabatic expansion method which Eucken and collaborators[14] have used previously with much success. We furthermore call attention to specific heat values for the paraffins obtained by Lewis and McAdams[10] by a flow method not designated in detail. Inasmuch as the flow method is known to introduce systematic errors easily, it is not astonishing that they find C_p values at 50°C for methane and ethane which are about 1.2 calories larger than those from spectroscopic data. However, they find in agreement with this work an increase in specific heat of the paraffins from methane to butane, which is, as they prefer to state, proportional to the number of carbon atoms. If their error is indeed systematic, as may be expected, their values should give the same slope as the values obtained from this investigation. This is actually the case within one percent accuracy, which speaks for the correctness of Sage and Lacey's value for n-butane.

As may be seen above, the accuracy of the values for the olefines depends on the accuracy of the values for the respective paraffins and at higher temperatures it depends also on the assumption that at any temperature the ratio of the specific heats of an olefine and the respective paraffin is constant, an assumption which is practically fulfilled in the case of ethane and ethylene as has been stated above in more detail.

[14] A. Eucken and K. von Lüde, Zeits. f. physik. Chemie **B5**, 413 (1929); A. Eucken and A. Parts, ibid. **B20**, 184 (1933).

Acknowledgments

Grateful acknowledgment is made to the directors of the Shell Development Company and especially to Dr. E. C. Williams for their continuous interest in this work and their permission to publish it.

Mr. W. Thurston has collaborated in securing data by the molecular beam method. Mr. F. Rust has prepared most of the pure gases. Both have helped with the numerical calculation of the specific heat data presented.

OCTOBER, 1936 JOURNAL OF CHEMICAL PHYSICS VOLUME 4

An Elementary Deduction of Gibbs' Adsorption Theorem

E. A. GUGGENHEIM, *Sir William Ramsay Laboratories of Inorgamic and Physical Chemistry, University College, London, England*

(Received June 11, 1936)

1. INTRODUCTION

IN the thermodynamics of surfaces there is no theorem more important than that known as "Gibbs' adsorption theorem," which determines how the surface tension of a solution varies when the composition is varied at constant temperature. Its derivation by Gibbs has all the logical conviction and elegance characteristic of Gibbs. But the abstract character of his proof makes it difficult to follow by anyone not thoroughly conversant with Gibbs' methods. Owing to the numerous applications of the theorem to all branches of surface chemistry and particularly colloid chemistry it is very desirable to have a more elementary proof.

Various attempts in this direction have already

been made. Of these the place of honor must without question be given to a proof by Koenig and Swain.[1] This proof is accurate, clear and convincing to anyone who is able to follow it. It however postulates a familiarity with the thermodynamic functions known as free energy and chemical potentials. It therefore seems to the author for some purposes insufficiently elementary. The proof is in fact almost exactly Gibbs' proof translated into less abstract and more comprehensible terms.

Of a very different class is the alleged proof of Milner,[2] which is reproduced in numerous elementary textbooks, and a somewhat similar proof of Harlow and Willows.[3] In neither of these treatments is the formula derived an accurate expression of Gibbs' adsorption theorem in its most general form. Both these treatments assume firstly that the solution contains only two components, secondly that the solution is ideal and thirdly that one of the components, regarded as solute, is present in very small quantity compared with the other, regarded as the solvent. Actually many of the systems to which the theorem is most widely applied have none of these properties. These treatments also have the drawback of relating the surface tension to the osmotic pressure instead of to the partial vapor pressures, a drawback common to numerous thermodynamic discussions of a past generation. We shall return to a more detailed criticism of Milner's formulae in a later section.

There is also a proof by Porter,[4] which does avoid the introduction of the quite irrevelant osmotic pressure, but there is a step in the argument which we are unable to follow.[5] Moreover the proof involves unnecessary approximations, in particular an inexact form of Raoult's law is assumed. Finally the proof seems in no respect easier to follow than that of Gibbs.

The proof which we shall give makes no reference to any thermodynamic potential functions and yet is free from restriction to ideal solutions or solutions of only two components. We consider that an elementary proof of such an important thermodynamic theorem is highly illuminating and instructive, provided it is logical and accurate. Alleged elementary proofs in which simplicity is obtained at the expense of clear and exact reasoning are to be deprecated. As there is so much loose reasoning prevalent in elementary thermodynamics due to confusion between the total reversible work of a process and the net or useful reversible work (in the terminology of Lewis and Randall) we shall commence with a brief discussion of these two expressions. We shall next discuss an important theorem equivalent to the formula called Gibbs-Duhem-Margules. An illuminating elementary proof of this theorem has been given by Bjerrum.[6] The Gibbs-Duhem-Margules relation has nothing to do with surfaces but its form is very similar to that of the Gibbs adsorption formula. It is therefore perhaps not altogether surprising that we are able to derive the latter from the former in a brief and simple manner.

2. Reversible Work and Net (or Useful) Reversible Work

If we consider two completely defined states I and II of a system, the two states being of the same temperature, then the work done by the system in passing isothermally from the state I to the state II has a maximum value if the path of the change is a reversible one; this maximum value is the same for all reversible paths and is called the (total) reversible work. It will be denoted by w.

In the particular case that in states I and II the whole system is at the same external pressure P, then one part of the reversible work may be regarded as done against this external pressure. If we denote by V^{I} and V^{II} the initial and final volumes of the system, this part of the work is evidently $P(V^{\mathrm{II}}-V^{\mathrm{I}})$. If we subtract this quantity from the (total) reversible work, we obtain the residue $w-P(V^{\mathrm{II}}-V^{\mathrm{I}})$ which is available for doing electrical work or other useful work. It has therefore been called by Lewis and Randall[7] the net (reversible) work of the process. It will be denoted by w'. In the more general case that the initial and final states are not at the same pressure

[1] Koenig and Swain, J. Chem. Phys. **1**, 723 (1933).
[2] Milner, Phil. Mag. **13**, 96 (1907).
[3] Harlow and Willows, Trans. Faraday Soc. **11**, 53 (1915).
[4] Porter, Trans. Faraday Soc. **11**, 51 (1915).
[5] The step in question is worded: "since dN and dn must be in the same proportion as N and n."
[6] Bjerrum, Zeits. f. physik. Chemie **104**, 410 (1923).
[7] Lewis and Randall, *Thermodynamics* (McGraw-Hill Book Company, 1923), p. 157.

or that there are phases at different pressures, the net (reversible) work is defined by

$$w' = w - \sum P^{II} V^{II} + \sum P^{I} V^{I}, \qquad (2.1)$$

the summation sign $\sum$ extending over the various phases.

Let us now compare the values of w and w' for two important processes. The first is the evaporation of one mole of a component from a condensed phase (crystal, single liquid, or solution) through a membrane permeable only to the vapor of this particular component to the vapor phase containing only this component. If P denotes the pressure on the condensed phase, p that of the vapor, v the partial molar volume of the particular component in the condensed phase and u its molar volume in the vapor, then evidently

$$w = pu - Pv, \qquad (2.2)$$

$$w' = 0. \qquad (2.3)$$

The second, and more interesting, process that we shall consider is the transfer of one mole of a component from one condensed phase denoted by the superscript α to another condensed phase denoted by the superscript β. The simplest method of reversible transfer is the familiar distillation in three stages:

(1) evaporate from α through membrane permeable only to vapor

$$w = p^{\alpha} u^{\alpha} - P^{\alpha} v^{\alpha}, \qquad (2.4)$$

(2) expand from p^{α} the partial vapor pressure over α to p^{β} the partial vapor pressure over β

$$w = \int_{p=p^{\alpha}}^{p=p^{\beta}} p\,du, \qquad (2.5)$$

(3) condense into β through membrane permeable only to vapor

$$w = -p^{\beta} u^{\beta} + P^{\beta} v^{\beta}. \qquad (2.6)$$

For the complete transfer, we have by addition

$$w = p^{\alpha} u^{\alpha} - P^{\alpha} v^{\alpha} + \int_{p=p^{\alpha}}^{p=p^{\beta}} p\,du - p^{\beta} u^{\beta} + P^{\beta} v^{\beta} \qquad (2.7)$$

or integrating by parts

$$w = -\int_{p^{\alpha}}^{p^{\beta}} u\,dp - P^{\alpha} v^{\alpha} + P^{\beta} v^{\beta}. \qquad (2.8)$$

Hence, according to the definition (2.1) of w', we obtain the extremely simple yet exact formula

$$w' = -\int_{p^{\alpha}}^{p^{\beta}} u\,dp. \qquad (2.9)$$

If the vapor behaves as a perfect gas, then

$$u = RT/p, \qquad (2.10)$$

where T is the absolute temperature and R the gas constant. Hence by substituting into (2.9), we obtain

$$w' = -\int_{p^{\alpha}}^{p^{\beta}} (RT/p)\,dp, \quad = RT \log (p^{\alpha}/p^{\beta}). \qquad (2.11)$$

If on the other hand the vapor does not behave as a perfect gas, then following G. N. Lewis[8] we define the fugacity p^* by the relation

$$\int_{p^0}^{p} u\,dp = RT \log (p^*/p^0), \qquad (2.12)$$

where p^0 is some pressure sufficiently low for the vapor to behave as a perfect gas. Substituting into (2.9) we obtain

$$w' = RT \log (p^{*\alpha}/p^{*\beta}). \qquad (2.13)$$

For the sake of simplicity we shall write for the general case

$$w' = RT \log (p^{\alpha}/p^{\beta}) \qquad (2.14)$$

on the understanding that if the vapor is not a perfect gas then p^{α}, p^{β} denote the fugacities and not the partial vapor pressures. With this reservation we shall usually refer to p^{α}, p^{β} as the partial vapor pressures, though strictly they denote fugacities if the vapors do not behave as perfect gases.

Suppose that two phases α and β at the same temperature, but not necessarily at the same external pressure, are in equilibrium with respect to a particular component i. Then there is no tendency for this component to distil over from the one phase to the other and so its partial vapor pressure must have the same value over both phases:

$$p_i^{\alpha} = p_i^{\beta}. \qquad (2.15)$$

By substitution of (2.15) into (2.14), we obtain

$$w' = 0. \qquad (2.16)$$

That is to say, the condition for the equilibrium with respect to a given component of two phases

[8] Lewis, Proc. Am. Acad. **37**, 49 (1901); Zeits. f. physik. Chemie **38**, 205 (1901).

at the same temperature, but not necessarily at the same pressure, is that the net work of transfer of the component from the one phase to the other be zero. It is with respect to this condition that the net reversible work w' is more important than the reversible work w. In particular the net work of transfer of a component from the interior of a phase to its surface is zero, provided the surface is in equilibrium with the interior.

3. Gibbs-Duhem-Margules Theorem

This theorem can be expressed in a very simple form by making use of the conception of net work. Consider two solutions at the same temperature and differing only infinitesimally in composition; then the net work of transfer of a finite quantity, say one mole, of any single component will evidently be infinitesimal. But the net work of transfer of a finite quantity of either solution into the other solution is an infinitesimal of a higher order or effectively zero. This last statement is equivalent to the Gibbs-Duhem-Margules relation. It can be expressed mathematically as follows: consider a mixture composed of n_1 moles of component 1, n_2 moles of component 2 and so on, and imagine its composition to be varied at constant temperature and pressure, then

$$n_1RTd\log p_1+n_2RTd\log p_2+\cdots=0 \quad (3.1)$$

or dividing throughout by RT

$$n_1d\log p_1+n_2d\log p_2+\cdots=0. \quad (3.2)$$

As an elementary proof of this important theorem has been given by Bjerrum[9] we shall merely illustrate it by a simple example. In a mixture of 0.40 mole of alcohol to 0.60 mole of water the partial vapor pressure of the alcohol is 34.2 mm and that of the water is 18.35 mm. In a mixture of 0.41 mole of alcohol to 0.59 mole of water the partial vapor pressure of the alcohol is 34.6 mm and that of the water is 18.25 mm. The net work of transfer of one mole of alcohol from the first mixture to the second is RT log (34.2/34.6) and the net work of transfer of one mole of water is RT log (18.35/18.25). These quantities are of opposite sign and both are of course small compared to RT because there is only a small difference in the composition of the two mixtures. But the net work of transfer of one mole of the first mixture, made up of 0.40 mole alcohol+0.60 mole water, into the second mixture will be

$$\begin{aligned}0.40RT\log(34.2/34.6)+0.60RT\log(18.35/18.2)\\ =RT\{0.40\log(34.2/34.6)+0.60\log(18.35/18.2)\}\\ =RT(-0.0046+0.0049),\end{aligned}$$

which is numerically very much smaller than either of the two terms.

The special form of the theorem which we shall use is the following: if to a large, effectively infinite, volume of a phase we add a finite quantity of another phase of the same temperature, the same pressure and infinitesimally different composition, the net work is zero (strictly an infinitesimal of a higher order). As we shall apply this theorem to a system containing free surfaces, which may not be ignored, it is necessary to be clear as to the conditions of validity of the theorem in the presence of such surfaces. These conditions are simple. We may apply the theorem in the form stated above even in the presence of free surfaces, provided these surfaces are in equilibrium with the volume phases which bound them and that the process of mixing does not create or destroy any free surfaces.

4. Gibbs' Adsorption Theorem

After these preliminaries the actual proof of the adsorption theorem is extraordinarily simple. In the diagram $KABCDEFGJ$ is the cross section of the wall of a container. HC is a partition separating the small volume $ABCH$, from the much larger, effectively infinite, volume $HDEF$. The partition HC is hinged at H and can be rotated slightly so as to allow the contents of the two compartments $ABCH$ and $HDEF$ to mix. $ABCH$ is filled with a solution of composition such that the components 1, 2, $\cdots$ have partial vapor pressures (strictly fugacities) p_1, p_2, $\cdots$. $HDEF$ is filled with a solution of slightly different composition such that the components 1, 2, $\cdots$ have partial vapor pressures (strictly fugacities) p_1+dp_1, p_2+dp_2, $\cdots$. AH is a cover which can be slid from the position AH to the position HG, each supposed to be of area unity. This lid is imagined to have the following properties:

(1) The composition of the solution in contact with the lid remains absolutely uniform right up the surface of the lid.

[9] Bjerrum, Zeits. f. physik. Chemie **104**, 410 (1923).

(2) The interfacial tension between the lid and the solution in contact with it is independent of the composition of the solution.

Actually according to the Gibbs adsorption theorem, which it is our object to prove, these two properties are not independent but thermodynamically equivalent to each other.

Suppose that we rotate the partition *HC* so that the two solutions mix. Then, since the mixing takes place without the formation or disappearance of any free surfaces, we may apply the Gibbs-Duhem-Margules relation and so the net reversible work of this process is zero. Now let us imagine the system in its original state and let us bring it to the same final state as before by a different path. Let us commence by gradually sliding the lid across from the position *AH* to the position *HG*. As we do so we gradually build up a free surface *AH* and destroy the free surface *HG*. In so doing we wish to keep unaltered the compositions of the interiors of the mixtures. This we can do by distilling over from the right to the left such amounts (positive or negative) of each component as are present in excess at the free surface on the left. If we do this then the surface tension of the two free surfaces, the one expanding, the other contracting will each remain constant throughout. After the lid has been moved to *HG* we rotate the partition *HC* so that the solutions mix. Since the mixing takes place again without formation or disappearance of any free surfaces, we may again apply the Gibbs-Duhem-Margules theorem and therefore the net work of mixing is again zero. But after mixing we can evidently slide the lid back to its old position *AH* without any work. But we have now reached the same final position as by the first and simpler procedure. Hence the net work is zero for the series of processes: sliding the lid from *AH* to *HG*, mixing solutions, sliding lid back to *AH*. But we have already pointed out that the net reversible work of the last two processes is zero; hence it must also be zero for the first process. All that remains to be done is to write down the net work of the process of moving the lid across from *AH* to *HG* while at the same time distilling over such amounts of the components as to keep the composition of each interior and therefore each surface tension unaltered and then equate this net work to zero.

Let $\Gamma_1, \Gamma_2, \cdots$ denote the number of moles of the components 1, 2, $\cdots$ in excess (positive or negative) per unit area of free surface over what would be present if the composition remained uniform right up the surface. Then $\Gamma_1, \Gamma_2, \cdots$, are the quantities of the components 1, 2, $\cdots$ that are distilled over from the right to the left. The net reversible work of these distillations is

$$\Gamma_1 RTd \log p_1 + \Gamma_2 RTd \log p_2 + \cdots. \quad (4.1)$$

If γ denotes the surface tension of the mixture on the left and $\gamma + d\gamma$ that of the mixture on the right, then the work done by the surface tension when the lid is moved from *AH* to *HG* is evidently $d\gamma$. Adding this to the net work of the distillations and equating to zero, we obtain

$$d\gamma + \Gamma_1 RTd \log p_1 + \Gamma_2 RTd \log p_2 + \cdots = 0 \quad (4.2)$$

or

$$-d\gamma = \Gamma_1 RTd \log p_1 + \Gamma_2 RTd \log p_2 + \cdots = 0. \quad (4.3)$$

This is the accurate and general form of the Gibbs adsorption theorem.

5. Physical Meaning of Γ and Invariant Form of Adsorption Formula

Actually formula (4.3) is applicable to the surface separating any two phases, but we wish to confine our attention to surfaces separating a liquid mixture from a vapor phase. We may then assume that every component of the solution has a volume concentration in the vapor phase negligible compared with that in the liquid phase. We may therefore with sufficient accuracy define the Γ_i as follows.[10] If we compare a portion of the liquid containing unit area of free surface with another very nearly equal portion in the interior of the liquid then the former will contain Γ_i moles of each component i more than the latter. This definition is sufficient for the derivation given above of formula (4.3). It is however not a complete definition of the Γ_i because it leaves unspecified the relation between the quantity of liquid with free surface and the quantity of liquid in the interior. For instance we might choose the two quantities of liquid to be of identical mass, or to contain exactly the same total number of molecules, or to have exactly the same volume or to satisfy any one of an infinite number of alter-

[10] Cf. Guggenheim and Adam, Proc. Roy. Soc. **A139**, 223 (1933).

native conditions. The choice is immaterial as far as the validity of (4.3) is concerned. This means that the actual values of the individual Γ_i occurring in (4.3) are of little physical significance. It therefore seems desirable to transform formula (4.3) into another formula involving quantities with values independent of the quantity of liquid in the interior with which we compare the liquid having a free surface. We can do this and at the same time remove another defect in formula (4.3) namely, the following. For variations of composition at constant temperature and pressure, the differentials $d \log p_1$ are not all mutually independent, since they are related by the Gibbs-Duhem-Margules formula

$$n_1 RTd \log p_1 + n_2 RTd \log p_2 + \cdots = 0. \quad (5.1)$$

Let us now multiply (5.1) by Γ_1/n_1 and subtract from (4.3). We obtain

$$-d\gamma = \left(\Gamma_2 - \frac{n_2}{n_1}\Gamma_1\right) RTd \log p_2 + \left(\Gamma_3 - \frac{n_3}{n_1}\Gamma_1\right) RTd \log p_3 + \cdots. \quad (5.2)$$

We have thus eliminated p_1 and have obtained a formula involving only the independent variables $p_2, p_3 \cdots$. We may write (5.2) in the abbreviated form

$$-d\gamma = \Gamma_2^{(1)} RTd \log p_2 + \Gamma_3^{(1)} RTd \log p_3 + \cdots, \quad (5.3)$$

where we define $\Gamma_2^{(1)}, \Gamma_3^{(1)} \cdots$ by

$$\begin{aligned} \Gamma_2^{(1)} &= \Gamma_2 - (n_2/n_1)\Gamma_1, \\ \Gamma_3^{(1)} &= \Gamma_3 - (n_3/n_1)\Gamma_1. \\ &\cdots\cdots\cdots \end{aligned} \quad (5.4)$$

We may thus regard $\Gamma_2^{(1)}, \Gamma_3^{(1)}, \cdots$ as measures of the quantities of the components 2, 3, $\cdots$ adsorbed per unit area, when we take component 1 as reference substance with $\Gamma_1^{(1)}$ zero by definition. Now it is easy to prove that the quantities $\Gamma_2^{(1)}\ \Gamma_3^{(1)}, \cdots$ thus defined have values independent of the quantity of homogeneous liquid with which we compare the liquid with unit free surface. For suppose we increase the quantity of homogeneous liquid in the ratio $1+x : 1$. Then since the total number $n_i+\Gamma_i$ of moles of each component i in the system with unit free surface has a definite value, independent of any convention, each Γ_i will have to be decreased by the amount $n_i x$. If we denote by the symbol $\rightarrow$ the variation due to increasing the quantity of homogeneous liquid used as reference to define the Γ_i, we thus have

$$n_i \rightarrow n_i + n_i x, \quad (5.5)$$

$$\Gamma_i \rightarrow \Gamma_i - n_i x, \quad (5.6)$$

$$\Gamma_1 \rightarrow \Gamma_1 - n_1 x. \quad (5.7)$$

Hence we deduce

$$\Gamma_i - (n_i/n_1)\Gamma_1 \rightarrow \Gamma_i - (n_i/n_1)\Gamma_1 \quad (5.8)$$

or in other words the $\Gamma_i^{(1)}$ remain invariant. Thus formula (5.3) has two advantages over formula (4.3); the first that the differentials are independently variable and the second that the quantities $\Gamma_i^{(1)}$ have values completely defined by the system and independent of any arbitrary choice. Readers familiar with Gibbs' treatment will recognize the quantities $\Gamma_i^{(1)}$ to be the same as those introduced by Gibbs[11] and designated $\Gamma_{i(1)}$ by him, but our definition is quite different from and much less abstract than that of Gibbs.

6. Relation between Surface Tension and Osmotic Pressure

We shall show that in the special case of a system of only two components there is a differential relation between the surface tension and the osmotic pressure of the solution. This relation is of small intrinsic interest and, in the author's opinion, of little value. The reason for not ignoring it is that it is this relation, not the Gibbs adsorption formula, that was derived by Milner by an elementary proof.

In a two component system if the component 1 is regarded as solvent and the component 2 is regarded as the solute, the osmotic pressure π is related to the vapor pressure of the solvent by the formula

$$d\pi = -(RT/v_1)d \log p_1, \quad (6.1)$$

where v_1 is the molar volume of the solvent. This formula is thermodynamically accurate subject to the assumption that v_1 is independent of the composition (mixing without volume change) and independent of the pressure (compressibility negligible); the formula is independent of any assumption of ideality of the solution. But for a

[11] Gibbs, *Collected Works*, Vol. I, p. 234.

two component system the Gibbs-Duhem-Margules relation is

$$n_1 d \log p_1 + n_2 d \log p_2 = 0 \qquad (6.2)$$

and the Gibbs adsorption equation is

$$-d\gamma = \Gamma_1 RT d \log p_1 + \Gamma_2 RT d \log p_2. \qquad (6.3)$$

If we eliminate p_1 and p_2 between the three Eqs. (6.1), (6.2), (6.3) we obtain

$$-d\gamma = \{\Gamma_2 - (n_2/n_1)\Gamma_1\}(n_1 v_1/n_2) d\pi. \qquad (6.4)$$

If we introduce the quantity $\Gamma_2^{(1)}$ defined above, we have

$$-d\gamma = \Gamma_2^{(1)}(n_1 v_1/n_2) d\pi \qquad (6.5)$$

or

$$-d\gamma = (\Gamma_2^{(1)}/m) d\pi, \qquad (6.6)$$

where m denotes the number of moles of solute per unit volume of solvent. Instead of using the quantity $\Gamma_2^{(1)}$, we might fix the values of Γ_1, Γ_2 according to the arbitrary convention that the solution having a free surface be compared with a portion of homogeneous liquid having an equal volume (but a different mass, different total number of moles, and different numbers of moles of each component). We shall for convenience refer to this convention as the (v) convention. If we ignore any expansion or contraction when a molecule is taken from the interior of the liquid to the surface, the (v) convention is represented by the equation

$$\Gamma_1^{(v)} v_1 + \Gamma_2^{(v)} v_2 = 0, \qquad (6.7)$$

the superscript (v) referring to the particular convention used to fix the values of Γ_1 and Γ_2.[10] If we eliminate Γ_1 between (6.7) and (6.4) we obtain

$$-d\gamma = \Gamma_2^{(v)}(n_1 v_1 + n_2 v_2/n_2) d\pi \qquad (6.8)$$

or

$$-d\gamma = (\Gamma_2^{(v)}/c) d\pi, \qquad (6.9)$$

where c denotes the number of moles of solute per unit volume of solution. Eq. (6.9) is the accurate expression of the formula deduced by Milner.

7. Milner's Formula

We shall now review briefly what Milner does in his alleged deduction of the Gibbs adsorption theorem. He tacitly assumes that there are only two components and uses the (v) convention to fix the values of Γ_1 and Γ_2. Subject to this arbitrary convention he correctly derives the formula

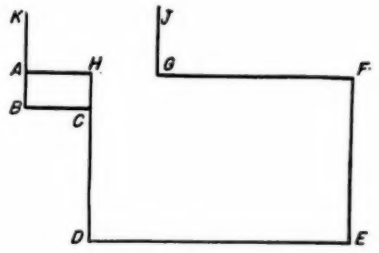

FIG. 1.

$$-d\gamma = (\Gamma_2^{(v)}/c) d\pi. \qquad (7.1)$$

He then assumes for π the formula

$$\pi = RTc, \qquad (7.2)$$

which is inaccurate even for an ideal solution. By combining (7.2) with (7.1) he obtains the inaccurate formula

$$-d\gamma = \Gamma_2^{(v)} RT d \log c, \qquad (7.3)$$

which he incorrectly calls the Gibbs adsorption theorem.

The accurate formula for the osmotic pressure for an ideal solution of negligible compressibility is

$$\pi = -(RT/v_1) \log \{n_1/(n_1+n_2)\}. \qquad (7.4)$$

If this is substituted into (7.1), we obtain

$$-d\gamma = -\Gamma_2^{(v)} \frac{n_1 v_1 + n_2 v_2}{n_2 v_1} RT d \log \frac{n_1}{n_1+n_2} \qquad (7.5)$$

or by a simple transformation

$$-d\gamma = \Gamma_2^{(v)} \frac{n_1 v_1 + n_2 v_2}{n_1 v_1} RT d \log \frac{n_2}{n_1+n_2}. \qquad (7.6)$$

This is the formula which Milner would have obtained if he had used the accurate formula for the osmotic pressure of an ideal solution. But it is to be noted that this formula is valid only for ideal solutions, whereas the Gibbs adsorption theorem is applicable and often applied to solutions that are by no means ideal. A further objection to Milner's formula (7.1) is that it holds only for $\Gamma_2^{(v)}$ defined according to the arbitrary (v) convention. The formula (6.5) for $\Gamma_2^{(1)}$ is different from Milner's formula even for ideal solutions except at infinite dilution. Finally Milner's formula is applicable only to binary solutions, whereas the Gibbs adsorption equation is, of course, applicable to mixtures of any number of components.

LETTERS TO THE EDITOR

This section will accept reports of new work, provided these are terse and contain few figures, and especially few halftone cuts. The Editorial Board will not hold itself responsible for opinions expressed by the correspondents. Contributions to this section must reach the office of the Managing Editor not later than the 15th of the month preceding that of the issue in which the letter is to appear. No proof will be sent to the authors. The usual publication charge ($3.00 per page) will not be made and no reprints will be furnished free.

The Rate of Oxidation of Carbon Monoxide in Presence of Nitrogen Dioxide

The effect of nitrogen dioxide has been studied by Crist and Roehling.[1] They suggested that the reaction had a complicated chain mechanism for low concentrations of nitrogen dioxide and that it was homogeneous for larger amounts of the catalyst.

We have studied the reaction in Pyrex, quartz, aluminum, and Pyrex treated with a potassium chloride solution. It was found that the reaction for low nitrogen dioxide pressures (0.06→5 mm) was greatly affected by the surface volume ratio and by the material of the reaction vessel. The rate was comparatively small in the Pyrex vessel washed with a potassium chloride solution. At higher pressures of nitrogen dioxide the reaction was unaffected by the nature of the vessel.

The homogeneous portion appears to consist of the reactions:

$$2\,NO+O_2=2\,NO_2, \quad (1)$$

$$2\,NO_2=2\,NO+O_2, \quad (2)$$

$$NO_2+CO=CO_2+NO. \quad (3)$$

The experimental method was varied so as to isolate these reactions. In a mixture with the approximate concentrations, total nitrogen dioxide = 10 mm, oxygen = 600 mm, and carbon monoxide = 50 mm, the reaction was found to be first order with respect to both carbon monoxide and nitrogen dioxide and proportional to the square root of the oxygen pressure. When the oxygen concentration is large it would be practically constant and the rate would be expressed by

$$-\frac{dco}{dt}=k_3[NO_2][CO].$$

Then, in order to obtain k_3 we calculate the nitrogen dioxide on the assumption that it is constant at the equilibrium concentration. The values of k_3 at 385°C and 527°C are, respectively, $1.12\times10^2(\pm0.07)$ sec.$^{-1}$ and $8.50\times10^3(\pm0.20)$ sec.$^{-1}$.

In order that reaction (1) should determine the rate, the mixture taken was approximately as follows: nitrogen dioxide = 10 mm, carbon monoxide = 600 mm and oxygen = 20 mm. Since the oxygen pressure is low the nitrogen dioxide concentration will also be small and the amount of nitrogen dioxide lost by reaction (2) will be relatively small. The results show that the reaction under these conditions is first order with respect to oxygen, independent of the carbon monoxide, and proportional to the square of the nitric oxide when its concentration is not too large. This is in accordance with the equation

$$-\frac{dO_2}{dt}=k_1[NO]^2[O_2].$$

The results are in Table I.

TABLE I. *Rate constants for the oxidation of nitric oxide.*

Temperature = 385°C		Temperature = 527°C	
Pressure in mm of NO (Total)	$k_1\times10^{-9}$ cc^2 mole^{-2} sec.$^{-1}$	Pressure in mm of NO (Total)	$k_1\times10^{-9}$ cc^2 mole^2 sec.$^{-1}$
6.80	2.02	7.37	4.21
10.0	2.05	7.65	4.37
11.5	1.80	10.8	4.20
15.4	1.48	13.4	3.92
17.4	1.47	15.7	3.38
25.2	0.79	15.8	3.37
		16.0	3.45
		19.0	3.68
		28.0	2.47

The decrease of the rate constant at higher nitrogen dioxide pressures could be due to increased nitrogen dioxide decomposition. The best value for k_1 would then be that obtained at the lower concentration of nitrogen dioxide. The value of the constant at 385°C is in fairly good agreement with the work of Bodenstein.[2] The constant at 527°C is in accordance with the predictions that the temperature coefficient should become positive at temperatures above 400°C.

R. H. CRIST
G. M. CALHOUN

Department of Chemistry,
Columbia University,
New York, N. Y.,
August 31, 1936.

[1] Crist and Roehling, J. Am. Chem. Soc. **57**, 2196 (1935).
[2] Kassel, *Kinetics of Homogeneous Gas Reactions* (Chemical Catalog Co., 1932), p. 157.